Characterization of the human NLR protein NLRC5

vorgelegt von

Andreas Heinrich Neerincx

aus

Emmerich am Rhein

Köln 2013

Berichterstatter: Prof. Dr. Jonathan Howard

                               Prof. Dr. Mats Paulsson

Tag der mündlichen Prüfung: 14.01.2013

Table of Contents

Abbreviations

°C	Degree Celsius
α	anti
µg	microgramme
µl	microlitre
A	desoxyadenosine
A20	TNFAIP3, tumor necrosis factor, alpha-induced protein 3
aa	amino acid
AAA+	ATPases associated with various cellular activities
AAMP	angio-associated migratory cell protein
AD	transcription activation domain
ADP	adenosine diphosphate
AIM2	absent in melanoma 2
APAF1	apoptotic protease-activating factor 1
APC	Allophycocyanin
APS	ammonium persulfate
ASC	apoptosis-associated speck-like protein containing a CARD
ATP	adenosine triphosphate
BIR	baculovirus inhibitory repeat
BLS	bare lymphocyte syndrome
BMDMs	bone marrow-derived macrophages
bp	base pairs
BS	Blau Syndrome
BSA	bovine serum albumin
C	desoxycytidine
CIITA	MHC class II transcriptional activator
CARD	caspase activating and recruitment domain
CC	coiled-coil
CREB	cyclic-AMP-responsive-element-binding protein
CD	Crohn's Disease
CD4	cluster of differentiation 4
CD8	cluster of differentiation 8
cDNA	complementary DNA
CHX	Cycloheximide
cIAP	cellular inhibitor of apoptosis protein
CLR	C-type lectin receptor
CMV	cytomegalovirus
C-terminus	carboxyl-terminus
DAI	DNA-dependent activator of IRFs
DAMPs	danger-associated molecular pattern
DAP	diaminopimelic acid
DISC	death-induced signalling complex
DMEM	Dulbecco's modified Eagle's medium

DMSO	dimethylsulfoxide
DNA	desoxyribonucleic acid
dNTP	desoxynucleotide triphosphate
ds	double stranded
DTT	dithiothreitol
EDTA	ethylenediaminetetraacetic acid
ELISA	enzyme-linked immunosorbent assay
EOS	early onset sarcoidosis
Erbin	Erbb2 interacting protein
ERK	axtracellular-signal-regulated kinase
et al.	*et alii*; and others
ETI	effector-triggered immunity
FBS	fetal bovine serum
g	gravitational force
g	gramme
G	desoxyguanosine
GAPDH	glycerinealdehyde-3-phosphate-dehydrogenase
GTP	guanosine triphosphate
h	hour
HA	hemagglutinin
HAU	hemagglutinin unit
HC	heavy chain
HEK	human embryonic kidney
HIN200	hematopoietic interferon-inducible nuclear antigens with 200 amino acid repeats
HLA	human leukocyte antigens
hNLRC5	human NLRC5
HRP	horseradish peroxidise
i.e.	id est; that is
ie-DAP	γ-D-glutamyl-meso-diaminopimelic acid
IF	immunofluorescence
IFI16	interferon-γ-inducible protein 16
IFN	interferon
Ig	immunoglobulin
IKK	IκB kinase
IκBα	NF-κB inhibitor-alpha
IL	interleukin
IP	immunoprecipitation
IRF	interferon regulatory factor
JNK	c-Jun N-terminal kinase
kb	kilobase pairs
kDa	kilodalton
LB	Lysogeny broth
LC	light chain
LepB	Leptomycin B

LPS	lipopolysaccharide
LRR	leucine-rich repeat
M	molar
mAB	monoclonal antibody
MAMP	microbe-asscociated molecular pattern
MAPK	mitogen-activated protein kinase
MAVS	mitochondrial antiviral-signalling protein
MCS	multiple cloning site
MDA5	melanoma differentiation associated gene 5
MDP	muramyl dipeptide
MEF	mouse embryonic fibroblast
mg	milligramme
MHC	major histocompatibility complex
min	minute
ml	millilitre
mM	millimolar
mNLRC5	murine NLRC5
MOI	multiplicity of infection
mRNA	messenger RNA
MyD88	myeloid differentiation primary response gene 88
NACHT	domain present in NAIP, CIITA, HET-E and TP1
NAIP	neuronal apoptosis inhibitory protein
NBD	nucleotide-binding domain
NEMO	NF-κB essential modulator
NF-AT	nuclear factor of activated T cells
NF-κB	nuclear factor κ-light-chain-enhancer of activated B cells
NF-Y	nuclear factor binding to the y box
ng	nanogram
NIK	NF-κB-inducing kinase
NLR	nucleotide-binding domain and leucine-rich repeat containing protein
NLRC	nucleotide-binding domain and leucine-rich repeat containing protein containing a CARD domain
NLRP	nucleotide-binding domain and leucine-rich repeat containing protein containing a PYRIN domain
NLS	nuclear localization signal
№	number
NOD	Nucleotide-binding oligomerization domain
NP40	Nonidet P 40
nRLU	normalized relative light unit
N-terminus	amino-terminus
OD	optical density
ONPG	*o*-Nitrophenyl-γ-D-galactopyranosid
P	phosphate
pAB	polyclonal antibody

PAGE	polyacrylamid gelelectrophoresis
PBS	phosphate buffered solution
PCR	polymerase chain reaction
PFA	paraformaldehyde
PGN	peptidoglycan
PRR	pattern recognition receptor
PYD	pyrin domain
PYHIN	pyrin and HIN domain-containing protein
qRT-PCR	quantitative real-time PCR
R protein	resistance protein
RD	repressor domain
RFX5	regulatory factor X 5
RFX-ANK	RFX-associated ankyrin-containing protein
RFX-AP	RFX-associated protein
RIG-I	retinoic acid-inducible gene I
RIP2	receptor interacting serine/threonine-protein kinase 2
RNA	ribonucleic acid
ROS	reactive oxygen species
rpm	rounds per minute
RT	room temperature
RT-PCR	reverse transcription PCR
SD	standard deviation
SDS	sodium dodecyl sulphate
SEAP	secreted alkaline phosphatise
sec	seconds
SeV	Sendai Virus
siRNA	small interfering RNA
ss	single stranded
STAND	signal transduction ATPases with numerous domains
STING	stimulator of interferon genes
T	desoxythymidine
TAB	TAK1-binding protein
TAF	TATA-box binding protein (TBP) associated factor
TAK	transforming growth factor (TGF)-beta activated kinase
TBE	TRIS-Borat-EDTA
TBK	TANK-binding kinase
TEMED	N,N,N',N',-Tetramethylethylendiamin
TFs	transcription factors
TIR	Toll-IL-1 receptor
TLR	Toll-like receptor
TNF(-α)	tumor necrosis factor(-alpha)
TRAF	TNR-receptor associated factor
TriDAP	L-Ala-D-γ-Glu-mDAP

TRIF	Toll/IL-1R domain containing adaptor inducing IFN-
TRIS	Tris(hydroxymethyl)-aminomethan
Triton X-100	polyethylene glycol p-(1,1,3,3-tetramethylbutyl)-phenyl ether
Tween 20	polyoxyethylen-(20)-sorbitan monolaureate
u	unit
Ub	ubiquitin
UV	ultra violet
V	volt
WB	western blot
wt	wildtype
XIAP	X-linked inhibitor of apoptosis

Amino acid abbreviations

Amino acid	Three letter code	One letter code
Alanine	Ala	A
Arginine	Arg	R
Asparagine	Asn	N
Aspartate	Asp	D
Cysteine	Cys	C
Glutamate	Glu	E
Glutamine	Gln	Q
Glycine	Gly	G
Histidine	His	H
Isoleucine	Ile	I
Leucine	Leu	L
Lysine	Lys	K
Methionine	Met	M
Phenylalanine	Phe	F
Proline	Pro	P
Serine	Ser	S
Threonine	Thr	T
Tryptophane	Trp	W
Tyrosine	Tyr	Y
Valine	Val	V

1 Introduction

1.1 Innate Immunity and Pattern Recognition Receptors

Multicellular organisms are constantly exposed to a variety of different microbes. To keep their integrity and to cope with potentially harmful pathogens, vertebrates have evolved a rapidly responding innate immune system as well as a less rapid responding adaptive immune system. Both immune responses are triggered by different immune receptors, which are either germline-encoded to confer innate immunity or are assembled by complex somatic gene-rearrangements to assign adaptive immunity (Iwasaki and Medzhitov, 2010). The receptors triggering innate immunity are called pattern recognition receptors (PRRs), since they recognise specific structures unique to microbes that are not found in the host. These invariant structures are termed microbe associated molecular patterns (MAMPs). To date, a broad variety of different PRRs have been identified in mammals. These PRRs can either be membrane-bound, like the Toll-like receptors (TLRs) or C-type lectin receptors (CLRs) but also cytosolic, like the nucleotide-binding domain, leucine-rich repeat containing receptors (NLRs) or RIG-I-like receptors (RLRs). To date, several mutations in PRRs and downstream signalling components associated with severe immune-related diseases were described, in particular in TLR and NLR signalling, uncovering their importance in innate immune recognition and subsequent clearing of infecting pathogens (reviewed in Netea *et al.*, 2012; Kufer and Sansonetti, 2011).

1.2 Membrane-bound Pattern Recognition Receptors

Among the membrane-bound PRRs, TLRs are probably the best studied family. The first human TLR, TLR 4, was identified in 1997 (Medzhitov *et al.*, 1997). TLRs are closely related to the interleukin (IL)-1 receptor and the *Drosophila* Toll receptor which was previously reported to mediate anti-fungal immunity in flies (Medzhitov *et al.*, 1997; Lemaitre *et al.*, 1996). The TLR family in humans comprises 10 different family members, whereas 12 different TLRs have been reported in mice. All TLRs are type I transmembrane proteins and consist of an extracellular leucine-rich-repeat (LRR) domain, a central transmembrane domain and a cytoplasmic Toll/interleukin-1 receptor (TIR) domain (Kumar *et al.*, 2011a). Although TLRs mediate extracellular pathogen recognition, they are not exclusively located in the plasma membrane. In fact, among the 10 different TLRs in humans, TLR1, TLR2, TLR4, TLR5 and TLR6 are expressed at the cell surface, whereas TLR3, TLR7, TLR8 and TLR9 are expressed in the endocytic compartment (Kumar *et al.*, 2011a). TLRs are able to recognize a broad variety of microbe-associated molecular patterns (MAMPs), including lipopeptides, detected by TLR2 together with TLR1 or TLR6 (Takeda *et al.*, 2002), nu-

cleic acids, detected by TLR3 (Alexopoulou *et al.*, 2001), TLR7, TLR8 (Heil *et al.*, 2004) or TLR9 (Hemmi *et al.*, 2000), as well additional bacterial derived products, including LPS, detected by TLR4 (Medzhitov *et al.*, 1997) or flagellin, detected by TLR5 (Mizel *et al.*, 2003; Smith *et al.*, 2003; Hayashi *et al.*, 2001).

Upon activation by their ligands, dimerisation was reported for at least some TLR receptors, including TLR2 with TLR1 and TLR6 (Jin *et al.*, 2007; Takeda *et al.*, 2002), TLR3 (Wang *et al.*, 2012) and TLR4 (Park *et al.*, 2009) to mediate downstream signalling by recruitment of TIR-domain containing adaptor molecules, such as myeloid differentiation primary response gene 88 (MyD88), Toll/IL-1R domain containing adaptor inducing IFN-β (TRIF), TIR domain containing adaptor protein (TIRAP) and TRIF-related adaptor molecule (TRAM) (Kumar *et al.*, 2011a; Saitoh *et al.*, 2004b; Saitoh *et al.*, 2004a). Except TLR3, all TLRs are able to recruit MyD88, which activates nuclear factor "kappa-light-chain-enhancer" of activated B-cells (NF-κB) or mitogen-activated protein kinase (MAPK) pathways. TRIF, in contrast, is recruited to TLR3 and TLR4 following activation and triggers downstream NF-κB and interferon regulatory factor 3 (IRF3) signalling, resulting in type I interferon and cytokine production (Kawai and Akira, 2010). TRAM and TIRAP serve as adaptor molecules, important for the specific recruitment of MyD88 and TRIF, and provide a basis for diversity in TLR signalling (Kumar *et al.*, 2011a). Among all TLRs, TLR4 is the only TLR which is able to bind all of the four adaptor proteins and requires additional molecules for LPS-recognition, including LPS-binding protein (LBP), CD14 and myeloid differentiation protein 2 (MD-2) (Peri and Piazza, 2012; Akashi-Takamura and Miyake, 2008; Shimazu *et al.*, 1999). TLR signalling in general can be divided into a MyD88-dependent and a MyD88-independent (TRIF-dependent) signalling cascade.

In the MyD88-dependent pathway, MyD88 activates the insulin receptor associated kinase 4 (IRAK4). Subsequently, IRAK 1 and 2 are phosphorylated and recruited to form an active signalling complex together with TNF-receptor associated factor 6 (TRAF6). TRAF6 is an E3-Ligase which assembles lysine 63-linked polyubiquitin chains on itself together with IRAK1. For that purpose, two additional enzymes, the ubiquitin-activating enzyme Ubc13 and the ubiquitin-conjugating enzyme Uev1A are recruited and form the fully active ubiquitin-transfer complex together with TRAF6 (refer to figure 1.1; MyD88-dependent TLR signalling). Subsequently, ubiquitinated TRAF6 acts as a signalling mediator in TLR signalling and interacts with TAK1, a member of the mitogen-activated protein kinase kinase kinase (MAPKKK) family (Yamaguchi *et al.*, 1995). Two proteins called TAB1 and TAB2 have been identified to play crucial roles as scaffolding proteins for TAK1 and bind to ubiquitinated TRAF6 (Akira and Takeda, 2004). The activated TAK1/TRAF6 complex subsequently mediates phosphorylation of downstream targets such as the IκB kinase complex (IKK) and MAPKs (Ninomiya-Tsuji *et al.*, 1999). The IκB kinase

complex (IKK) consists of IKK-α, IKK-β and NF-κB essential modulator (NEMO or IKK-γ) and is responsible for phosphorylation of the inhibitor of NF-κB (IκB). Phosphorylation of IκB leads to its degradation and to the release of bound p65/p50, which initiates transcription of early-phase NF-κB responsive genes (Karin and Ben-Neriah, 2000). A schematic overview of the processes starting from TLR dimerization upon ligand binding and ending up in NF-κB activation is depicted in figure 1.1.

The MyD88-independent or TRIF-dependent pathway mainly plays a role in nucleic acid recognizing TLRs, such as TLR3, as well as partly in TLR4 signalling, resulting in IRF3-dependent type I interferon activation and late phase NF-κB activation (Akira and Takeda, 2004). It has been shown that noncanonical IKKs, for example the kinase IKK-ε, as well as the TANK-binding kinase-1 (TBK1) mediate activation of IRF3 downstream of TRIF (Fitzgerald *et al.*, 2003b; Fitzgerald *et al.*, 2003a; Sharma *et al.*, 2003a; Yamamoto *et al.*, 2002). Phosphorylation in its C-terminal regulatory domain leads to dimerisation and nuclear translocation of IRF3 where it acts as a transcription factor in conjunction with co-activators such as p300 and CREB-binding protein for early phase IFN-β release. Furthermore, IRF3 also induces and cooperates with another IRF called IRF7, which is involved in later phase IFN-α and IFN-β expression (Akira and Takeda, 2004; Sato *et al.*, 2000). Taken together, TRIF is involved in type I IFN production, but can also trigger late phase NF-κB activation via at least two different MyD88-independent pathways (Akira and Takeda, 2004).

The physiological importance of TLR signalling is highlighted by hereditary cases of severe diseases caused by pathogen infection (reviewed in Casanova *et al.*, 2012). Well studied examples are mutations in MyD88 and IRAK4, abolishing functional protein production. The absence of these proteins result in impaired cytokine production, followed by increased bacterial infection diseases (reviewed in Netea *et al.*, 2012). Interestingly, MyD88-IRAK4 deficiency is most problematic in early childhood, but less in the adulthood, indicating the development of adaptive immune responses over time (Netea *et al.*, 2012; Bousfiha *et al.*, 2010). Another example affects the MyD88-independent/TRIF-dependent signalling pathway downstream of TLR3, including mutations in TLR3 itself, in TRIF and in additional downstream molecules. These patients are highly susceptible to herpesvirus encephalitis, but not to diseases caused by other infecting pathogens, most likely due to altered type I IFN release (Netea *et al.*, 2012; Bousfiha *et al.*, 2010; Zhang *et al.*, 2007).

A second group of transmembrane receptors are Dectin-1 and Dectin-2, two members of the C-type lectin superfamily. Although, this superfamily consists of 17 subgroups with more than 1000 proteins, in mammals only Dectin-1 and Dectin-2 seem to function as PRRs to detect microbial derived molecules. C-type lectin receptors (CLRs) consist of an extracellular stalk re-

gion, a central transmembrane domain and a cytoplasmic signalling region (reviewed in Sancho and Reis e Sousa, 2012).
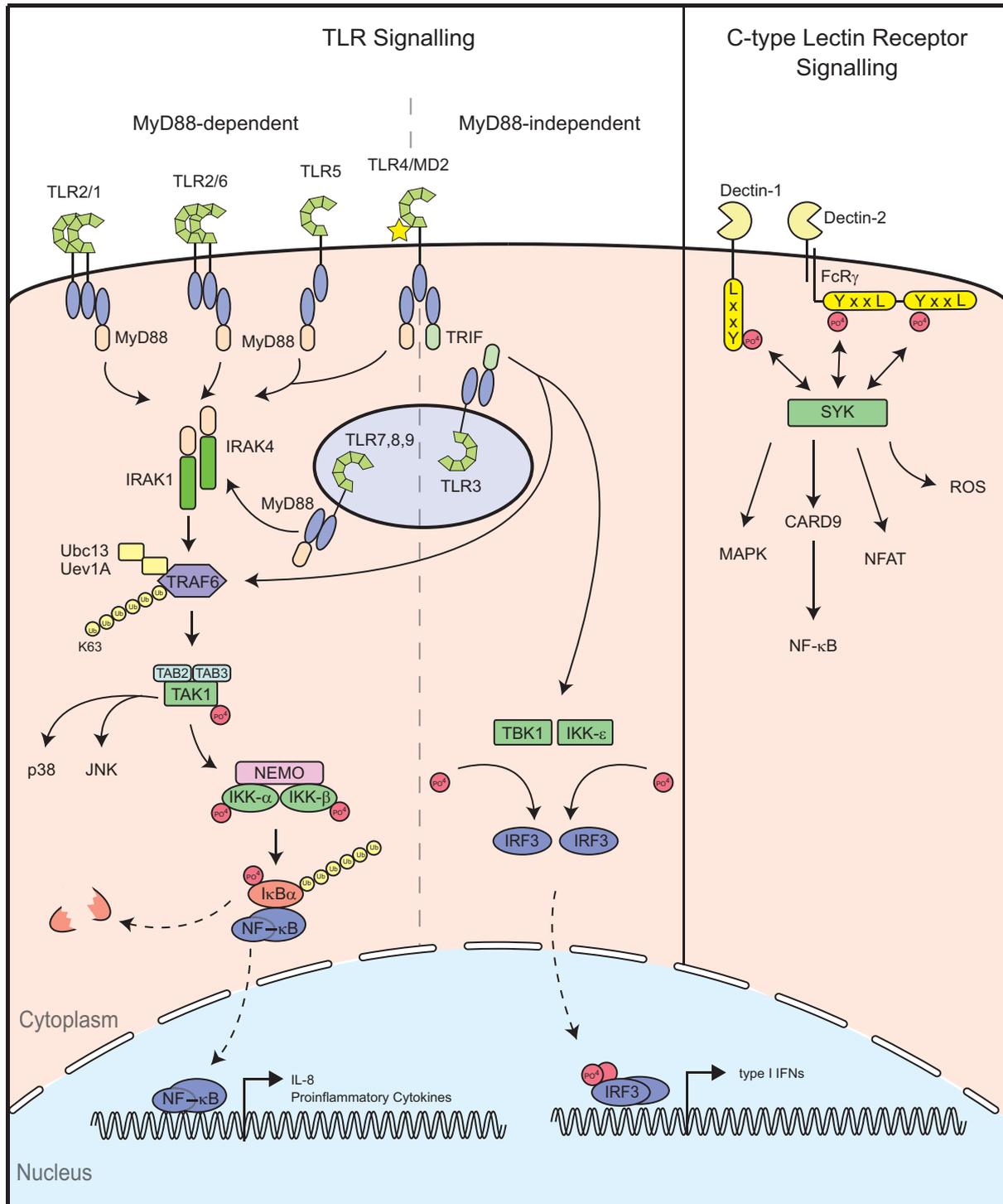
Figure 1.1 Membrane-bound PRR signalling
Detection of extracellular MAMPs is mediated by membrane-bound Toll-like receptors (TLRs) or membrane-bound C-type lectin receptors (CLR). TLR signalling can be divided into MyD88-dependent (left part) and MyD88-independent/TRIF-dependent (middle part) signalling. Recruitment of MyD88 results in canonical NF-κB activation, whereas TRIF recruitment results in type I IFN activation via the kinases TBK1 and IKK-ε. CLR signalling is mediated by the central kinase Syk, activating different transcription factors, like NF-κB or NFAT as well as MAPK pathways and ROS production (based on Sancho and Reis e Sousa, 2012; Kawai and Akira, 2010; Akira and Takeda, 2004).

Although this cytoplasmic region can harbour different signalling motifs with mostly unknown signalling functions, the role of Dectin-1 and Dectin-2 with an immunoreceptor tyrosine-based activation motif (ITAM) and a hemITAM motif, respectively, has been linked to innate immunity (Sancho and Reis e Sousa, 2012). Both Dectin-1 and Dectin-2 are activated by the fungal cell wall components β-1-3-glycans and α-mannose, respectively. Upon activation, they dimerize and recruit the tyrosine kinase Syk, which is able to activate a variety of signalling pathways, like NF-κB via the adaptor CARD9, MAPK pathways, the transcription factor nuclear factor of activated T cells (NFAT) or reactive oxygen species (ROS) production (Sancho and Reis e Sousa, 2012). Importantly, Dectin-1 and Dectin-2 do not only function as PRRs to trigger innate immunity, but can also impact cell migration, phagocytosis or cargo transport in general (Sancho and Reis e Sousa, 2012).

An overview of membrane bound PRRs and the activated signalling pathways are depicted in figure 1.1.

1.3 Cytosolic Pattern Recognition Receptors

Even though membrane bound PRRs are able to cope with a variety of different pathogens, when pathogens enter the cytoplasm, these receptors become useless.

From that point on, intracellular PRRs undertake pathogen recognition and innate immunity activation. Examples are the RIG-I-like receptors (RLRs), DNA-binding proteins like the DNA-dependent activator of IFN-regulatory factors (DAI), members of the PYHIN protein family, such as absent in melanoma 2 (AIM2) and nucleotide-binding domain-leucine-rich repeat-containing proteins (NLRs) (Schattgen and Fitzgerald, 2011; Wilkins and Gale, 2010).

Most of these cytoplasmic receptors are activated by pathogen-derived molecules. RLRs and DNA receptors are responsible for viral nucleic acid recognition whereas NLR proteins are mainly, but not exclusively, activated upon stimulation by bacterial-derived products and danger molecules. In the following paragraph, the different protein families and their signalling pathways will be briefly introduced.

The RLR family consists of three different members, namely retinoic-acid inducible gene I (RIG-I), melanoma differentiation associated gene 5 (MDA5) and laboratory of genetics and physiology 2 (LGP2). RLRs are expressed ubiquitously in most cell types and are closely related to each other. Moreover, they share a similar structure belonging to the DExD/H box-containing RNA helicase family. They consist of a C-terminal regulatory domain (RD), which is important to confer recognition specificity for 5'-ppp dsRNA bound by the central helicase domain. Furthermore, RIG-I and MDA5 have two additional N-terminal caspase recruitment and activation (CARD) domains (Schmidt *et al.*, 2011). Although LGP2 lacks the N-terminal CARD domain and

was thus proposed to have inhibitory function (Komuro and Horvath, 2006; Rothenfusser *et al.*, 2005), another study reported a defect in type I IFN response in LGP2$^{-/-}$ mice upon viral infection (Venkataraman *et al.*, 2007).

To date, the molecular basis of ligand binding to RIG-I has been investigated in great detail. *In vitro* assays revealed, that RIG-I interacts with 5'-ppp-ssRNA and dsRNA in an ATP-independent manner through its C-terminal repressor domain (RD) and helicase domain (Gee *et al.*, 2008; Hornung *et al.*, 2006; Pichlmair *et al.*, 2006). Subsequent ATP binding induces conformational changes, leading to exposure of the CARD domains (Kowalinski *et al.*, 2011; Luo *et al.*, 2011; O'Neill and Bowie, 2011). Due to structural similarities, a related mechanism is also plausible for other RLRs (O'Neill and Bowie, 2011). In contrast to RIG-I, MDA5 is selectively activated by the dsRNA mimic poly(I:C) (Yoneyama and Fujita, 2009; Kato *et al.*, 2006). Although detailed information of the subsequent ATP-dependent activation is still missing, it has been established, that both RIG-I and MDA5 interact through homotypic CARD-CARD interactions with the signalling-adaptor molecule IPS-1 (also known as MAVS, VISA or Cardif) (Kawai *et al.*, 2005; Meylan *et al.*, 2005; Seth *et al.*, 2005; Xu *et al.*, 2005). IPS-1 itself is associated to the outer mitochondrial membrane and consists of an N-terminal CARD domain, a central proline-rich-region (PRR) as well as a C-terminal transmembrane domain which is important for its function (Seth *et al.*, 2005). RIG-I and MDA5 activation result in type I IFN production, mediated by the adaptor protein TRAF3 (refer to figure 1.3; right part). An interaction between IPS-1 and TRAF3 was reported to be essential for type I IFN via recruitment of the kinases (TANK)-binding kinase 1 (TBK1) and IKK-ε with subsequent activation of the transcription factors IRF3/7 (Fitzgerald *et al.*, 2003b; Sharma *et al.*, 2003b). Moreover, RIG-I and MDA5 also activate NF-κB, likely by recruitment of TRAF2 and TRAF6 (Xu *et al.*, 2005). This signalling platform consists of several additional factors including Fas-associated death domain (FADD), receptor interacting protein 1 (RIP1), as well as of proteins involved in the TNF-receptor (TNFR)-mediated signalling complex, for example TNFR-associated DD (TRADD) (Yoneyama and Fujita, 2009). For complete RIG-I activation, another adaptor protein called stimulator of interferon genes (STING), also known as mediator of IRF-3 activation (MITA), interacts directly with RIG-I, thus functioning as a scaffold (Ishikawa and Barber, 2008; Zhong *et al.*, 2008) (also refer to Figure 1.3; right part).

Another group of intracellular nucleic acid receptors mediates DNA recognition. The fact that dsDNA occurs in the cytoplasm only during a pathogen infection makes it an efficient target for innate immune responses. Moreover, cytoplasmic DNA is able to trigger different pathways (reviewed in Hornung and Latz, 2010). First, DNA receptors can induce transcriptional reprogramming, i.e. NF-κB activation or IRF activation, second, dsDNA can be transcribed by RNA polymerase III to elicit RIG-I (Ablasser *et al.*, 2009; Chiu *et al.*, 2009) and finally, dsDNA can

induce IL-1β processing by activation of the AIM2 inflammasome (Burckstummer *et al.*, 2009; Fernandes-Alnemri *et al.*, 2009; Hornung *et al.*, 2009; Roberts *et al.*, 2009).

The first cytoplasmic receptor recognized to function as a dsDNA receptor was DNA-dependent activator of IRFs (DAI; also known as ZBP1) (Takaoka *et al.*, 2007). DAI is able to induce type I IFN responses in an IRF3-dependent manner (Takaoka *et al.*, 2007). However, DAI knock-down cells responded normally to DNA virus infection, thus it is likely that more than one receptor has evolved to detect dsDNA (Hornung and Latz, 2010; Wang *et al.*, 2008).

In 2009, Chiu and colleagues, as well as Ablasser and colleagues, unveiled a dsDNA-dependent type I IFN response, which was RIG-I-, MAVS- and IRF3-dependent. During the study, they uncovered a mechanism, by which AT-rich cytoplasmic DNA serves as a template for *de novo* synthesis of RNA by DNA-dependent RNA polymerase III. The *de novo* synthesized RNA then activates RIG-I and induced type I IFN responses (Ablasser *et al.*, 2009; Chiu *et al.*, 2009). Both studies not only elucidated a new pathway of dsDNA recognition, but also solved a long-standing mystery why DNA-dependent RNA polymerase is present in the cytoplasm, where normally no DNA is present (Ablasser *et al.*, 2009; Chiu *et al.*, 2009).

Finally, dsDNA recognition is also mediated by the recently discovered PYHIN protein family with its most prominent members absent in melanoma 2 (AIM2) and interferon inducible protein (IFI16). This protein homooligomerizes upon activation and interacts with the apoptosis-associated speck like protein containing a CARD (ASC) to form multi-protein structures called inflammasomes (refer to figure 1.3).

PYHIN proteins consist of an N-terminal PYRIN domain and one or more C-terminal HIN200 domains. The C-terminal HIN200 domain is able to bind directly to dsDNA, thus, this family appears to be composed of intracellular nucleotide sensors. In human, the PYHIN family consists of 4 members and the first PYHIN protein discovered to form inflammasome structures was AIM2 (Burckstummer *et al.*, 2009; Fernandes-Alnemri *et al.*, 2009; Hornung *et al.*, 2009; Roberts *et al.*, 2009). Another PYHIN protein, IFI16, was discussed to be involved in type I IFN responses against dsDNA (Unterholzner *et al.*, 2010) and later inflammasome formation by IFI16 was observed. Interestingly, the IFI16 inflammasome is the only nuclear inflammasome reported so far (Kerur *et al.*, 2011).

1.4 Nucleotide-binding domain, leucine-rich repeat containing proteins (NLRs)

NLR proteins are the largest family of cytosolic PRRs in mammals, including 22 members in humans (Ting *et al.*, 2006). They have a common tripartite structure, which consists of an N-terminal effector domain, a central ATPase domain present in NAIP, CIITA, the fungal protein HET-E and the telomerase subunits TP-1 (NACHT domain) and a C-terminal leucine-rich re-

peat containing region (reviewed in Kufer and Sansonetti, 2011; Koonin and Aravind, 2000). NLR proteins belong to the STAND subclass of AAA ATPases, thus they are able to bind and hydrolyse ATP (reviewed in Kufer and Sansonetti, 2011; Danot *et al.*, 2009; Hanson and Whiteheart, 2005). The detailed function of ATP-binding and hydrolysis in NLR activation is not well understood, but structural data on the closely related human apoptotic protease-activating factor-1 (Apaf-1) suggests a model in which the N-terminal effector domain is buried by the C-terminal WD40 region in an ADP-dependent manner and thus is not accessible for downstream signalling in the inactive molecule (Riedl and Salvesen, 2007; Bao *et al.*, 2005). Upon binding of the Apaf-1 ligand cytochrome c and upon exchange of ADP for ATP, Apaf-1 forms an oligomeric complex termed apoptosome. This apoptosome mediates caspase-9 activation and triggers apoptotic cell death (Riedl *et al.*, 2005). Inactivation of Apaf-1 then is brought about by ATP hydrolysis resulting in the complex disassembly.

On the basis of their N-terminal effector domains, NLR proteins can be divided into three different groups. The two main groups, the Nodosome or NLRC NLRs and the Inflammasome or NLRP NLRs harbour an N-terminal CARD or PYRIN domain, respectively (reviewed in Kufer, 2008; Fritz *et al.*, 2006). The third group is characterized by an effector domain excluding CARD or PYRIN. The neuronal apoptosis-inhibitory protein (NAIP) for example harbours a baculovirus inhibitor of apoptosis domain (BIR) (Mercer *et al.*, 2000), whereas NLRX1 possesses a mitochondrial targeting sequence (Tattoli *et al.*, 2008).

However, some NLRs also harbour a less characterized N-terminal domain, as for example NLRC3 or NLRC5. A schematic overview of NLR proteins is depicted in figure 1.2.

Interestingly, NLR proteins are highly conserved and similar proteins can also be found in plants. Notably, plants lack an adaptive immune system, thus immune responses completely rely on innate immune detection mediated by membrane-bound PRRs and NLR proteins, called resistance proteins (R-proteins) as key players. These R-proteins have a similar structure, consisting of an N-terminal effector domain, which can either be a coiled-coil (CC) or Toll/interleukin-1 (TIR) domain, a central nucleotide binding domain (NB-ARC) and C-terminal leucine rich repeats (LRRs). Analogous to animal NLR proteins, they serve as immune receptors, although plant NLRs rather sense modified host proteins ('modified self' model) and pathogen-derived effector proteins to provoke effector triggered immunity (ETI) (reviewed in Maekawa *et al.*, 2012).

In the following paragraphs, the different groups of NLR proteins will be discussed in more detail.

NLR proteins
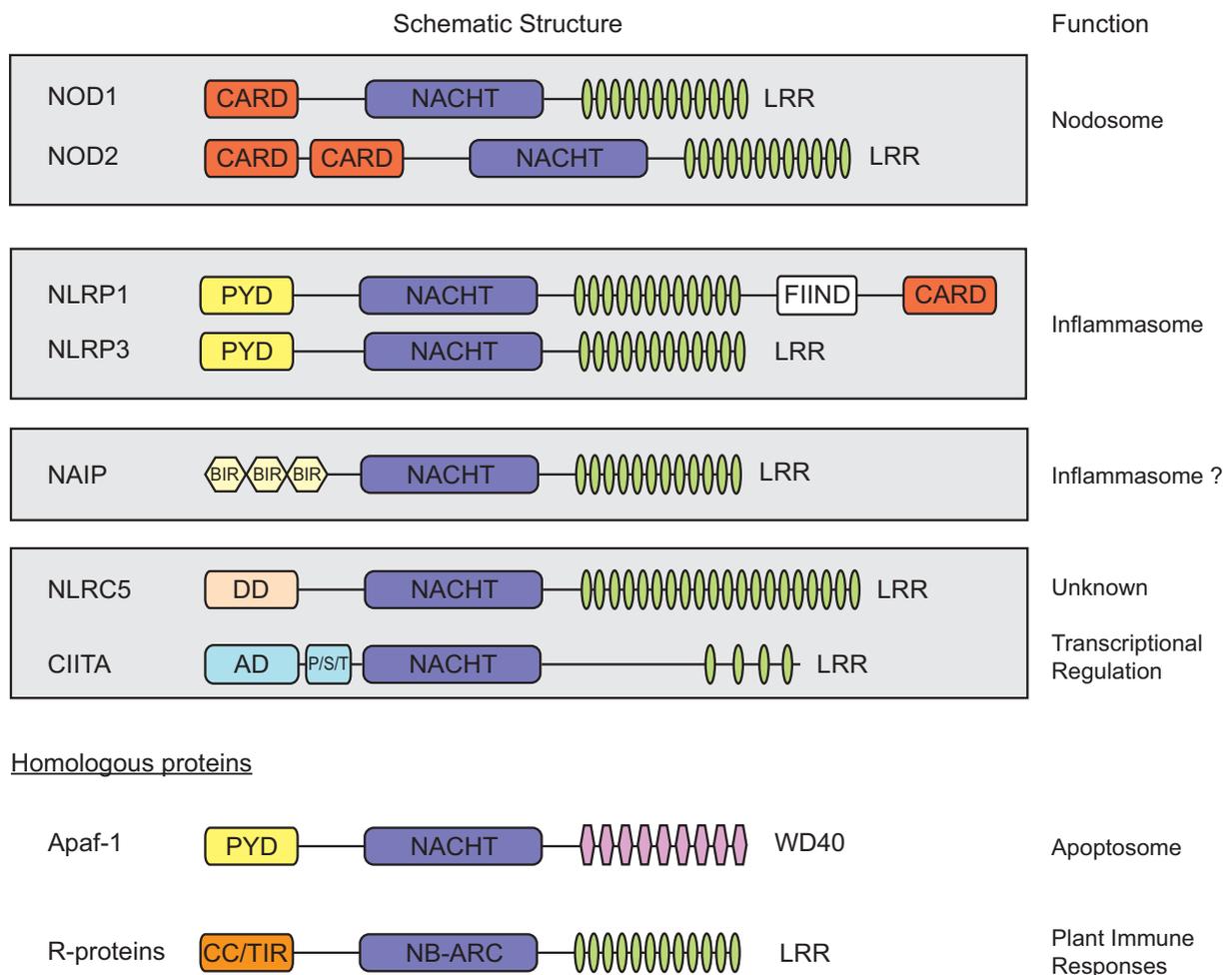
Figure 1.2 Structure of human NLR proteins
Schematic overview of the human NLR family and homologous proteins. NLR proteins are grouped by their different N-terminal signalling domains which determine their signalling abilities. NLR proteins are highly homologous to the apoptotic mediator Apaf-1. Furthermore, NLR proteins are not restricted to animals, but play a crucial role as resistance proteins (R-proteins) in plant immune responses (based on Kufer and Sansonetti, 2011; Fritz *et al.*, 2006).

1.4.1 The Nodosome NLRs

The Nodosome NLR family is characterized by the presence of an N-terminal caspase activation and recruitment domain (CARD). This domain was first identified in an alignment study from 1996 by Bucher and colleagues and was found in proteins involved in apoptotic signalling (Bucher *et al.*, 1996). Later, this domain was termed caspase recruitment domain (Hofmann *et al.*, 1997).

The so far most extensively studied members of the Nodosome NLR family are NOD1 and NOD2. Both protein possess the typical tripartite NLR structure, except that NOD2 harbours a prolonged N-terminus consisting of two CARD domains, in contrast NOD1 possesses only one CARD domain (Ogura *et al.*, 2001; Inohara *et al.*, 1999). The first functional characterizations of NOD1 and NOD2 were published by the Nuñez group in 1999 and 2001, respectively, showing that both proteins activate NF-κB by involvement of the receptor interacting protein kinase 2 (RIP2) (Ogura *et al.*, 2001; Inohara *et al.*, 2000; Inohara *et al.*, 1999). The elicitors for NOD1 and NOD2 were identified in 2003, when several groups reported distinct substructures of peptidoglycan (PGN) that are recognized by NOD1 and NOD2 (Chamaillard *et al.*, 2003; Girardin *et al.*, 2003b; Girardin *et al.*, 2003a; Inohara *et al.*, 2003). The minimal structure that is recognized by NOD1 was identified as γ-D-glutamyl-meso-diaminopimelic acid (ie-DAP), a structure which is found in PGN of Gram-negative bacteria (Chamaillard *et al.*, 2003; Girardin *et al.*, 2003b). The minimal structure that elicits NOD2 is muramyl dipeptide, present in PGN of both Gram-positive and Gram-negative bacteria (Girardin *et al.*, 2003a; Inohara *et al.*, 2003). The LRR region is pivotal for the recognition of PGN in both NOD1 and NOD2 (Girardin *et al.*, 2005; Tanabe *et al.*, 2004) and there is now evidence for a direct interaction between NOD1 and TriDAP (Laroui *et al.*, 2011) and NOD2 and MDP (Grimes *et al.*, 2012; Mo *et al.*, 2012). Upon recognition of PGN fragments, NOD1 and NOD2 are thought to undergo conformational changes resulting in an interaction with the receptor interacting protein kinase 2 (RIP2) (Ogura *et al.*, 2001; Inohara *et al.*, 2000). Subsequently, RIP2 gets ubiquitinated at lysine 63, which serves as a docking site for the TAK1/TAB2/TAB3 complex. Although the E3 ligase being responsible for this event remains somewhat unclear, it was initially proposed that TRAF2, TRAF5, TRAF6 and ITCH are responsible for this event (Tao *et al.*, 2009; Hasegawa *et al.*, 2008; Abbott *et al.*, 2007). Recently it became evident that cellular inhibitor of apoptosis 1 (cIAP1) and cellular inhibitor of apoptosis 2 (cIAP2) as well as the X-linked inhibitor of apoptosis (XIAP) play an essential role in RIP2 ubiquitination (Bertrand *et al.*, 2009; Krieg *et al.*, 2009) and a role for the linear ubiquitin assembly complex (LUBAC) in NOD2 signalling was reported (Damgaard *et al.*, 2012). Similar to TLR signalling, the TAB-TAK complex activates the IKK complex, consisting of IKK-α, IKK-β and IKK-γ (NEMO). Subsequently, IKK-α and IKK-β phosphorylate IκBα, leading to ubiquitination and degradation. As a result, the canonical NF-κB subunits p50 and p65 can translocate to the nucleus and bind to NF-κB-specific promoter sites (reviewed in Correa *et al.*, 2012).

NOD1 and NOD2 are not only directly controlled through binding of the elicitor, but further by factor acting downstream in the signalling cascades. Some examples are the de-ubiquitinating enzyme A20, which de-ubiquitinates RIP2 and inhibits NF-κB activation (Hase-

gawa *et al.*, 2008). AAMP that inhibit both NOD1- and NOD2-mediated NF-κB activation (Bielig *et al.*, 2009) and Erbin that exerts an inhibitory function specific for NOD2-mediated NF-κB signalling (Kufer *et al.*, 2006; McDonald *et al.*, 2005). To conclude, even though NOD1 and NOD2 were identified over 10 years ago, the details of their signalling pathways still remain unclear.

Interestingly, several mutations in the NOD1-encoding gene *CARD4* and the NOD2-encoding gene *CARD15* are linked to severe inflammatory disorders. Polymorphisms in *CARD4*, for example, are linked to asthma and increased levels of serum IgE and mutations in *CARD15* are associated with increased susceptibility to Crohn's Disease (CD), Blau syndrome (BS) and early-onset sarcoidosis (EOS). The increased susceptibility to CD is caused by several amino acid substitutions in or near the LRR of NOD2, results in a loss-of-function mutation, whereas BS and EOS are linked to constitutive NF-κB activation, triggered by gain-of-function NOD2 variants (reviewed in Franchi *et al.*, 2009).

1.4.2 The Inflammasome NLRs

The group of inflammasome NLRs, or NLRPs, is the largest sub-group of NLR proteins with similar PYRIN-domain containing structures. They functionally differ from the Nodosome NLRs since they are responsible for IL-1β and IL-18 processing, two cytokines that play crucial roles in immunity. Inflammasomes are high-molecular-weight structures, which assemble in the cytoplasm. They consist of NLRP proteins together with an adaptor protein called apoptosis-associated speck-like protein (ASC) and recruit pro-caspase-1. This in turn leads to activation of caspase-1 and subsequent cleavage of pro-IL-1β or pro-IL-18 into the biological active forms IL-1β and IL-18 (reviewed in Gross *et al.*, 2011). Although most NLRP proteins are still uncharacterized, inflammasome formation was reported for NLRP1, NLRP3, NLRP6 and NLRP12. Additionally, inflammasome assembly was also observed for NLRC4, a CARD-containing NLR protein, as well as for a recently discovered protein family, called PYHIN proteins (Rathinam *et al.*, 2012; Schattgen and Fitzgerald, 2011). As depicted in figure 1.3, inflammasome NLR proteins form different inflammasome complexes.

The best studied inflammasome is the NLRP3 inflammasome (Martinon *et al.*, 2002). Upon activation and oligomerization, NLRP3 recruits the adaptor protein ASC (Mariathasan *et al.*, 2004). ASC binds to NLRP3 through its PYRIN domain, providing an exposed CARD domain that is important for caspase-1 recruitment. Caspase-1 is expressed as a zymogen and oligomerization with the inflammasome activates a process known as autoproteolysis, leading to self-cleavage and caspase-1 activation (Cohen, 1997).

NLRP3 inflammasome signalling is tightly controlled on different levels of activation. For example, it has been shown that expression of pro-IL-1β is highly inducible by LPS (Bauernfeind *et al.*, 2009; Unlu *et al.*, 2007). Moreover, expression of NLRP3 itself is inducible by LPS in an NF-κB-dependent manner, a process that is necessary but not sufficient for NLRP3 inflammasome activation (Bauernfeind *et al.*, 2009). Finally, inflammasome formation also depends on an activating stimulus. For the best-studied member NLRP3 several stimuli have been reported to trigger inflammasome assembly. On the one hand, NLRP3 is activated by several pathogens (i.e. *Staphylococcus aureus, Listeria monocytogenes, Klebsiella pneumoniae, Candida albicans* and influenza A virus) (Rathinam *et al.*, 2012). On the other hand, host-derived cellular molecules referred to as danger molecules activate the inflammasome. An important role in this process plays extracellular ATP, hyaluronan, amyloid-β fibrils as well as uric acid crystals (Gasse *et al.*, 2009; Yamasaki *et al.*, 2009; Halle *et al.*, 2008; Mariathasan *et al.*, 2006).

Due to this broad diversity of elicitors a direct binding of the elicitors to the inflammasome seems unlikely. Rather, three models were proposed, in which the stimuli mentioned above trigger either potassium (K^+) efflux, ROS production or phagolysosomal destabilization, all of them resulting in NLRP3 inflammasome formation (reviewed in Rathinam *et al.*, 2012; Jin and Flavell, 2010).

Interestingly, the CARD-containing NLRC4 protein is also able to form inflammasomes, but in contrast to NLRP3, the NLRC4 inflammasome is independent of ASC, since caspase-1 is able to directly bind to the N-terminal CARD domain of NLRC4. It was reported, that the NLRC4 inflammasome assembles upon bacterial stimuli. Several groups analysed assembly upon stimulation with flagellin derived from many different bacteria but NLRC4 inflammasomes also assemble after detection of a critical type III secretion system (T3SS) protein, which is shared by many different bacteria (Gong and Shao, 2012; Miao *et al.*, 2010). The detailed mechanism of NLRC4 activation was long time veiled with no evidence for direct binding of flagellin to NLRC4. In 2011, two groups reported a necessity of NAIP2 and NAIP5 in recognition of bacterial T3SS protein and flagellin, respectively. Furthermore, direct binding between NLRC4 and NAIP2 or NAIP5 was observed, which in turn bind bacterial derived products, demonstrating that a receptor-ligand-model mediated by additional proteins could be conceivable for activation of other inflammasomes as well (Kofoed and Vance, 2011; Zhao *et al.*, 2011) (refer to figure 1.3).

NLRP6 and NLRP12 were one of the first proteins to be referred to function as inflammasomes after transfection and overexpression (Grenier *et al.*, 2002; Wang *et al.*, 2002). To date, there has been no activator for NLRP6 identified yet, but recent work demonstrated the involvement of NLRP6 in intestinal homeostasis including its function as a negative regulator of inflammatory signalling (Anand *et al.*, 2012; Chen *et al.*, 2011; Elinav *et al.*, 2011; Normand *et al.*,

2011). NLRP12 was reported to function as an antagonist of proinflammatory signals, induced by TLR, but its involvement in migration of dendritic cells and myeloid cells was also reported. Nevertheless, it seems to be dispensable for caspase-1 activation upon different stimuli (reviewed in Rathinam *et al.*, 2012).

NLRP1 is unique among NLR proteins, since the NLRP1 inflammasome can bypass the necessity of the adaptor protein ASC because of a C-terminal CARD domain in the NLRP1 protein. Nevertheless, ASC is able to enhance NLRP1 inflammasome activity (Rathinam *et al.*, 2012). Interestingly, NLRP1 harbours an additional domain between LRR and CARD, called function-to-find (FIIND) (refer to figure 1.2). Even though its function remains to be elucidated, autoproteolytical cleavage can be observed, resulting in a CARD-lacking NLRP3-like NLRP1 protein (D'Osualdo *et al.*, 2011). The only known activator of human NLRP1 so far is the bacterial peptidoglycan component muramyl dipeptide (MDP), inducing inflammasome formation in a NOD2-dependent manner in the presence of ATP (Faustin *et al.*, 2007; Hsu *et al.*, 2008). Confusingly, murine NLRP1 lacks the N-terminal PYRIN domain (D'Osualdo and Reed, 2012).

Finally, PYHIN family members also assemble to inflammasomes by recruitment of the adaptor proteins ASC, similar to NLRP3 (refer to section 1.3) (reviewed in Schattgen and Fitzgerald, 2011).
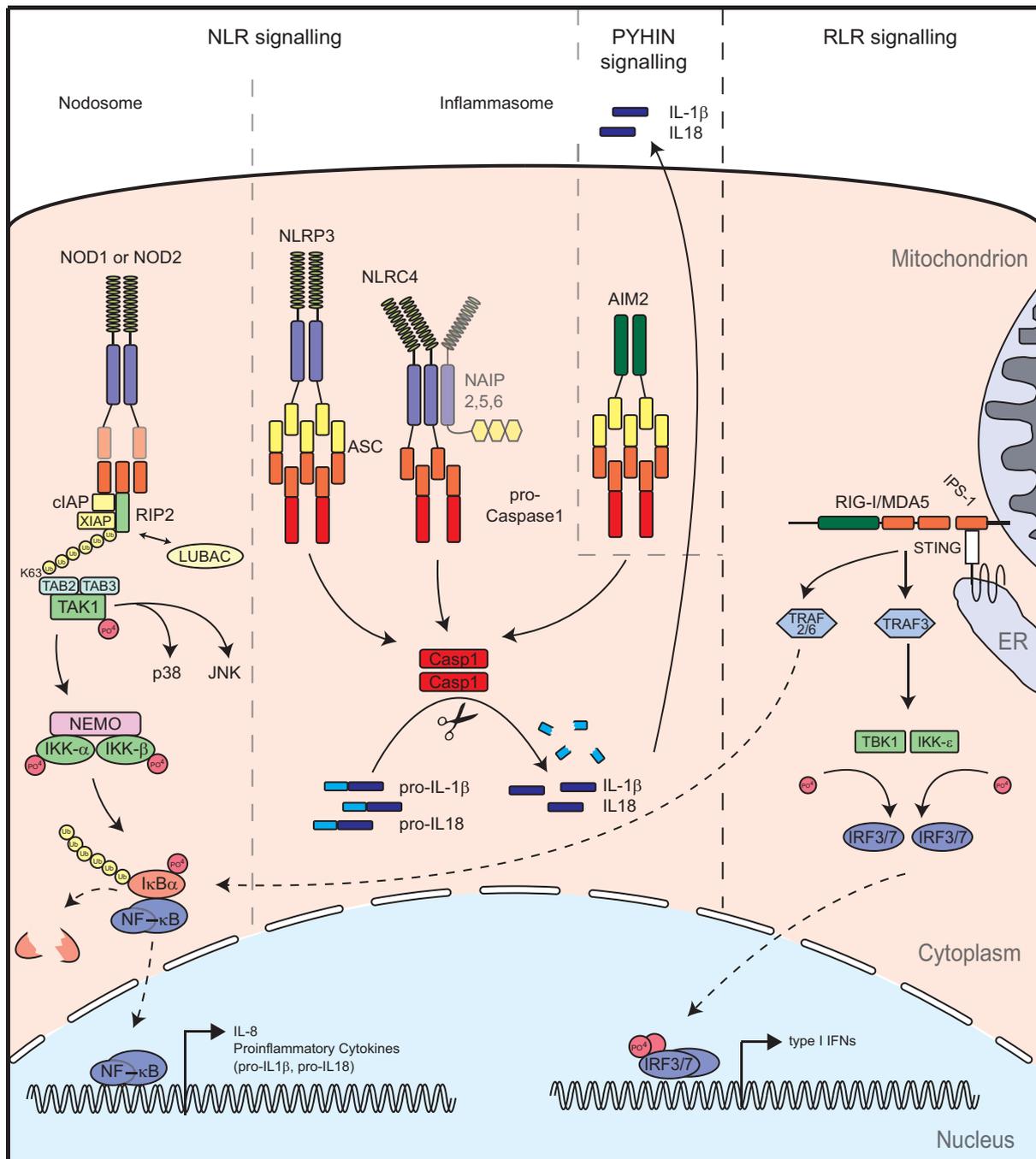
Figure 1.3 Cytoplasmic PRR signalling

Signalling of the intracellular NLR proteins, PYHIN proteins and RLRs proteins.

Upon activation of NOD1 or NOD2 by bacterial PGN fragments, they trigger the canonical NF-κB pathway through the RIP2 kinase (left part). Inflammasome activation results in caspase-1 activation and IL-1β and IL-18 processing. A similar pathway is utilized by the PYHIN domain protein AIM2 (middle part). On the right hand side RLR signalling is outlined, which mainly results in type I IFN activation and TRAF2/6-dependent NF-κB activation (based on Correa *et al.*, 2012; Gong and Shao, 2012; Rathinam *et al.*, 2012; Kato *et al.*, 2011; Schattgen and Fitzgerald, 2011).

## 1.4.3 The MHC class II transcriptional activator CIITA: a function apart from pattern recognition

As previously introduced, most NLR proteins are involved in either NF-κB signalling or IL-1β/IL-18 processing. Nonetheless, other functions beyond pathogen recognition have been reported for several NLRs (reviewed in Kufer and Sansonetti, 2011). The best characterized NLR protein with a PRR-unrelated function is the MHC class II transcriptional activator (CIITA). It shares the typical NLR tripartite structure, including NACHT domain and LRR domain, but harbours an N-terminal transcription activation domain (AD) followed by a proline/serine/threonine-rich region (P/S/T) (reviewed in Krawczyk and Reith, 2006).

CIITA was originally discovered by an expression cloning approach using MHC class II deficient R2.25 cells, derived from the Burkitt Lymphoma B cell line Raji (Steimle *et al.*, 1993; Hume and Lee, 1989; Long *et al.*, 1984; Accolla, 1983). Steimle and colleagues identified a cDNA that completely restored MHC class II expression, termed MHC class II transcriptional activator (CIITA) (Steimle *et al.*, 1993). Polymorphisms in CIITA are associated with a severe immunodeficiency in patients, characterized by the lack of MHC class II expression, hence called bare lymphocyte syndrome (BLS) (Steimle *et al.*, 1993). Interestingly, the genes encoding the MHC class II molecules are intact in these patients, thus mutations were supposed to involve genes having a regulatory function for MHC molecule transcription (Krawczyk and Reith, 2006; Reith and Mach, 2001).

MHC molecules are pivotal for antigen presentation in antigen-presenting cells (APCs), like macrophages and dendritic cells (DCs) (Vyas *et al.*, 2008). They are responsible for the transport and cell-surface-presentation of small peptides to T cell receptors (TCRs) (reviewed in van der Merwe and Dushek, 2010). Depending on the source, antigen presentation is performed by two different pathways. Cytosolic antigens deriving from intracellular bacteria or viruses as well as cellular proteins are presented at the cell surface via the MHC class I pathway, whereas exogenous antigens present in the endocytic compartment are presented on the cell surface via the MHC class II pathways. Although the principle of antigen presentation is similar in class I and class II, the pathways differ from each other in some major aspects. A brief overview is depicted in figure 1.4.

Antigens presented by MHC class II molecules are mainly of exogenous origin. They are taken up by phagocytosis and undergo endosomal degradation. MHC class II molecules are assembled in the ER and are composed of an α–chain and a β-chain, which are further stabilized by an invariant chain (Ii). Subsequently, the complex of MHC class II molecule and Ii is transported to a late endosomal compartment, termed MHC class II compartment (MIIC) (refer to figure 1.4; right part). This compartment is further provided with extracellular antigens by en-

dosomal fusion. Here, li is digested and only a small peptide termed class II-associated li peptide (CLIP) remains in the antigen-binding groove. Afterwards a helper molecule, HLA-DM, mediates the exchange of CLIP with an antigen, and as a consequence, the loaded MHC class II molecules are transported to the cell surface, where foreign antigens activate CD4$^+$ T cells (reviewed in Neefjes *et al.*, 2011). A brief summary of MHC class II loading is depicted in the right part of figure 1.4.
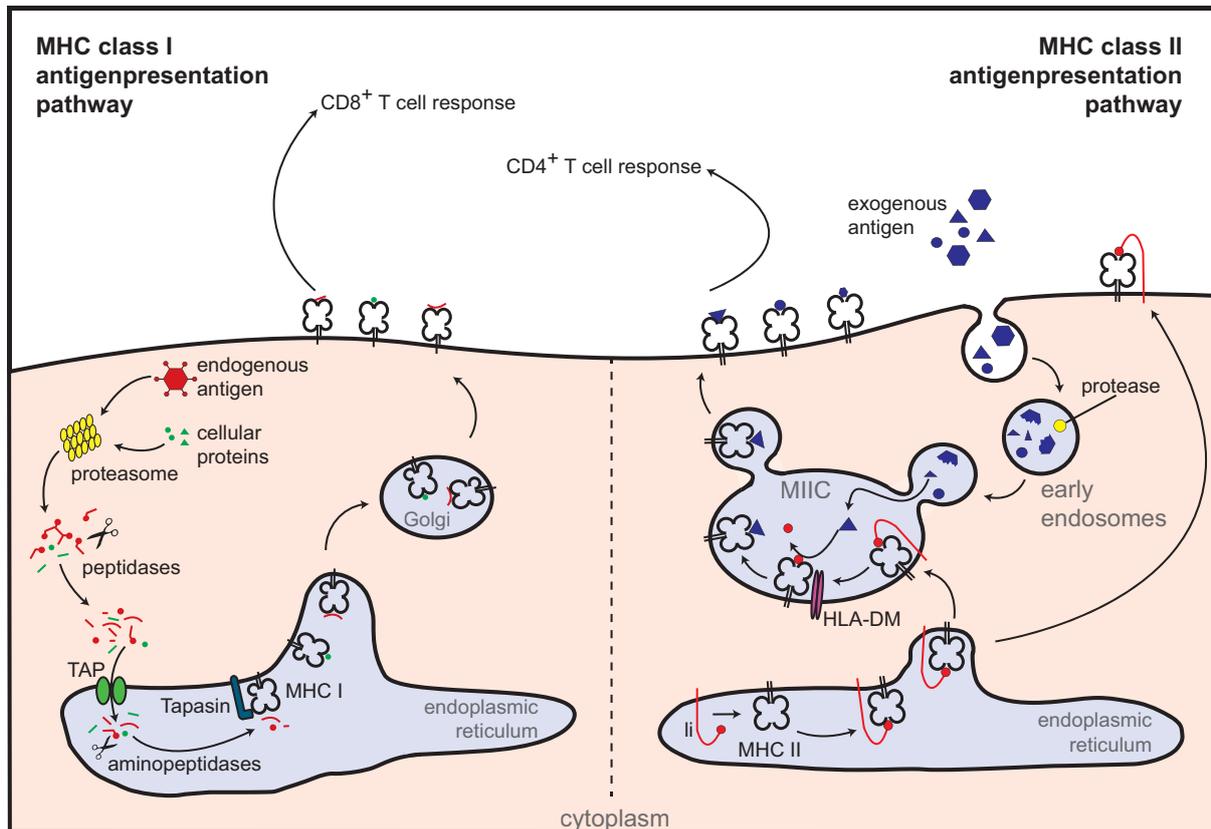
Figure 1.4 Antigen presentation by APCs
Endogenous antigens, either derived from endogenous pathogens or cellular proteins, are presented on the cell surface via MHC class I molecules. Loaded MHC class I molecules are recognized by CD8$^+$ T cells. Exogenous antigens are endocytosed and cleaved by proteases in the early endosomes. Mature MHC class II molecules are transported to a special compartment, termed MHC II compartment (MIIC), where loading of MHC class II molecules with the peptides takes place. Loaded MHC class II molecules are recognized by T cell receptors (TCR) on CD4$^+$ T cells (based on Neefjes *et al.*, 2011; Vyas *et al.*, 2008).

MHC class I molecules are key players in adaptive immune responses toward cytoplasmic pathogens, like certain bacteria and viruses. Antigens presented by MHC class I molecules are typically cytosolic and are generated by proteasomal degradation of proteins. Nontheless, DCs are uniquely able to take up exogenous peptides and present these via the MHC class I pathway, a process that is called cross-presentation. How this is mediated in detail remains to be elucidated,

currently both passive and active transport of peptides from phagosomes into the cytoplasm are discussed (Vyas *et al.*, 2008). Of note, many virus-infected cells, but notably also transformed cells show reduced or impaired MHC class I molecule expression, resulting in escaping of immuno-surveillance, although the underlying mechanism is still poorly understood (Reinis, 2011). However, complete absence of MHC class I antigen presentation typically results in natural killer (NK) cell-mediated lysis, known as "missing-self" hypothesis (Kumar and McNerney, 2005).

For that reason, antigen presentation of host-derived peptides by MHC class I molecules is of great importance to protect the cell from natural killer (NK) cell-mediated lysis. This protection is mediated by immediate degradation of newly synthesized proteins with subsequent loading of the peptides onto MHC class I moelcules (Reits *et al.*, 2000; Schubert *et al.*, 2000). Degradation is mediated by the 26S proteasome, which can either be supported by additional proteasomes called immunoproteasomes, or different subunits of the 20S proteasome subunit can be displaced by other immune specific subunits (Sijts and Kloetzel, 2011). Subsequently, the peptide fragments are transported into the endoplasmic reticulum (ER) by the peptide transporter TAP, where the MHC class I molecules are present as membrane-bound proteins stabilized by a subset of chaperones (figure 1.4; left part). In brief, the classical MHC class I molecules consist of heavy chains (encoded by the genes HLA-A, HLA-B and HLA-C) and one β_2-microglobulin chain. Peptide fragments are further cleaved to the appropriate loading size by aminopeptidases. The loading of peptides is mediated by the peptide-loading complex (PLC), including TAP, Tapasin (a chaperone) and the MHC class I molecule. Subsequently, the antigen-loaded molecules are transported to the cell surface via the Golgi-network, where antigen-bound MHC I molecules are detected by specific T-cell receptors on CD8$^+$ T cells (reviewed in Neefjes *et al.*, 2011). A brief summary is depicted in figure 1.4.

In order to preserve an uncontrolled immune reaction caused by APCs, such a powerful system has to be tightly regulated. This regulation is maintained on the one hand by the furnishing of antigens (for example proteasome modifications), but on the other hand, the MHC molecule expression itself is tightly regulated. In general, expression of MHC molecules is induced by IFN-γ, but the principle is slightly different between MHC class I and MHC class II. MHC class I gene promoters posses an interferon stimulatory response element (ISRE), which is occupied by IRF1 and triggers MHC class I expression upon IFN-γ stimulation (refer to figure 1.6) (Gobin *et al.*, 1999). Although the ISRE element is lacking in MHC class II gene promoters, these genes are also highly inducible upon IFN-γ stimulation, similar to MHC class I molecules. Responsible for the IFN-γ–dependent induction of MHC class II genes is CIITA, which itself is highly inducible by IFN-γ (Muhlethaler-Mottet *et al.*, 1997; Steimle *et al.*, 1994). Beside the involvement of CIITA in MHC class II gene expression, another protein was discovered in 1995, termed regulatory fac-

tor x 5 (RFX-5) (Steimle and Mach, 1995). In the following years, two additional proteins of the regulatory factor x family were described being indispensable for MHC expression, termed RFX-AP and RFX-ANK (or RFX-B) (Nagarajan *et al.*, 1999; Masternak *et al.*, 1998; Durand *et al.*, 1997). These proteins, termed RFX proteins, assemble to a trimeric RFX complex, called enhanceosome, which interacts with the MHC class II promoter. The MHC class II promoter consists of an S, X1, X2, Y motif (refer to figure 1.5) and the enhanceosome complex was reported to bind specifically to the X2-box inside of this motif (Steimle *et al.*, 1995). Together with additional DNA-binding factors called X2-binding protein (X2BP; a complex of cyclic-AMP-responsive-element-binding protein (CREB) and activating transcription factor (ATF)) (Moreno *et al.*, 1999; Moreno *et al.*, 1995) and nuclear factor binding to the Y box (NF-Y), as well as with an intact S-box sequence (Muhlethaler-Mottet *et al.*, 2004), they assemble a platform to recruit CIITA. CIITA as a non-DNA-binding co-activator is now able to recruit the general transcription machinery and elongation factors, as well as histone-modifying enzymes to activate MHC class II transcription (reviewed in Wright and Ting, 2006; Reith *et al.*, 2005). A schematic overview is depicted in figure 1.5.

For the function of CIITA, nuclear localization that relies on a functional NACHT domain is a prerequisite. In contrast to other NLR proteins, CIITA has a significant homology to GTP-binding proteins of the Ras-superfamily and CIITA was shown to bind GTP, rather than ATP (Chin *et al.*, 1997). Mutants lacking GTP-binding and hydrolysis activity loose their ability to shuttle to the nucleus (Harton *et al.*, 1999). Moreover, the LRR region and the N-terminal domain contribute to nuclear localization. An in-depth-analysis of the LRR region was performed by the group of Viktor Steimle, which identified several amino acids in the LRR region, pivotal for nuclear import and MHC class II transactivator activity (Camacho-Carvajal *et al.*, 2004; Hake *et al.*, 2000). Interestingly, a mutant that lacks the N-terminal AD and P/S/T domain (CIITA-L335) is not able to shuttle to the nucleus. When forced to the nucleus (NLS-L335), this mutant is able to dominant-negatively inhibit MHC class II expression, probably by a more efficient binding to the MHC class II promoter, than wildtype CIITA (Camacho-Carvajal *et al.*, 2004; Masternak *et al.*, 2000b; Bontron *et al.*, 1997). Thus, the N-terminal domain, the GTPase domain and the LRR domain do all contribute to nuclear localization (reviewed in Krawczyk and Reith, 2006).

As previously mentioned, additional components called enhanceosome are necessary for CIITA-dependent MHC class II expression. The enhanceosome components are expressed ubiquitously, thus regulation of MHC class II expression is dependent on a specific regulation of CIITA expression itself. In contrast to NLR proteins that act as PRRs, CIITA is not kept in an inactive state; instead CIITA apparently acquires full activity without an extra stimulus. In human, CIITA transcription is tightly regulated by four different promoters, pI to pIV, whereas only pI,

pIII and pIV are conserved in mice (Muhlethaler-Mottet *et al.*, 1997). Each promoter was shown to possess unique transcription initiation sites, resulting in four different CIITA isoforms that differ only in their N-terminal regions. The originally described CIITA (Steimle *et al.*, 1993) is transcribed from pIII. This promoter is mainly used in B cells, activated T cells and plasmacytoid dendritic cells (pDCs) (Krawczyk and Reith, 2006; Muhlethaler-Mottet *et al.*, 1997). In contrast to pIII, pI was found to be active only in DCs and, interestingly, it results in a transcript with a 5' 303 bp extension that encodes a CARD-domain (CIITA-FI) (refer to figure 1.5; upper part). Nevertheless, this CARD domain is neither involved in cell death regulation, nor in NF-κB activation. Rather, CIITA-FI is more potent to induce MHC class II expression *in vitro*, than CIITA-FIII (Nickerson *et al.*, 2001). In 2012, Zinzow-Kramer and colleagues created CIITA-pI-deficient mice, but could not link any essential function which is restricted to CIITA-FI, thus the function of the N-terminal CARD domain remains elusive (Zinzow-Kramer *et al.*, 2012).
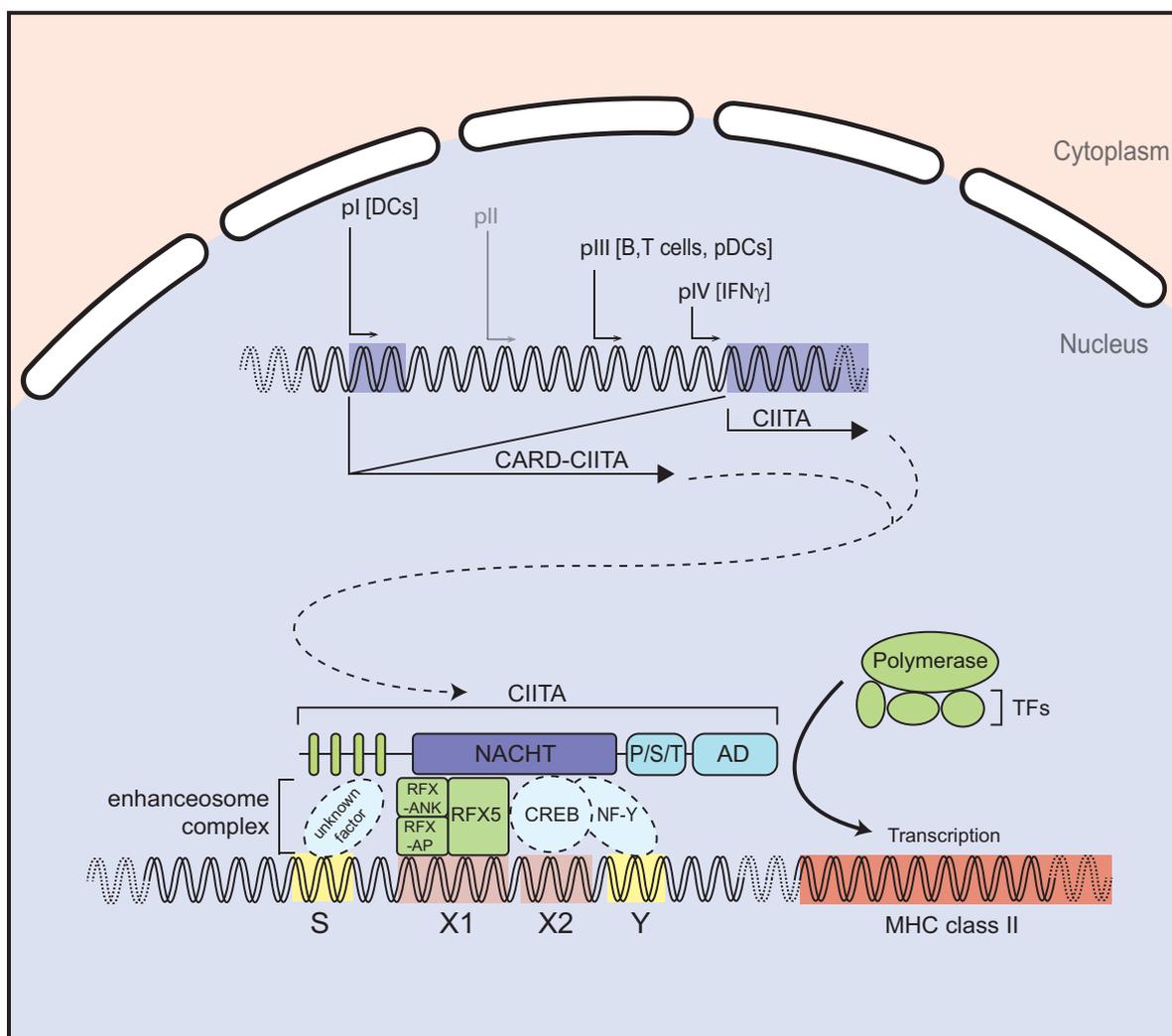
Figure 1.5 Structural overview of the MHC class II promoter elements
MHC class II molecule expression is tightly regulated by the MHC class II transcriptional activator CIITA. CIITA functions as a non-DNA-binding co-activator that is recruited to a DNA-binding complex called enhanceosome. CIITA itself is transcribed from four different promoters. It is only ubiquitously expressed in APCs (from pI or pIII). In most other cell types, CIITA expression is inducible upon IFN-γ

stimulation (pIV) in a broad variety of cells (based on Krawczyk and Reith, 2006; Ting and Trowsdale, 2002).

MHC class II expression is further highly inducible by the cytokine IL-4 in B cells (Boothby *et al.*, 1988) and by IFN-γ in the majority of non-APCs (reviewed in Reith and Mach, 2001). Responsible for the tremendous upregulation of MHC class II by IFN-γ is the induction of CIITA-FIV, which is highly inducible by IFN-γ (Muhlethaler-Mottet *et al.*, 1998; Muhlethaler-Mottet *et al.*, 1997). Nonetheless, it has been shown that CIITA-FI is also partly induced after IFN-γ stimulation (Pai *et al.*, 2002). Upregulation is mediated by the classical IFN-γ pathways, which requires IRF1 and STAT1 (Muhlethaler-Mottet *et al.*, 1998). CIITA-FIV is mainly identical to FIII except for a small 3 kDa N-terminal truncation. A schematic overview of MHC class II promoter activation by CIITA and additional factors is depicted in figure 1.5.

In contrast to MHC class II, MHC class I molecules are expressed in almost all nucleated cells, although differences in expression strength are detectable among different tissues (van den Elsen *et al.*, 2004). Noteworthy to mention here, that MHC class I self-antigen-presentation protects cells from 'missing-self'-mediated lysis by NK cells (Karre, 2002). Transcription of MHC class I genes, such as the three classical human MHC class I genes HLA-A, HLA-B and HLA-C and the β_2-microglobulin-gene, are under the control of different promoter elements and vary among tissues and cell types (Johnson, 2003). Different enhancer elements are responsible for basal transcription or inducible transcription of MHC class I genes. The basal transcription is dependent on the general transcription factor TAF1 ($TAF_{II}250$), whereas the inducible transcription pathway is TAF1-independent (Howcroft *et al.*, 2003). This transcription pathway can be initiated from different promoter sites, depicted in figure 1.6.

These sites include (1) enhancer A element, (2) interferon-regulatory-response element (ISRE), and (3) S, X1, X2, Y-motif. Both enhancer A and ISRE element were analysed in detail by two studies from Gobin and co-workers showing that NF-κB is able to strongly induce HLA-A and moderately induce HLA-B, but not other classical MHC class I loci (Gobin *et al.*, 1998a), whereas ISRE mediates interferon-driven induction of classical HLA-A, HLA-B and HLA-C molecules, rather than non-classical HLA-E, F and G (Gobin *et al.*, 1999). This explains the induction of MHC class I expression by TNF-α (mediated by binding of NF-κB to enhancer A) and IFN-γ (mediated by binding of IRF1 to ISRE). Notably, the S, X1, X2, Y motif is present in both MHC class I and MHC class II promoter regions, showing close sequence homologies (van den Elsen *et al.*, 2004). In MHC class II expression, this motif was connected to CIITA-enhanceosome-dependent activation, as described earlier in this paragraph and two early studies from Martin and

colleagues, as well as from Gobin and colleagues identified CIITA as an inducer of MHC class I promoter, strongly depending on the X1, X2, Y-box (Gobin *et al.*, 1998b; Gobin *et al.*, 1997; Martin *et al.*, 1997). Moreover, the RFX-complex subunits (enhanceosome) were discussed for being essential for CIITA-dependent MHC class I activation. Additional factors involved in complete MHC class II expression such as X2BP and NF-Y were further analysed in the context of MHC class I activation. Their data suggest that a complex consisting of the enhanceosome, X2BP and NF-Y is only assembled on the X1, X2, Y motif. As a result, a similar complex as assembling at the MHC class II promoter is also assembled at the MHC class I promoter (Gobin *et al.*, 2001). A schematic overview of the components so far identified to be involved in MHC class I activation is depicted in figure 1.6.
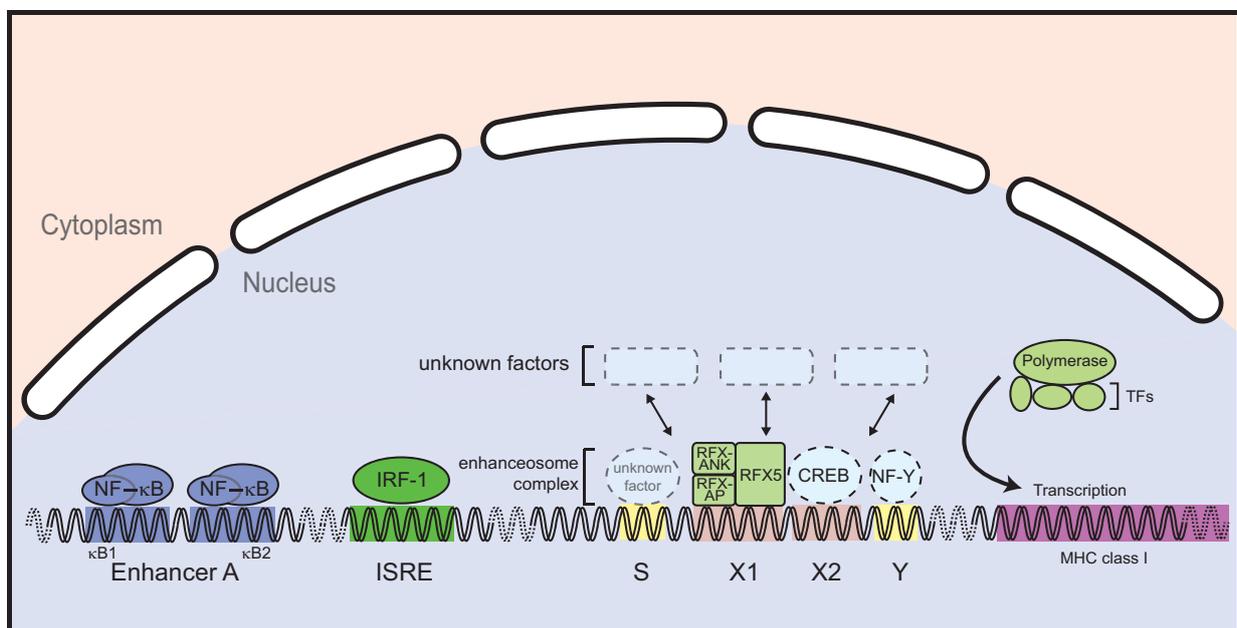
Figure 1.6 Structural overview of the classical MHC class I promoter region
MHC class I is ubiquitously expressed among a broad variety of nucleated cell types (driven by an upstream promoter element), but is also highly inducible by NF-κB (enhancer A) or IRF-1 (ISRE) pathway activation. Additionally, the enhanceosome complex mediates MHC class I induction by a yet poorly described mechanism (based on Krawczyk and Reith, 2006; van den Elsen *et al.*, 2004).

The involvement of CIITA in MHC class I and II expression was further examined in CIITA knock-out mice (Itoh-Lindstrom *et al.*, 1999). Although several groups reported an involvement of CIITA in MHC class I expression *in vitro*, this could not be validated *in vivo*. Rather, CIITA-deficient mice did not show any difference in MHC class I surface expression in B cells (Itoh-Lindstrom *et al.*, 1999). Taking this into consideration, together with the fact that MHC class I and II pathways present peptides from distinct sources, differential mechanisms to control ex-

pression seems plausible. Nevertheless, similarities between MHC class I and II are obvious. Thus, overlapping regulatory factors together with additional and unique regulatory proteins could perceive the difference between MHC class I and II expression.

1.5 Aim of the study

In the last decade, many NLR proteins have been characterized as receptors for pathogen associated molecular patterns (PAMPs) or host-derived danger associated molecular pattern (DAMPs) in host immune responses. However, additional biological activities of NLR proteins have been reported (reviewed in Kufer and Sansonetti, 2011). The best studied NLR protein with a non-PRR function is the MHC class II transcriptional activator CIITA, which was reported to tightly control the transcription of classical MHC class II genes and its involvement in MHC class I transcription was also implicated *in vitro* (reviewed in Krawczyk and Reith, 2006).

The aim of this thesis was to unravel the biological function of the previously uncharacterized NLR protein NLRC5. To this end, a thorough functional characterization of NLRC5 was conducted to elucidate the contribution of NLRC5 to cell-autonomous immune responses and MHC expression in human cells.

In the first part of this thesis, we analysed the expression of NLRC5 in different human tissues and cells, including expression analyses of NLRC5 upon a variety of different immunity activating stimuli. We furthermore characterized the function of NLRC5 in different innate immune pathways.

In the second part, we investigated the contribution of NLRC5 to MHC transcriptional regulation and analysed the underlying mechanism in more detail. Moreover, we investigated the involvement of the different domains of NLRC5 in signalling activity, drawing connections to the well-studied model-NLR CIITA.

2 Material and Methods

2.1 Material

2.1.1 Chemicals and enzymes

All chemicals were purchased from Roth, Merck or Sigma-Aldrich, unless otherwise noted.

All enzymes were purchased from Fermentas / Thermo Scientific.

2.1.2 Kits

All kits were purchased from Macherey-Nagel, unless otherwise noted.

The human cDNA panels were purchased from Clontech, hereafter Human MTC Panel I (Cat. #636742), Human MTC Panel II (Cat. #636743), Human Immune System MTC Panel (Cat. #636748) and Human Blood Fractions (Cat. #636750).

2.1.3 Cell lines and Bacteria

B16F10

B16F10 is a murine melanoma cell line, derived from murine BL6 melanoma cells. They were reported to be almost deficient in MHC class I and II surface molecule expression, but MHC surface expression can be induced upon different stimuli (Li *et al.*, 1996; Gorelik *et al.*, 1991; Gorelik *et al.*, 1985).

HEK293T cells

Human embryonic kidney 293 (HEK293) cells are derived from embryonic human kidney and due to their easy handling, are widely used in cell biology. The HEK293T cell line is a highly transfectable derivative of the HEK293 cell line, which stably expresses the SV40 large T-antigen. HEK293T cells were purchased from ATCC (#CRL 11268).

HEK-Blue™ IFN-α/β

HEK-Blue™ IFN-α/β cells (Invivogen; Cat. #hkb-ifnab) are derived from human embryonic kidney 293 (HEK293) cells by stable transfection with the human STAT2 and IRF9 genes to obtain a fully active type I IFN signalling pathway. Furthermore, they are stably transfected with a secreted embryonic alkaline phosphatise (SEAP) reporter under the control of the IFN-α/β

inducible ISG54 promoter. Stimulation of HEK-Blue™ IFN-α/β cells with human type I IFN leads to production and subsequent secretion of SEAP, which can be detected and quantified by QUANTI-Blue™ medium (Invivogen).

HeLa cells

HeLa cells are adherent human epithelial cells transformed by human papillomavirus 18 (HPV18), derived from a fatal cervical carcinoma. HeLa cells were purchased from ATCC (#CCL 2).

Primary human dermal fibroblasts

Primary human dermal fibroblasts were obtained by outgrowth from skin explants as previously described (Zigrino *et al.*, 2001).

THP-1 cells

THP-1 is a human acute monocyte leukemia cell line, derived from peripheral blood of a one year old human male with acute monocytic leukemia. THP-1 cells are non-adherent and grow in suspension, but can be differentiated into adherent macrophage-like cells using phorbol esters, such as phorbol 12-myristate 13-acetate (PMA). THP-1 cells were purchased from ATCC (#TIB 202, www.atcc.org/).

Escherichia coli XL1 Blue

The *E.coli* XL1 Blue is a non-pathogenic laboratory strain of the *E.coli* bacteria, which allows blue-white colour screening for recombinant plasmids and is an excellent host strain for routine cloning applications using plasmid or lambda vectors.

Genotype: endA1 gyrA96(nalR) thi-1 recA1 relA1 lac glnV44 F'[::Tn10 proAB+ lacIq Δ(lacZ)M15] hsdR17(rK- mK+)

Escherichia coli DH5α

The *E.coli* DH5α is a non-pathogenic laboratory strain of *E.coli* bacteria, commonly used for routine cloning applications.

Genotype: F-, *lac*1-, *rec*A1, *end*A1, *hsd*R17, Δ(*lac*ZYA-*arg*F), U169, F80d*lac*ZΔM15, *sup*E44, *thi*-1, *gyr*A96, *rel*A1

2.1.4 Plasmids

NLRC5 constructs

All FLAG-epitope tagged NLRC5 constructs were cloned using PCR cloning strategy with the indicated primer pairs. Myc-tagged NLRC5 constructs were cloned from the FLAG-tagged pCMV-Tag2B into myc-tagged pcDNA3.1-3xmyc-B.

All amino acid numbers refer to the full length NLRC5 isoform 1 sequence (gene bank reference number 156633662).

Name	Vector	Insert	Tag	Primer №	Reference
FLAG-NLRC5	pCMV-Tag2B	NLRC5 AA 1-1866	FLAG	85, 86	(Neerincx *et al.*, 2010)
FLAG-NLRC5 K234A	pCMV-Tag2B	NLRC5 AA 1-1866 K234A (Walker A mutant)	FLAG	182, 183	this study
FLAG-NLRC5 Iso3	pCMV-Tag2B	NLRC5 AA 1-720	FLAG	85, 173	(Neerincx *et al.*, 2010)
FLAG-NLRC5 DD	pCMV-Tag2B	NLRC5 AA 1-133	FLAG	172, 86	this study
FLAG-NLRC5 ΔDD NLS	pCMV-Tag2B	NLRC5 AA 110-1866	FLAG	334, 335	this study
FLAG-NLRC5 LRR	pCMV-Tag2B	NLRC5 AA 589-1866	FLAG	336, 86	this study
FLAG-2xNLS-NLRC5	pCMV-Tag2B	2xNLS-NLRC5 AA 1-1866	FLAG	337, 86	this study
MYC-NLRC5	pcDNA3.1-3xmyc-B	NLRC5 AA 1-1866	MYC	/	this study
MYC-NLRC5 K234A	pcDNA3.1-3xmyc-B	NLRC5 AA 1-1866 K234A (Walker A mutant)	MYC	/	this study
MYC-NLRC5 Iso3	pcDNA3.1-3xmyc-B	NLRC5 AA 1-720	MYC	/	this study

MYC-NLRC5 DD	pcDNA3.1-3xmyc-B	NLRC5 AA 1-133	MYC	/	this study
MYC-NLRC5 ΔDD NLS	pcDNA3.1-3xmyc-B	NLRC5 AA 110-1866	MYC	/	this study
MYC-NLRC5 LRR	pcDNA3.1-3xmyc-B	NLRC5 AA 589-1866	MYC	/	this study
MYC-2xNLS-NLRC5	pcDNA3.1-3xmyc-B	2xNLS-NLRC5 AA 1-1866	MYC	/	this study

CIITA constructs

CIITA expression plasmids in the EBV-based expression vector EBSB were previously described (Camacho-Carvajal *et al.*, 2004; Hake *et al.*, 2000; Steimle *et al.*, 1993).

Name	Vector	Insert	Tag	Reference
CIITA-FI	EBSB-PL	CIITA isoform I	No tag	(Camacho-Carvajal *et al.*, 2004; Hake *et al.*, 2000; Steimle *et al.*, 1993)
CIITA-FIII	EBSB-PL	CIITA isoform III	No tag	(Camacho-Carvajal *et al.*, 2004; Hake *et al.*, 2000; Steimle *et al.*, 1993)
FLAG-CIITA	pCMV-Tag2B	CIITA isoform III	FLAG	this study
GFP-CIITA	EBSB-PL	CIITA isoform III	EGFP	(Camacho-Carvajal *et al.*, 2004; Hake *et al.*, 2000; Steimle *et al.*, 1993)

Chimera constructs

All Chimera constructs were cloned into the pCMV-Tag2B backbone by PCR amplificiation of FLAG-NLRC5 or CIITA-FIII using the indicated primer pairs. The 2xNLS constructs were amplified from the FLAG-tagged chimera constructs using the indicated primer pairs.

Name	Vector	Insert	Tag	Primer №	Reference
FLAG-AD163-ΔDD-NLRC5	pCMV-Tag2B	CIITA AA 1-163 fused to NLRC5 AA 110-1866	FLAG	409-411, 86	this study
FLAG-AD335-ΔDD-NLRC5	pCMV-Tag2B	CIITA AA 1-335 fused to NLRC5 AA 110-1866	FLAG	409, 412-413, 86	this study
FLAG-CIITA_762_LRR_562	pCMV-Tag2B	CIITA AA 1-761 fused to NLRC5 AA 562-1866	FLAG	409, 429-430, 86	this study
FLAG-DD-ΔAD163-CIITA	pCMV-Tag2B	NLRC5 AA 1-142 fused to CIITA AA 163-1130	FLAG	85, 422-423, 426	this study
FLAG-DD-ΔAD335-CIITA	pCMV-Tag2B	NLRC5 AA 1-142 fused to CIITA AA 335-1130	FLAG	85, 424-425, 426	this study
FLAG-DD-ΔDD-Nod1	pCMV-Tag2B	NLRC5 AA 1-142 fused to Nod1 AA 126-953	FLAG	421, 433-435	this study
FLAG-2xNLS-DD-ΔDD-Nod1	pCMV-Tag2B	2xNLS-NLRC5 AA 1-142 fused to Nod1 AA 126-953	FLAG	337, 435	this study
FLAG-2xNLS-AD163-ΔDD-NLRC5	pCMV-Tag2B	2xNLS-CIITA AA 1-163 fused to NLRC5 AA 110-1866	FLAG	454, 86	this study
FLAG-2xNLS-AD335-ΔDD-NLRC5	pCMV-Tag2B	2xNLS-CIITA AA 1-335 fused to NLRC5 AA 110-1866	FLAG	454, 86	this study
FLAG-NLRC5_562_LRR_762	pCMV-Tag2B	NLRC5 AA 1-561 fused to CIITA AA 762-1133	FLAG	421, 426-428	this study

Obtained plasmids

Name	Vector	Insert	Tag	Reference
FLAG-NOD1	pCMV-Tag2B	NOD1 wt	FLAG	(Kufer *et al.*, 2008)
FLAG-NOD2	pCMV-Tag2B	NOD2 wt	FLAG	(Kufer *et al.*, 2006)
HLA-A230	pGL3-Luciferase	BglI-AhaII-HLA-A2.1 promoter fragment	No tag	(Gobin *et al.*, 1997)
HLA-B250	pGL3-Luciferase	AspI-AhaII HLA-B7 promoter fragment	No tag	(Gobin *et al.*, 1997)
HLA-B250"TCGCA"	pGL3-Luciferase	X1 box mutation of HLA-B250, described as mX1 mutation	No tag	(Gobin *et al.*, 1998b)
IFN-β-luciferase	/	125 bp fragment of the IFN-β gene with two ISRE sites, one NF-κB site and an Jun/IRF2 site	No tag	kindly provided by AG Bowie
IRF7-Gal4	/	IRF7 promoter region fused to a Gal4 DNA-binding domain	No tag	kindly provided by KA Fitzgerald
ISRE-luciferase	/	5 x ISRE enhancer and TATA box linked to luciferase gene	No tag	kindly provided by KA Fitzgerald
NF-κB-luciferase	NF-κB reporter Igκ-luciferase		No tag	(Munoz *et al.*, 1994)
pcDNA3.1-3xmyc-B	pcDNA3.1	3 x myc-tagged fused to MCS	MYC	H. Sillje (MPI Bio-chemistry, Martins-ried)
pcDNA3.1−β-gal	pcDNA3.1	β-galactosidase	No tag	(Kufer *et al.*, 2006)
pCMV-Tag2B	/	/	FLAG	Stratagene (Catalog #211172)

		five tandem repeats of the yeast GAL4 binding site fused to the firefly luciferase gene		
pFR-luciferase	/	five tandem repeats of the yeast GAL4 binding site fused to the firefly luciferase gene	No tag	Stratagene (Catalog #219000)
TBK1	pcDNA3	human TBK1	FLAG	(Fitzgerald *et al.*, 2003b)

2.1.5 Oligonucleotides

All oligonucleotides were applied from MWG Biotech.

Primer	Application	Primer №	Sequence
2xNLS-CIITA	Cloning of 2xNLS-AD-ΔDD-NLRC5 constructs	/	GGGGATATCAAGGATCCAAA AAAGAAGAGAAAGGTAGATC CAAAAAAGAAGAGAAAGGTA ATGCGTTGCCTGGCTCCA
B250_1	Cloning of B250-"TCGCA"-Luciferase	343	GCGCGGTACCGAGCTCTTAC GCGT
B250_2	Cloning of B250-"TCGCA"-Luciferase	344	GCGTCACGATGCGACTGGAA GAAGGACCCGACACAA
B250_3	Cloning of B250-"TCGCA"-Luciferase	345	GGGTCCTTCTTCCAGTCGCAT CGTGACGCGTCCCCA
B250_4	Cloning of B250-"TCGCA"-Luciferase	346	CGCGAAGCTTACTTAGATCG CAGATCTCGAGCC
CIITA_761_fwd1	Cloning of CIITA_762_LRR_562	429	CGCTTCTGGCTGGGCTGCC CACCTTCCTGGCGGG
CIITA_761_rev1	Cloning of CIITA_762_LRR_562	430	CCCGCCAGGAAGGTGGGCAG CCCAGCCAGAAAGCG
CIITA_cloning_fwd	Cloning of AD-ΔDD-NLRC5 constructs and CIITA_762_LRR_562	409	GCGCGAATTCATGCGTTGCC TGGCTCCA

CIITA_d163_fwd	Cloning of AD163-ΔDD-NLRC5	410	TGGAAGCCAGCTGAGCCCAGCCAACCTGAATCTCAGCTCC
CIITA_d163_rev	Cloning of AD163-ΔDD-NLRC5	411	GGAGCTGAGATTCAGGTTGGCTGGGCTCAGCTGGCTTCCA
CIITA_d335_fwd	Cloning of AD335-ΔDD-NLRC5 constructs	412	CCAACAAGCTTCCAAAATGGCCTAGCCAACCTGAATCTCAGCTCC
CIITA_d335_rev	Cloning of AD335-ΔDD-NLRC5 constructs	413	GGAGCTGAGATTCAGGTTGGCTAGGCCATTTTGGAAGCTTGTTGG
CIITA_XhoI_rev	Cloning of NLR5_562_LRR_762	426	GCGCCTCGAGTCATCTCAGGCTGATCCGTGAATC
EBSB_GFP_fwd	Cloning of EBSB-GFP-NLRC5 constructs	351	GCGCTCTAGAGCCACCATGGTGAGCAAGGGCGAGG
EBSB_NLRC5_fwd	Cloning of EBSB-NLRC5 constructs	352	GCGCTCTAGAGCCACCATGGACCCCGTTGGCCT
EBSB_NLRC5_rev	Cloning of EBSB-NLRC5 constructs	353	GCGCGGTACCTCATCAAGTACCCCAAGGGGC
GAPDH_fwd	RT-PCR	1	GGTATCGTGGAAGGACTCATGAC
GAPDH_rev	RT-PCR	2	ATGCCAGTGAGCTTCCCGTTCAG
hGAPDH_RT_fwd	qRT-PCR	305	CAACGACCACTTTGTCAAGC
hGAPDH_RT_rev	qRT-PCR	306	TCTTCCTCTTGTGCTCTTGC
HLA-B_fwd	qRT-PCR	369	CTACCCTGCGGAGATCA
HLA-B_rev	qRT-PCR	370	ACAGCCAGGCCAGCAACA
hRANTES_ep_fwd	RT-PCR	259	ATGAAGGTCTCCGCGGCACGCCT (published in Matsukura *et al.*, 1998)
hRANTES_ep_rev	RT-PCR	260	CTAGCTCATCTCCAAAGAGTTG (published in Matsukura *et al.*, 1998)

K234A_fwd	Cloning of NLRC5_K234A	182	GGCTGGCATGGGCGCGACCACGCTGGCCC
K234A_rev	Cloning of NLRC5_K234A	183	GGGCCAGCGTGGTCGCGCCCATGCCAGCC
NLRC5_562_fwd1	Cloning of NLRC5_562_LRR762	427	GGGCCTCTCAGACCACCTCATCTTCCAGCCTCCCGCC
NLRC5_562_rev1	Cloning of NLRC5_562_LRR762	428	GGCGGGAGGCTGGAAGATGAGGTGGTCTGAGAGGCC
NLRC5_cloning_fwd	Cloning of NLRC5	85	CTGCAGGAATTCGATATCATGGACCCCGTTGGCCTCCAG
NLRC5_cloning_rev	Cloning of NLRC5 and CIITA_762_LRR_562	86	CGGGCCCCCCTCGAGTCAAGTACCCCAAGGGGCCTG
NLRC5_dDD_NLS_fwd	Cloning of NLRC5 ΔDD NLS	334	GCGGTACCTAGCCAACCTGAA
NLRC5_dDD_NLS_rev	Cloning of NLRC5 ΔDD NLS	335	GAGCTGGCGGAATTCAAAAAGGAA
NLRC5_EcoRI_rev	Cloning of AD-ΔDD-NLRC5 constructs	414	GGCGGAATTCAAAAAGGAACAGGG
NLRC5_EcoRV_fwd1	Cloning of DD-ΔAD-CIITA constructs and NLRC5_562_LRR_762	421	GCGCGATATCATGGACCCCGTTGGCCT
NLRC5_I3_fwd	Detection of NLRC5 iso-form 3 expression	107	AGGCTGTGGGCAGATAGAGA
NLRC5_iso3_rev	Detection of NLRC5 iso-form 3 expression	271	ACCAGGCATCCCCAGC
NLRC5_iso4_fwd	Detection of NLRC5 iso-form 4 expression	272	TTTGCACTTCAGATCCAACG
NLRC5_iso4_rev	Detection of NLRC5 iso-form 4 expression	273	GATCAAGCAAACCGGAGATG
NLRC5_K234A_fwd	Cloning of NLRC5 K234A	182	GGCTGGCATGGGCGCGACCACGCTGGCCC

NLRC5_K234A_rev	Cloning of NLRC5 K234A	183	GGGCCAGCGTGGTCGCGCCC ATGCCAGCC
NLRC5_LRR_fwd	Cloning of NLRC5 LRR	336	GCGCGATATCGGTGCCAAGC AGGCTGCT
NLRC5_M_fwd	qRT-PCR	109	CTGCAGCCAAGTTCTTAGGG
NLRC5_M_rev	qRT-PCR	110	TCAGCTGAGGGAGTTGAGGT
NLRC5_N_rev	Cloning of NLRC5 Isoform 3	173	GCGCCTCGAGTTACTGCTTCT TGCACTGCTTCCG
NLRC5_N_fwd1	Cloning of DD-ΔAD163-CIITA and DD-ΔDD-Nod1	422	AGTGCAAGAAGCAGCAGCTA GAGCCCACTGTGGTGACTGG C
NLRC5_N_rev1	Cloning of DD-ΔAD163-CIITA	423	GCCAGTCACCACAGTGGGCT CTAGCTGCTGCTTCTTGCACT
NLRC5_N_fwd2	Cloning of DD-ΔAD335-CIITA	424	GCCAGTCACCACAGTGGGCT CTAGCTGCTGCTTCTTGCACT
NLRC5_N_rev2	Cloning of DD-ΔAD335-CIITA	425	TAGAACTGCTCCACCGGCTCC TCTAGCTGCTGCTTCTTGCAC T
NLRC5_N_fwd3	Cloning of DD-ΔDD-Nod1	433	AGTGCAAGAAGCAGCAGCTA GAGGTGAGCAGGTATACCCA GCAGC
NLRC5_N_rev3	Cloning of DD-ΔDD-Nod1	434	GCTGCTGGGTATACCTGCTC ACCTCTAGCTGCTGCTTCTTG CACT
NLRC5_NLS_fwd	Cloning of FLAG-2xNLS-NLRC5	337	GGGGATATCAAGGATCCAAA AAAGAAGAGAAAGGTAGATC CAAAAAAGAAGAGAAAGGTA ATGGACCCCGTTGGCCT
Nod1_XhoI_rev	Cloning of DD-ΔDD-Nod1	435	GCGCCTCGAGTCAGAAACAG ATAATCCGCTTCTCATCTTC
Seq_NLRC5_1	Sequencing of NLRC5	97	GGCAGCCCCACGCCTTC

Seq_NLRC5_2	Sequencing of NLRC5	98	CAATGGGACCCTCCTGCCTG
Seq_NLRC5_3	Sequencing of NLRC5	99	CACAGGCCCTGGGCACCAG
Seq_NLRC5_4	Sequencing of NLRC5	100	CTGGATTTTGATGGCTGTCCCCTG
Seq_NLRC5_5	Sequencing of NLRC5	101	GTGACGGCCAGAGGAAAGGG
Seq_NLRC5_6	Sequencing of NLRC5	102	GAAGCTGCCACCTCGGTCAC
Seq_NLRC5_7	Sequencing of NLRC5	103	GCTGCAGCTGAGCCAGACGG
Seq_NLRC5_8	Sequencing of NLRC5	104	CTTCCGGCCAGAGCACGTGTC
Seq_NLRC5_9	Sequencing of NLRC5	105	CTGAAGACATTTCGGCTGACCTCCAG
Seq_NLRC5_10	Sequencing of NLRC5	106	GATGCTTGGCTGCAATGCCCTG

2.1.6 siRNA

All siRNAs were applied from Qiagen.

Gene	Name	Number	Target
No Target	All Stars	SI1027281	No target
NLRC5	Hs_NLRC5_1	SI04143510	CAGGGTTCTCTCCCTGTTAGA
NLRC5	Hs_NLRC5_4	SI04300814	CTGCTTATCTTTGATGGGCTA
TBK1	siTBK1	published in (Sharma *et al.*, 2003b)	GCGGCAGAGTTAGGTGAA
TLR3	siTLR3	published in (Li *et al.*, 2005)	GGTATAGCCAGCTAACTAG

2.1.7 Antibodies

Primary Antibodies

All antibodies were diluted in 5 % milk powder in PBS.

Antigen	Source	Clone	Dilution	Reference
β-actin	mouse mAB	C4	WB 1:10000	Santa Cruz Biotechnology (sc-47778)
c-MYC	rabbit pAB	A-14	WB 1:1000	Santa Cruz Biotechnology (sc-789)
FLAG	mouse mAB	M2	WB 1:2000 IF 1:8000	Stratagene (#200471)
GAPDH	rabbit pAB	FL355	WB 1:1000	Santa Cruz Biotechnology (sc-25778)
GFP	mouse mAB	7.1/13.1	WB 1:2000	Roche (Cat. No. 11-814-460-001)
HLA-B/C	mouse mAB	/	WB 1:3000	gift from Anne Halenius
HLA-DR	mouse mAB	520B	WB 1:200	Santa Cruz Biotechnology (sc-69673)
MYC	mouse mAB	9E10	IF 1:1000	Roche (Cat. No. M4439)
NLRC5 3H8	rat mAB	3H8	WB 1:5	(Neerincx *et al.*, 2010)
NLRC5 5D4	rat mAB	5D4	WB 1:5	(Neerincx *et al.*, 2010)
NOD1	rat mAB	2A10	WB 1:100	(Kufer *et al.*, 2008)
NOD2	rat mAB	7E11	WB 1:100	(Kufer *et al.*, 2006)
TBK1	mouse mAB	108A429	WB 1:1000	Santa Cruz Biotechnology (sc-52957)
TLR3	goat pAB	N-14	WB 1:1000	Santa Cruz Biotechnology (sc-8691)
Tubulin	mouse mAB	4G5	WB 1:1000	Sigma-Aldrich (T7816)

Secondary Antibodies

All secondary antibodies were diluted 1:4000 in 5 % milk powder in PBS.

Antigen	Reference
Goat anti-Mouse IgG (H+L) – HRP conjugated	Bio-Rad (170-6516)
Goat anti-Rabbit IgG (H+L) – HRP conjugated	Bio-Rad (170-6515)
Goat anti-Rat IgG + IgM (H+L) – HRP conjugated	Santa Cruz Biotechnology (sc-789)
POD-conjugated Goat anti-Mouse LC specific	Dianova (115-035-174)
POD-conjugated Mouse anti-Rabbit LC specific	Dianova (211-032-171)

FACS Antibodies

Antigen	Source	Clone	Reference
anti-H-2k^b	mouse mAB	AF6-88.5	BD Pharmingen™ (#553568)
anti-IA/IE-Alexa647	mouse mAB	2G9	BD Pharmingen™ (#885893)
HLA-ABC-APC	mouse mAB	G46-2.6	BD Pharmingen™ (#562006)
IgG control-APC	mouse mAB	MOPC-21	BD Pharmingen™ (#555751)
Streptavidin-APC	/	Streptavidin	BD Pharmingen™ (#554067)

Antibody coupled beads

Antigen	Source	Clone	Reference
FLAG	mouse mAB	M2	Sigma-Aldrich (A2220)
MYC	mouse mAB	9E10	Santa Cruz Biotechnology (sc-40)

2.1.8 Instruments

Instrument	Manufacturer
Biofuge pico	Heraeus
Cell^R	Olympus
Centrifuge 5415R	Eppendorf
Centrifuge 5418	Eppendorf
Centro XS^3 LB960 Luminometer	Berthold Technologies
FACSCanto Flow Cytometer	BD Biosciences
Gel Electrophoresis System	Bio-Rad-Laboratories
Incubator	Heraeus
iQ5™ cycler (qRT-PCR cycler)	Bio-Rad-Laboratories
LAS-4000 Luminescent Image Analyser	Fujifilm
Microcentrifuge	Roth
Multifuge 4KR	Heraeus
Multipette plus dispenser	Eppendorf
Nano Photometer™	Implen GmBH
Neubauer Counting Chamber Improved	Labor Optik
Nunc-Immuno Wash 12	Nunc
Pipetboy acu	Integra Biosciences
Plate Reader bt 2	Anthos
Primus Thermocycler	MWG Biotech
PS-M3D Orbital Shaker	Grant-bio
Research pro Multichannel Pipettes	Eppendorf
roller mixer srt6	stuart
Steri-Cycle CO_2 Incubator, Model 381	Thermo Forma
Sterile Bench	Heraeus

Thermomixer comfort	Eppendorf
TRANS BLOT SD, Semi-Dry Transfer Cell	Bio-Rad Laboratories
Vortex Genie 2	Scientific Instruments

2.1.9 Software

Software	Company
Adobe Acrobat 9 Professional	Adobe Systems Incorporated
Adobe Illustrator CS5	Adobe
Adobe Photoshop CS5	Adobe
Bio-Rad iQ5 version 2.0	Bio-Rad Laboratories
Cell^R Software	Olympus
CellQuest software	BD Biosciences
Endnote X	Thomson Reuters
FACSDiva	BD Biosciences
ImageJ	(Schneider *et al.*, 2012)
Imagereader LAS-4000	Fujifilm
Microwin 2000	Berthold Technologies
Microsoft Office 2003	Microsoft

2.2 Methods

2.2.1 Cell Biological Methods

Cell Culture

Mouse melanoma B16F10, HEK293T cells and HeLa cells were cultivated at 37 °C with 5 % CO_2 in Dulbecco's Modified Eagle Medium (DMEM, Biochrom AG)) containing 10 % heat-inactivated Fetal Bovine Serum (FBS, Biowest) and penicillin/streptomycin (100 IU/ml and 100 mg/ml, respectively) (P/S) (Biochrom AG) under humidified conditions.

HEK-Blue™ IFN-α/β cells were grown at 37 °C with 5 % CO_2 in DMEM containing 10 % FBS, penicillin/streptomycin, 30 μg/ml blasticidine (Invivogen) and 100 μg/ml zeocin™ (Invivogen) under humidified conditions.

Primary human dermal fibroblasts (hFibr) were maintained at 37 °C with 5 % CO_2 in DMEM containing 10 % FBS and P/S under humidified conditions.

THP-1 cells were grown at 37 °C with 5 % CO_2 in Roswell Park Memorial Institute 1640 Medium (RPMI-1640, Biochrom AG) containing 10 % FBS and P/S under humidified conditions.

Cells were continuously tested for mycoplasma contamination.

Stimulation and Infection of Cells

$5x10^5$ THP-1 cells were seeded in 6 well dishes either directly before stimulation, or $5x10^5$ cells were seeded 24 h prior stimulation and differentiated with 100 nM PMA for 24 h. Stimulation was performed using 50 ng/ml tumor necrosis factor (TNF), 1 μM muramyl dipeptide (MDP), 50 ng/ml lipopolysaccharide (LPS), 0.5 μM phorbol 12-myristate 13-acetat (PMA), 100 ng/ml Pam3CSK or 100 μg/ml poly(I:C) for 6 to 24 h as indicated in the specific experiments. For infection of THP-1 cells with Sendai Virus (SeV, Charles River Laboratories), cells were seeded as for stimulation and infected with 80 hemagglutination units (HAU) / ml.

HeLa cells were seeded in 6 well dishes 16 to 18 h before stimulation to a confluence of about 60 %. Stimulation and infection was performed as described for THP-1 cells using 160 HAU / ml for 16 to 24 h.

Transient DNA transfection

For transient DNA transfection of adherent cells, cells were seeded in DMEM containing FBS and P/S in an adequate cell culture dish 24 h prior transfection in order to reach a cell density of about 50 to 70 %. To obtain an increasing expression time of the protein of interest (48 h to 72

h), cell density was reduced to 30 to 50 %. For transfection, Lipofectamine2000 (Invitrogen), FuGene6 (Roche) or XtremeGene9 (Roche) was used in a ratio of 1:3 (DNA : transfection reagent) in DMEM without supplements as described in the manufacturers' protocol. The ready-to-transfect transfection mixes were incubated 20 to 30 min prior transfection, to allow transfection complex formation.

For HeLa cell transfection, 6 h after transfection, the transfection medium was replaced by DMEM containing FBS and P/S.

For HEK293T cells, a medium change was conducted 16 to 24 h after transfection.

siRNA transfection

For siRNA transfection in THP-1 cells, $2x10^5$ cells were seeded into 24 well format in 500 µl RPMI containing FBS and P/S and differentiated for at least 24 h using 100 nM PMA. Shortly before siRNA transfection, the medium was replaced by 100 µl RPMI containing FBS and P/S. For transfection, 100 nM siRNA and 6 µl HiPerfect were diluted in 100 µl RPMI without supplements. The transfection mix was incubated 5 to 10 min at RT before added to the cells. 6 h after transfection, another 400 µl complete RPMI medium was added to the cells. One day after transfection, the medium was changed. 72 h after siRNA transfection, cells were stimulated and further analyses were performed as indicated.

For siRNA transfection in HeLa and hFibr, $5x10^4$ cells were seeded in 24 well format in 500 µl DMEM containing FBS and P/S one day prior transfection. siRNA transfection was performed in 100 µl DMEM without supplements containing 10 nM siRNA and 3 µl HiPerfect, as described in the manufacturer's protocol. 24 h after siRNA transfection, the medium was changed by DMEM containing FBS and P/S. siRNA silencing was performed for 72 h, unless specified otherwise. After 72 h, cells were stimulated with 100 µg/ml poly(I:C) or infected with 130 HAU/ml SeV for 16 to 18 h.

For further analyses, RNA was extracted by pooling three 24 well wells.

Luciferase reporter assay

For a cell based luciferase assay in 96 well format, $3x10^4$ cells per well were seeded in DMEM containing FBS and P/S about 4 to 6 h prior transfection. For NF-κB pathway activation, 13 ng luciferase reporter construct, for IRF7 pathway activation, 3 ng of IRF7-Gal4 together with 40 ng pFR-luciferase was transfected and for IFN-β, ISRE and MHC class I and II pathway activation, 20 ng luciferase reporter construct was transfected together with 10 ng of β-galactosidase plasmid as well as the indicated amount of plasmid of interest per well. For equal transfection conditions, the DNA amount was adjusted to 50 ng or 100 ng per well. The transfection was performed in

20 μl DMEM without supplements and 0.2 μl FuGene6 or XtremeGene (in case of 100 ng of total plasmid, 0.4 μl FuGene6 or XtremeGene) per well. The transfection mix was incubated for 20 min prior transfection. The luciferase readout was performed 20 to 24 h after transfection (Zurek *et al.*, 2011).

For activated luciferase reporter assays, cells were infected with SeV, using 130 HAU/ml 18 h prior luciferase readout.

For the readout, cells were lysed in 100 μl luciferase lysis buffer per well. Subsequently, 50 μl of cell lysate was used to determine luciferase activity using 100 μl luciferase readout buffer and the remaining 50 μl cell lysate was mixed with 100 μl ONPG development buffer to determine β-galactosidase activity. The luciferase readout was performed using a Centro XS^3 LB960 Lumi-nometer (Berthold Technologies). The β-galactosidase readout was performed using an anthos bt 2 plate reader.

Luciferase activity was normalized to β-galactosidase expression and mean and standard deviation were calculated from triplicates.

Luciferase lysis buffer:	25 mM TRIS pH 8.0, 8 mM MgCl$_2$, 15 % glycerol, 1 % Triton X-100, stored at 4 °C
Luciferase read out buffer:	Luciferase lysis buffer supplemented with 0.54 μg/ml D-Luciferin and 1.33 mM ATP, freshly prepared
ONPG dilution buffer:	60 mM Na$_2$HPO$_4$x2H$_2$O, 40 mM NaH$_2$PO$_4$, 10 mM KCl, 1 mM MgSO$_4$x7H$_2$O, pH 7.0
ONPG stock solution:	4 mg/ml ONPG in ONPG dilution buffer, stored at 4 °C
ONPG development buffer:	1:4 dilution of ONPG stock solution in ONPG dilution buffer, freshly prepared

HEK-IFN-α/β reporter assay

For detection of type I interferons, 3x10^4 HEK-Blue™ IFN-α/β cells were seeded in 20 μl of DMEM containing 10 % FBS and P/S under humidified conditions in 96 well plate format. These cells were stably transfected with the human STAT2 and IRF9 to maintain a completely functional type I IFN signalling pathway and were further transfected with a SEAP reporter gene under the control of the IFN-α/β inducible ISG54 promoter. Directly after seeding of the cells, the type I IFN supernatant was added to the cells and the cells were incubated for 16 to 24 h. After incubation, the levels of secreted SEAP were determined using QUANTI-Blue™ SEAP-detection medium. For that purpose, 20 to 50 μl of HEK-Blue™ IFN- α/β cell supernatant were

incubated with 180 to 150 μl of QUANTI-Blue™ SEAP-detection medium and incubated at 37 °C up to 1 h. SEAP activity was measured at 620 nm. All assays were performed in triplicates.

QUANTI-Blue SEAP-detection medium: Reconstituted in ddH2O according to the manufacturers' protocol

Indirect immunofluorescence

To accomplish indirect immunofluorescence microscopy, HeLa cells were seeded in 24 well format on sterilized glass coverslips in 500 μl DMEM containing FBS and P/S one day before transfection to a confluence of about 40 to 50 %. Shortly before transfection, the medium was replaced by 500 μl DMEM containing FBS but no antibiotics. Cells were transiently transfected with 1 μg of indicated plasmid using Lipofectamine2000 as described in the manufacturer's protocol. 6 h after transfection, the transfection medium was replaced by DMEM containing FBS and P/S. After 24 h, cells were either treated with 50 nM Leptomycin B (LepB) for 4h or left untreated. Subsequently, cells were fixed using 3 % paraformaldehyde (PFA) in PBS for 5 to 10 min. After fixation, cells were washed three times using PBS and then permeabilized for 5 min using 0.5 % Triton X100 in cold PBS. After three additional washing steps with PBS, cells were incubated in 3 % BSA in PBS to block unspecific protein interactions. Antibody staining was performed for 1h at RT using either anti-myc antibody or anti-FLAG M2 antibody, diluted 1:1000 and 1:8000, respectively. For visualization of anti-c-myc or anti-FLAG M2 antibody, samples were incubated with Alexa488-conjugated anti-mouse antibody for an additional hour at RT. Finally, unbound antibody was removed by three additional washing steps and cells were mounted in Prolong® Gold Antifade Reagent (Invitrogen). Image acquisition was performed using a Cell^R microscope and processed using ImageJ (Schneider *et al.*, 2012).

0.5 % Triton:	1x PBS + 0.5 % Triton X-100
3 % PFA Solution:	1x PBS + 3 % (v/v) PFA
3 % BSA:	1x PBS + 3 % BSA
PBS (10x):	1,37 M NaCl, 26.82 mM KCl, 80.9 mM $Na_2HPO_4 x2H_2O$, 17.63 mM KH_2PO_4, pH 7.4

2.2.2 Molecular Biological Methods

Production of chemically competent bacteria

For production of chemical competent bacteria, a 500 ml LB medium culture of DH5α bacteria inoculated from a single bacterial colony was incubated over night at 37 °C. This culture was subsequently used to inoculate a second LB bacterial culture, growing at 20 °C and shaking at 200 rpm until the bacterial culture has reached an OD_{600} of 0.3 to 0.6. Next, the culture was chilled on ice for about 10 min and pelleted at 4 °C and subsequently washed with 150 ml of cold transformation buffer. Finally, the culture was centrifuged again and the pellet was resuspended in 40 ml transformation buffer and 3 ml DMSO and aliquots of about 500 µl were frozen in liquid nitrogen and stored at -80 °C.

LB medium:	10 g Tryptone, 10 g NaCl, 5 g Yeast Extract add 1 L H_2O, autoclaved
LB agar plates:	15 g Agar Powder added to 1 L LB medium, supplemented with antibiotics (50 µg/ml Kanamycin, 100 µg/ml Ampicillin, 4 °C)
Transformation buffer:	15 mM $CaCl_2$, 250 mM KCl, 10 mM PIPES, 55 mM $MnCL_2x4H_2O$, pH 6.7, sterile filtrated

Heat-shock transformation of chemical competent bacteria

Chemical competent bacteria E.*coli* DH5α were carefully thawn on ice. For retransformation of plasmid DNA, 100 ng of the plasmid of interest was added to 50 µl of chemically competent bacteria and incubated for 30 min on ice. After 30 min, a heat-shock was performed for 90 sec at 42 °C followed by a short incubation on ice. Next, 250 µl of LB medium was added to the 50 µl transformed bacteria sample. Depending on the resistance marker of the plasmid, the transformed bacteria were incubated for one hour at 37 °C shaking prior plating (for kanamycin) or were directly plated on LB agar plates (for ampicillin) containing either 50 µg / ml kanamycin or 100 µg / ml ampicillin.

Isolation of plasmid DNA from E.*coli* DH5*a*

For plasmid isolation from E.*coli*, bacteria were either cultured in 5 ml LB containing antibiotics (for Miniprep) or in 100 ml LB containing antibiotics (for Maxiprep) over night at 37 °C shaking . The next day, bacteria were pelleted for 15 min at 4000 x g at 4 °C. Isolation of plasmid DNA was performed using the NucleoBond PC20 (Macherey-Nagel) or PC500 (Macherey-Nagel)

plasmid preparation kit as described in the manufacturer's protocol. The plasmid DNA pellet was resuspended in 100 to 200 µl 10 mM TRIS pH 8. The plasmid DNA concentration and purity was determined using a nanodrop photometer measuring absorption of 260 and 280 nm.

Isolation of RNA from human cells

RNA was isolated from human cells using the RNeasy Mini Kit (Qiagen) according to the manufacturers' protocol. RNA was eluted with RNase free water. RNA concentration and purity was measured using a nanodrop photometer measuring absorbance at 260 to 280 nm.

Reverse transcription of RNA

1 µg of isolated RNA was reverse transcribed into cDNA using the RevertAid First Strand cDNA Synthesis Kit (Fermentas) with Oligo(dT)$_{18}$ primer referring to the manufacturer's protocol.

End-point RT-PCR

End-point RT-PCR of cDNA samples was performed according to following protocol.

Substance	Volume
cDNA	50 to 100 ng
Taq Buffer (+KCl; -MgCl$_2$) (10 x)	5 µl
MgCl$_2$ (25 mM)	4 µl
dNTPs (10 mM)	2 µl
Taq DNA Polymerase (5 u/µl)	0.5 µl
primer fwd	10 pmol
primer rev	10 pmol
H$_2$O	up to 50 µl

The PCR was run using the following conditions.

Time	Temperature	
1 min	94 °C	
15 sec	94 °C	25-30x (depending on the gene of interest)
30 sec	55 °C	
30 sec	72 °C	
5 min	72 °C	
∞	4 °C	

The PCR fragments were subsequently analysed on a 1 to 2 % (agarose in TBE buffer) agarose gel.

Amplification of DNA fragments

For cloning of NLRC5 and CIITA fusion proteins, the fragments of interest was amplified by PCR from FLAG-NLRC5 or CIITA-FIII with the primers indicated above, using the 2xPhusion® High-Fidelity PCR Master Mix (Finnzymes) as described in the manufacturer's protocol. Subsequently, the PCR product was digested using the appropriated restriction enzymes for 4 h at 37 °C. The digested PCR fragments were purified using a 1 to 2 % preparation gel with further gel extraction using the ExtractIT-Kit (Macherey-Nagel).

Site-directed mutagenesis

Point mutation introduction was performed by PCR using the QuikChange™ Site-Directed Mutagenesis procedure (Stratagene). Reaction mixes were prepared according to the following protocol.

Substance	Volume
plasmid DNA (100 ng/μl)	2.5 μl
2x Phusion™ Master Mix	25 μl
primer fwd (10 pmol/μl)	1 μl
primer rev (10 pmol/μl)	1 μl
H$_2$O	up to 50μl

The PCR was run using the following conditions.

Time	Temperature	
30 sec	98 °C	
10 sec	98 °C	
30 sec	65 °C	25x
3 min	72 °C	
5 min	72 °C	
∞	4 °C	

To digest plasmid DNA, 1.5 µl DpnI (+6 µl Buffer + 3.5 µl H$_2$O) was added to the PCR mix and incubated at 37 °C for 2 h. Subsequently, 5 µl PCR sample was transformed into 50 µl of chemical competent bacteria.

Restriction digestion of plasmid DNA

For restriction of plasmid DNA, 1 to 2 µg of plasmid DNA was digested using 5 u of the appropriate restriction enzyme for 4 h at 37 °C. Buffer and temperature conditions were adjusted according to the specific enzyme. Simultaneous digestion with two restriction enzymes was performed as suggested form the Thermo Fischer / Fermentas DoubleDigest™ website (http://www.fermentas.com/en/tools/doubledigest/).

Agarose gel electrophoresis

DNA fragments were separated and analysed by agarose gel electrophoresis using 1 to 2 % agarose dissolved by boiling in 1 x TBE. The liquid agarose was poured into a gel and mixed with 0.5 µg/ml ethidium bromide. Samples were dosed with 10 x DNA loading buffer or 6 x low range DNA loading buffer. GeneRuler Low Range DNA Ladder (Fermentas; Cat. Nr. SM1191) or Lambda Hind III/phiX Hae III Marker (Roth; CP49) were used as standards. The gel was run at 80 V and bands were detected under UV light.

10 x TBE (TRIS-borate EDTA):	0.89 M TRIS, 0.89 M boric acid, 20 mM Na$_2$EDTA pH 8.0
	The working solution was prepared by 1:10 dilution in ddH$_2$O and addition of 20 % methanol.
6 x DNA loading buffer:	2 % glycerol in ddH$_2$O, supplemented with brome phenol blue

Ligation of DNA fragments

Digested DNA fragments were ligated using the Rapid DNA Ligation Kit (Fermentas) according to the manufacturer's protocol. Ligation was performed using a ratio of 2:1 or 3:1 (insert : vector DNA fragment).

Quantitative real-time PCR

Quantitative real-time PCR (qRT-PCR) was performed using a Bio-Rad iQ™ cycler and the iQ ™ SYBR® Green Supermix. For each qRT-PCR reaction, 50 ng cDNA in a volume of 25 µl

PCR Mix was used. For qRT-PCR reactions of human cDNA panel, 1 µl of stock cDNA was used per qRT-PCR reaction.

The reaction was prepared as follows:

Reagent	Volume/Concentration
2x iQ ™ SYBR® Green Supermix	12.5 µl
primer fwd	0.07 µl / 7.5 pmol
primer rev	0.07 µl / 7.5 pmol
H_2O	add 20 µl

The indicated cDNA amount in a volume of 5 µl ddH_2O was added to each reaction. Reaction mixes were prepared on ice and drops were collected by centrifugation before starting the reaction. The PCR was performed in 96 well PCR plate format under following conditions:

Temperature	Time	
95 °C	3 min	1 x
95 °C	15 sec	40 x
60 °C	1 min	
55 °C	30 sec	81 x
25 °C	∞	1 x

2.2.3 Biochemical Methods

Protein concentration measurement

Protein concentrations were determined using the Bio-Rad DC Protein Assay according to the manufacturer's protocol.

Protein Separation and detection

Proteins were separated as previously described (Laemmli, 1970). Separation was performed using either a 7.5 % or 10 % TRIS-buffered SDS-Polyacrylamide-Gel. Samples were dosed with 6 x Laemmli loading buffer containing β-mercaptoethanol and boiled 5 min at 95 °C prior loading. Samples were run at 120 to 180 V until the dye front completely drained off the gel.

6 x Laemmli buffer:	7 ml 0.5 M Tris/0.4 % SDS pH 6.8, 3 ml glycerol, 1 g SDS, bromophenole blue, 60 µl β-mercaptoethanol added directly before use
Separation gel:	2.1 ml ddH$_2$O, 2.5 ml acrylamide (40 %), 5 ml 0.5 M TRIS/0.4 % SDS pH 8.8, 25 µl TEMED, 50 µl APS
Stacking gel:	4.5 ml ddH$_2$O, 650 µl acrylamide (40 %), 1.25 ml 0.5 M TRIS/0.4 % SDS pH 6.8, 25 µl TEMED, 50 µl APS
SDS-PAGE running buffer (10 x):	250 mM TRIS, 1.92 M glycine, 34.67 mM SDS; working solution was prepared by 1:10 dilution in ddH$_2$O.

Separated proteins were transferred on nitrocellulose membrane by semi-dry western blotting at 15 V for 50 min. Blot efficiency was controlled by Ponceau-S staining.

PBS-T	1x PBS + 0.05 % Tween20
Ponceau-S solution:	0.2 % Ponceau S, 3 % acetic acid
Transfer buffer (10 x):	250 mM TRIS, 1.92 mM glycine
	The working solution was prepared by 1:10 dilution in ddH$_2$O and addition of 20 % methanol.

Membranes were blocked using 5 % milk powder in PBS to avoid unspecific binding of antibodies.

All primary antibodies were diluted in 5 % milk powder in PBS and incubated for at least 1 h at RT or over night incubation at 4 °C.

After primary antibody incubation, the membrane was washed 3 times with PBS containing 0.05 % Tween20. Secondary antibodies were diluted in 5 % milk powder in PBS and incubated for 1 h at RT. Proteins were detected using SuperSignal West Pico Chemiluminescent Substrate or Femto maximum Sensitivity Substrate (Thermo Scientific). Signals were recorded on an electronic imaging system (LAS4000, Fujifilm).

Co-Immunoprecipitation

For Co-Immunoprecipitation of overexpressed proteins, HEK293T cells were seeded in 10 cm dishes one day prior transfection. Cells were transiently transfected with 1 to 3 µg of each plasmid as indicated using Lipofectamine2000 or FuGENE6, according to the manufacturers' protocol. 24 h after transfection, cells were lysed in NP40 or RIPA lysis buffer containing phosphate inhibitors (20 µM β-glycerophosphate, 5 mM NaF, 100 µM Na$_3$VO$_4$), protease inhibitors (1 tablet

for 50 ml lysis buffer) and 2 mM EDTA. The lysates were incubated on ice for 20 min and subsequently cleared by centrifugation at 14.000 x g and 4 °C. 50µl of supernatant was stored for input samples and remaining supernatant was utilized directly for immunoprecipitation using 20 µl anti-FLAG M2 (Sigma-Aldrich) or 20 µl anti-myc beads (Santa Cruz) for 4 h at 4 °C on an end-to-end rotator. After precipitation, beads were washed 5 times using NP40 or RIPA lysis buffer with additives. The washed beads were dosed with equal amounts of 2 x Laemmli buffer. For SDS-PAGE analysis, 15 µl input or 10 µl of IP were loaded.

NP40 lysis buffer:	150 mM NaCl, 50 mM TRIS pH 7.4, 1 % NP40, 4 °C
	freshly add EDTA, protease and phosphate inhibitors
RIPA lysis buffer:	150 mM NaCl, 50 mM TRIS pH7.4, 1 % Triton X-100, 0.1 % SDS, 0.5 % deoxycholic acid sodium salt, 4°C
	freshly add EDTA, protease and phosphate inhibitors

Subcellular fractionation of HeLa cells

For stimulation of HeLa cells, $5x10^6$ cells were seeded in a 10 cm dish one day before stimulation. For activation of TLR3, cells were stimulated with 100 µg/ml poly(I:C) for 24 h. After 24 h, the medium was changed and nuclear export was blocked using 50 nM Leptomycin B for 4 h. Subsequently, subcellular fractionation was performed using the Qproteome Compartment Kit (Qiagen Cat. # 37502) as described in the manufacturer's protocol.

The cytosolic and the nuclear fraction were directly used for IP using 20 µl anti-NLRC5 3H8 antibody-coupled protein G sepharose beads (incubation of 70 µl protein G sepharose beads with 1400 µl anti-NLRC5 3H8 antibody hybridoma supernatant over night). Beads were processed as described in Co-Immunoprecipitation part.

Cytokine Profiling and ELISA

For cytokine profiling, Proteome Profiler Human Cytokine Array Panel A kit from R & D Systems (Catalog Number ARY005) was used. Quantification was performed by recording the signal on a LAS4000 ECL camera system and densitometric quantification to the internal controls after background subtraction (ImageJ).

ELISA for IFN-β, RANTES, and IP-10 was performed using a MultiAnalyte ELISArray kit from SABiosciences (MEH-007A) according to the manufacturer's instructions.

Secretion of CCL5/RANTES from human cells was measured using the DuoSet ELISA Development Kit from R & D Systems (Catalog Number DY278), according to the manufacturer's protocol.

Flow cytometry

For FACS analysis of THP-1 cells, cells were seeded in 24 well format and siRNA knock-down was performed as previously described. For flow cytometry preparation, cells were washed and trypsinized for 15 min. Subsequently, 2×10^5 were transferred to a 96 well plate and washed two times using PBS supplemented with 0.1 % FBS. HLA-A/B/C or IgG1 control staining was performed in 20 µl 2 % BSA in PBS supplemented with 3 µl FACS antibody for 45 min on ice. After incubation, cells were washed two additional times to remove unbound antibody residues. Subsequently, cells were fixed in 1 % PFA in PBS for 30 min on ice. After two additional washing steps with PBS containing 0.1 % FBS, cells can be directly analysed or stored at 4 °C up to one week. Samples were analysed using a FACSCanto Flow Cytometer and analysed with FACSDiva.

B16F10 cells were transfected in 12 well plates with EBSB-GFP-NLRC5 or CIITA constructs and selected with antibiotics for 4 weeks. FACS analysis was performed as previously described (Steimle *et al.*, 1993). Cells were stained for MHC class II expression with Alexa Fluor 647-coupled anti-IA/IE mAB 2G9 (BD Biosciences), for MHC class I expression with biotinylated anti H-2k^b Ab AF6-88.5 (BD Biosciences), followed by secondary staining with Streptavidin-allophycocyanin (BD Biosciences), or appropriate controls. Cells were analysed on a FACSCanto instrument using CellQuest software (BD Biosciences).

3 Results

3.1 A Role for the human nucleotide-binding domain, leucine-rich repeat-containing family member NLRC5 in antiviral responses

3.1.1 Structure of NLRC5

Sequence comparisons of NLRC5 show the same overall multidomain architecture composed of effector, NACHT, winged helix, superhelical and leucine-rich repeat (LRR) domains which are found in all other human NLRs. Differences exist in the type of effector domain and the significantly longer LRR receptor domain. The NLRC5 effector domain (residues 1–101) is composed of five α-helices and shows no sequence homology to CARD or PYD domains. This indicates that the NLRC5 effector domain although structurally similar to CARD and PYD domains features a different interface. The NACHT domain obtains all typical features important for nucleotide hydrolysis followed by a winged helix domain and a superhelical domain. Thus, NLRC5 is a typical Apaf-like ATPase likely capable of ATP hydrolysis which is required for conformational changes leading to activation. The LRR domain in NLRC5 differs from other LRRs in respect to its length of more than 1000 residues. Structurally, leucine-rich repeats of that length should form more than a full LRR circle, resulting in a LRR helix (personal communication R. Schwarzenbacher). A model is depicted in figure 3.1 A.

3.1.2 Expression and Induction of NLRC5

To get a first insight into the role of NLRC5, we analysed the overall expression of NLRC5 in different human cells and tissues using qRT-PCR. In line with available microarray data (www.biogps.org), we detected highest expression of NLRC5 in cells of the hematopoietic compartment, in both CD4$^+$ and CD8$^+$ T cells, and to a lesser extent in macrophages (CD14$^+$). In tissue-derived cDNA, highest expression was observed in lymph nodes, spleen, bone marrow and tonsils (Figure 3.1 B).

Accordingly, we found high amounts of NLRC5 in cell lines of thymoid (Jurkat) and myeloid (THP-1) origin, whereas other cells lines, derived from human embryonic kidney (HEK293T) and colon (CaCo2) only displayed marginal expression (Figure 3.1 C).

During the cloning of the NLRC5 open reading frame from a human leukocyte cDNA library, we could obtain different splice variants, of which five of them were already contained in databases (www.uniprot.org). Interestingly, the different variants all share the common 5' region

encoding the effector domain and the central NACHT domain, but differed in the length of the LRR (Figure 3.1 D).
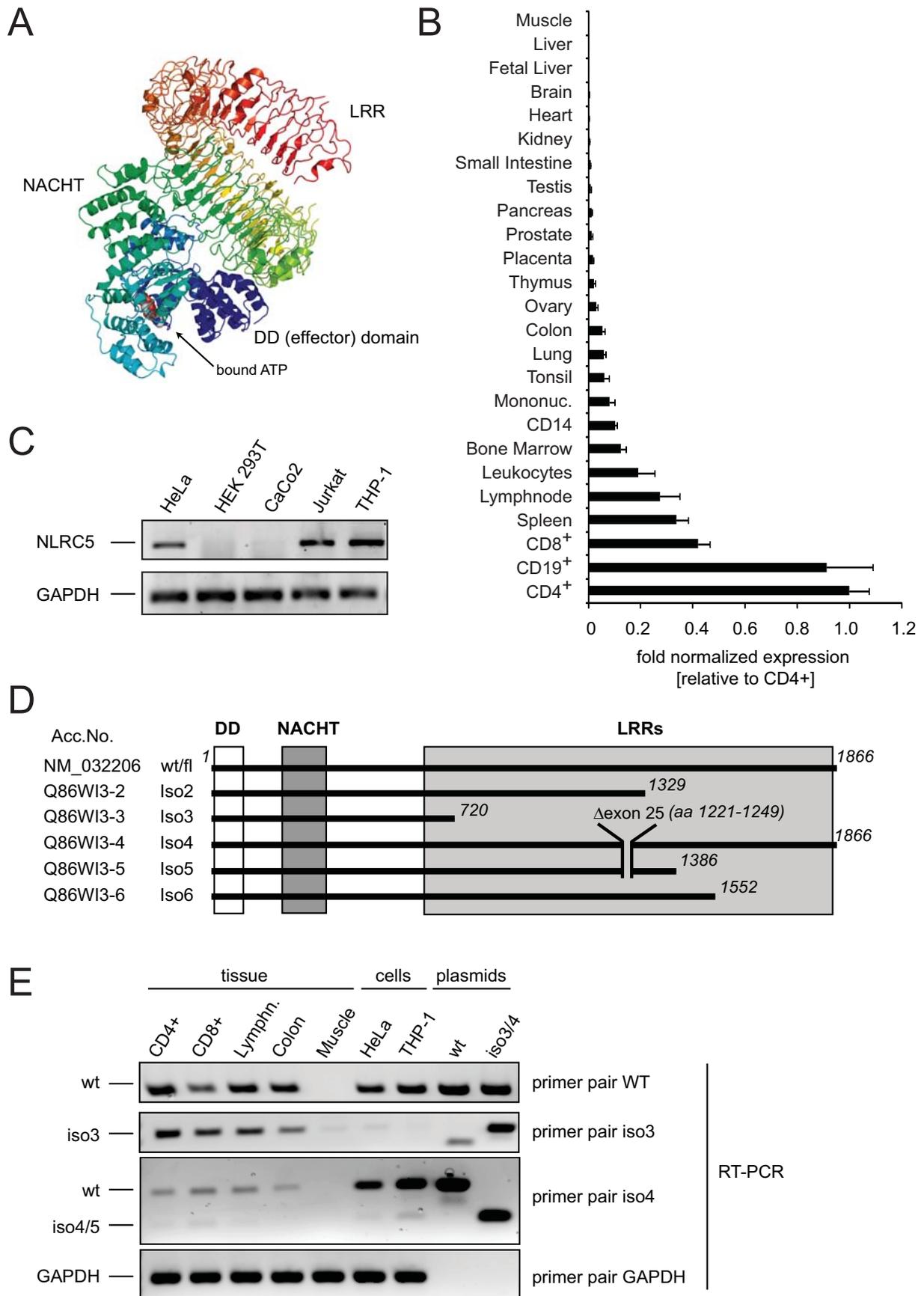
Figure 3.1 Structure and expression of endogenous NLRC5

A) Model of the NLRC5 structure. The N-terminal effector domain and the nucleotide-binding domain (NACHT) with a bound ATP molecule (blue) are based on the Apaf-1 effector domain structure (Protein Data Bank entry 1z6t). The C-terminal LRRs (red to yellow) are based on the TLR4 LRRs (Protein Data Bank entry 2z64). The figure was prepared with Pymol. The positions of the domains are indicated. Model generated by R. Schwarzenbacher.

B) qRT-PCR expression pattern of the indicated tissues and blood cells from a human cDNA library. The NLRC5 mRNA expression level was normalized to GAPDH expression and is represented relative to the NLRC5 expression in CD4^{+} T cells (set to 1). The reactions were performed in replication. Mean ± SD (n=3) is depicted. The order was determined by increasing NLRC5 mRNA expression.

C) RT-PCR analysis of NLRC5 mRNA levels of the indicated cell lines. GAPDH served as a control.

D) Schematic representation of putative NLRC5 splice variants. Position of effector domain (DD), nucleotide-binding domain (NACHT) and leucine-rich repeats (LRR) domain is highlighted with white/grey boxes. The italic numbers refer to amino acid numbers. Uniprot database (www.uniprot.org) accession number is indicated on the left.

E) RT-PCR analysis of the indicated tissue samples and cell types using isoform specific primer pairs. NLRC5 wildtype (also termed full length or isoform 1) expression, isoform 3 expression and isoform 4/5 expression (detection of missing exon 25) was accessed using the indicated primer pairs. Plasmids encoding full-length NLRC5 (wt) or NLRC5 isoform 3 or 4 (iso 3/4) served as controls. Amplification of GAPDH served as a standard.

As already mentioned, the LRR region of NLRC5 is unusually long, and modelling indicated a large helical conformation rather than the typical horseshoe structure of other NLRs. For other NLR proteins like NOD1 and NOD2, it has been shown, that activation by an elicitor is completely based on the presence of the LRR region (Girardin *et al.*, 2005; Tanabe *et al.*, 2004), and to date, there is some evidence for a direct interaction between elicitor and LRR in the case of both NOD1 and NOD2 (Grimes *et al.*, 2012; Mo *et al.*, 2012; Laroui *et al.*, 2011). Thus, different truncated versions of the LRRs might give rise not only to different elicitor sensing specificities of NLRC5 but might also change the LRR domain from the helical to a classical horseshoe-like structure found in other LRRs. Of note, isoform 3 lacking the whole LRR region was the prevalent cDNA obtained. Sequence analysis revealed that a differential splicing of exon 5 leads to a premature stop codon introduction. Another cDNA sequence we obtained (isoform 4) is almost identical to full length NLRC5, except lacking exon 25, which leads to a deletion of the amino acids 1221 to 1249. To elucidate the presence of these splice variants in different tissues, we designed a primer pair allowing the specific amplification of isoform 3. Moreover, another primer pair was used to detect the deletion of exon 25 present in isoform 4 and also 5. Both primer pairs were able to specifically amplify the corresponding isoforms as shown by PCR using plasmids containing full-length or NLRC5 isoform DNA. Analysis of different tissues with high expression of NLRC5 full-length (Figure 3.1 B) revealed NLRC5 isoform 3 expression in CD4^{+}, CD8^{+} cells, lymph nodes and to a lesser extend in colon (Figure 3.1 C). However, expression of

isoform 4/5 was detected only at very low levels in CD4^{+} cells, lymph node and colon and slightly stronger in CD8^{+} cells. Similar to full-length NLRC5, also isoform 3 and isoform 4/5 were absent in muscle cells. In HeLa and THP-1 cells that strongly express NLRC5 full-length, NLRC5 isoform 3 was not robustly detectable; however isoform 4/5 was expressed at low levels in THP-1 cells (Figure 3.1 E).

Expression of many NLRs is induced by many PAMPs and inflammatory cytokines. NOD2 expression, for example, is upregulated by bacterial challenge, single-stranded RNA and IFN-γ (Sabbah *et al.*, 2009; Oh *et al.*, 2005; Rosenstiel *et al.*, 2003). Furthermore, it was recently shown that NF-κB-mediated signalling is a prerequisite of NLRP3 activation by inducing NLRP3 expression (Bauernfeind *et al.*, 2009). We therefore ask, whether the expression of NLRC5 might also be influenced by PAMP stimulation and/or inflammatory mediators. We could previously show, that NLRC5 is robustly expressed in CD14^{+} cells as well as in mononuclear cells, so we analysed the expression of NLRC5 in the human monocytic cell line THP-1. Although, we could detect NLRC5 expression on mRNA level in these cells, the expression level was not upregulated after 6 h challenging with tumor necrosis factor (TNF), muramyl dipeptide (MDP), lipopolysaccharide (LPS), phorbol 12-myristate 13-acetate (PMA) or Pam3CSK4 (activation of TLR1 and TLR2) in comparison to untreated control cells. All of the tested compounds induced inflammatory responses in the cells, monitored by induction of IL-8 mRNA. However, no obvious changes in NLRC5 mRNA levels were observed (Figure 3.2 A).

Similar to THP-1, epithelial HeLa cells also express detectable amounts of NLRC5 on mRNA level (Figure 3.1 B). Interestingly, expression was highly inducible in HeLa cells after stimulation with the dsRNA analog poly(I:C) in these cells, as detectable on mRNA level (Figure 3.2 B) and on protein level (Figure 3.2 C). Moreover, whereas NLRC5 protein levels were at the detection limit in untreated HeLa cells, NLRC5 was robustly detectable after 24 h of poly(I:C) treatment (Figure 3.2 B). Furthermore, poly(I:C) failed to induce NLRC5 expression in the colon cell line CaCo2 (Figure 3.2 C). CaCo2 cells are known to be deficient of TLR3 signalling (Vijay-Kumar *et al.*, 2005; Alexopoulou *et al.*, 2001) indicating that NLRC5 expression is induced by poly(I:C) in a TLR3-dependent manner (Figure 3.2 C). To substantiate that the induction of NLRC5 was mediated by the TLR3 pathway and not by other pattern recognition receptors activated by poly(I:C), siRNA-mediated knock-down of TLR3 and its downstream kinase TBK1 were performed. This kinase is pivotal for the phosphorylation of IRF3 and thus expression of IFN-β (Fitzgerald *et al.*, 2003b). Knock-down of TBK1 was assured by Western blot and demonstrated that NLRC5 induction upon poly(I:C) stimulation was mediated by the TLR3/TBK1 pathway (Figure 3.2 D) . Thus, upregulation of NLRC5 by poly(I:C) is dependent on a functional TLR3 signalling pathway activation.
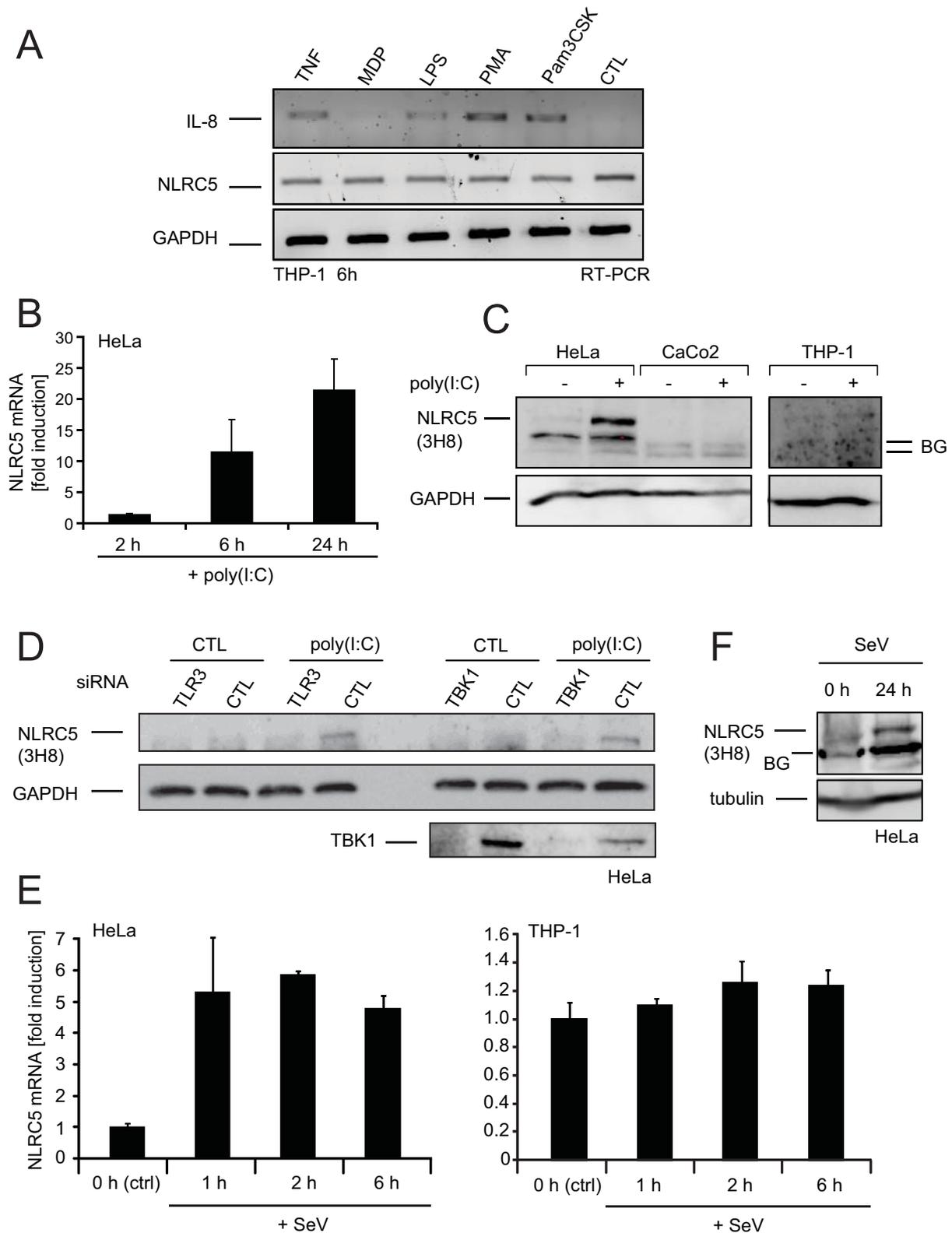
Figure 3.2 Induction of NLRC5 expression by viral PAMPs

A) NLRC5 mRNA levels of PAMP-treated THP-1 cells. THP-1 cells were treated with 50 ng/ml tumor necrosis factor (TNF), 1 µM muramyl dipeptide (MDP), 50 ng/ml lipopolysaccharide (LPS), 0.5 µM phorbol 12-myristate 13-acetate (PMA), or 100 ng/ml Pam3CSK. After 6 h of PAMP stimulation, RNA was extracted and cDNA synthesis was performed. RT-PCR was conducted amplifying NLRC5 and GAPDH cDNA as a control. Interleukin-8 (IL-8) served as internal control for successful stimulation.

B) Quantitative RT-PCR expression analysis of HeLa cells stimulated with 100 µg/ml poly(I:C) for the indicated time points. The data are normalized to GAPDH. Mean ± SD (n=3) is depicted.

C) Western blot analysis of HeLa cells, CaCo2 cells or THP-1 cells treated with 100 µg/ml poly(I:C) for 24 h. Detection with anti-NLRC5 3H8 is shown. BG indicates background bands. Reprobing with GAPDH served as loading control.

D) HeLa cells were transfected with siRNA targeting TLR3 or TBK1 or transfected with a non-targeting control CTRL for 48 h. After 48 h, the cells were stimulated with 100 µg/ml poly(I:C) for additional 24 h or left untreated. Detection with anti-NLRC5 3H8 is shown, reprobing with TBK1 served as knockdown control (bottom panel). Reprobing with GAPDH served as loading control.

E) Quantitative RT-PCR analysis of HeLa and THP-1 cells, treated with SeV for the indicated time. The data are normalized to GAPDH expression. Mean ± SD (n=3) is depicted.

F) Western blot analysis of HeLa cells treated for 24 h with Sendai virus. Detection with the anti-NLRC5 antibody 3H8 is shown. Probing for anti-tubulin served as a loading control.

A commonly used viral infection model in innate immunity is the single-stranded RNA containing Sendai Virus (SeV) model, which mainly leads to the activation of the RIG-I pathway, resulting in type I IFN expression. Based on the poly(I:C) dependent upregulation of NLRC5, we wondered, whether infection with SeV also induces NLRC5 expression. In line with the upregulation by poly(I:C), infection of cells with SeV led to an approximately 6-fold increase in NLRC5 mRNA levels in HeLa cells (Figure 3.2 E) and increased protein expression (Figure 3.2 F). In contrast, as with poly(I:C), only a marginal (below 2-fold) induction of NLRC5 mRNA was obtained in THP-1 upon SeV infection (Figure 3.2 E). This showed that not only double-stranded RNA but also single-stranded RNA or other viral signatures on SeV are able to induce NLRC5 expression. Furthermore, these experiments revealed that NLRC5 is differentially inducible in different cell types.

3.1.3 Innate Immune Signalling of NLRC5

Most NLRs activate pro-inflammatory pathways such as NF-κB or IL-1β processing (Kufer and Sansonetti, 2011). Since NLRC5 is mainly expressed by cells and tissues of the immune system and is highly inducible upon viral stimuli, we assumed a role for NLRC5 in one of these pathways. To test the ability of NLRC5 to activate a specific immune related pathway, we performed luciferase reporter assays in HEK293T cells (Zurek *et al.*, 2011). This method is based on the fact, that overexpression of NLR proteins as for example NOD1 and NOD2 induces autoactivation, which is mediated by oligomerization of these proteins (Ogura *et al.*, 2001; Inohara *et al.*, 1999). We assumed that this property is shared by NLRC5. Indeed, overexpression of NLRC5 in HEK293T cells induced specific homooligomerization of NLRC5, whereas NLRC5 did not strongly interact with NLRP3 or NOD1. Thus, NLRC5 was also able to homooligomerize and

the reporter assay is also feasible for NLRC5 (Figure 3.3 A). Next, we tested the ability of NLRC5 to activate signalling pathways, which play important roles in immune signalling. Increasing amounts of NLRC5 were expressed in HEK293T cells, and activation of inflammatory pathways was monitored using luciferase-reporter constructs. NF-κB, IFN-β, IRF3 (data not shown), IRF7, and ISRE reporter were tested, because they represent the most relevant innate immune pathways induced by viral and bacterial pathogens (Akira *et al.*, 2006).
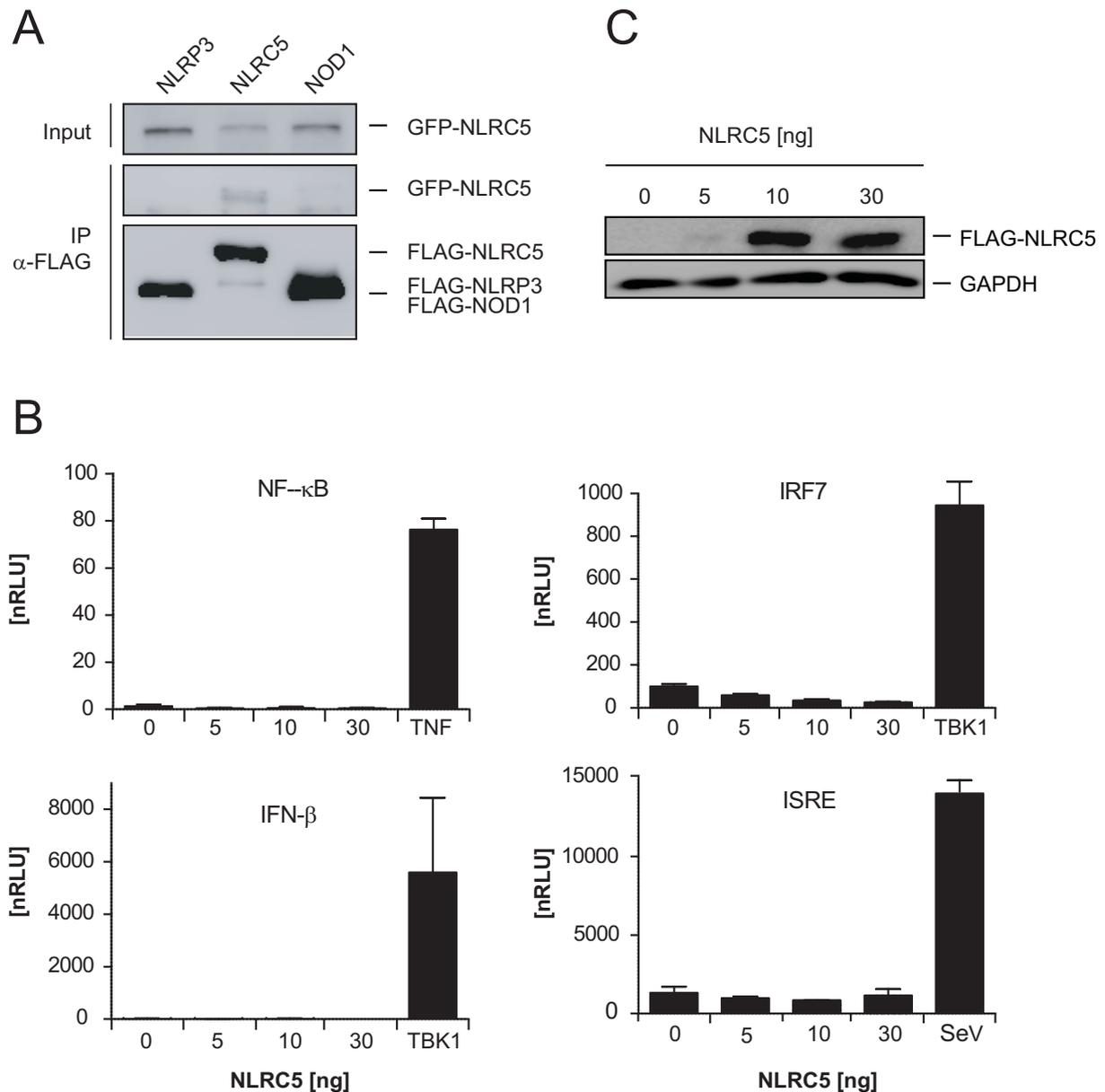
Figure 3.3 NLRC5 oligomerization and signalling
A) FLAG-tagged NLRs (NLRP3, NLRC5 and NOD1) were coexpressed with GFP-tagged NLRC5 in HEK293T cells for 24 h. FLAG-NLRC5 were immunoprecipitated with anti-FLAG antibody and GFP-NLRC5 was detected in the lysate (Input) or in the immunoprecipitation (IP).

B) Effect of NLRC5 on NF-κB, IRF7, IFN-β or ISRE signalling pathways using a HEK293T-based luciferase reporter assay in 96 wells. TNF stimulation, TBK1 overexpression or SeV infection served as internal positive controls. Read-out was performed 16 h after transfection. Depicted are normalized relative light units (nRLU) of triplicate measurements (Mean (n=3) ± S.D).
C) Expression control of variant amounts of NLRC5 taken from ISRE-luciferase promoter activation assay. Blots were probed with anti-FLAG antibody and reprobed with anti-GAPDH antibody.

Although the tested reporter were significantly inducible by appropriate controls like TNF stimulation (for NF-κB pathway induction) or SeV-infection/TBK1 overexpression (for IFN pathway induction), we were not able to activate any reporter by transfection of increasing amounts of NLRC5 (Figure 3.3 B). Expression of NLRC5 was further verified on protein level by western blot analysis in one representative experiment (Figure 3.3 C). To rule out the possibility that the failure of NLRC5 to induce inflammatory pathways was due to negative regulation by its LRRs, we repeated the experiments with a form of NLRC5 lacking the LRR domain (Isoform 3; Figure 3.1 C). This protein formed a SDS stable dimer when overexpressed in HEK293T cells, likely being indicative for robust autoactivation (later depicted in figure 3.12 E). However, using this construct we obtained virtually the same result as with full-length NLRC5 (data not shown), suggesting that NLRC5 indeed is unable to activate the tested pathways upon overexpression in HEK293T cells.

In conclusion, NLRC5 failed to induce the most prominent inflammatory pathways, suggesting either, that an essential adaptor is lacking in HEK293T cells, or that NLRC5 is linked to signalling pathways that have not been tested here.

To date, most of the already characterized NLR proteins are involved in innate immunity activation, although some NLRs also possess inhibitory function on innate immune pathways (reviewed in Kufer and Sansonetti, 2011). A very prominent example is the mitochondrial-located NLRX1, which was reported to inhibit antiviral immunity and NF-κB signalling (Allen *et al.*, 2011; Xia *et al.*, 2011). Taking this into consideration together with the fact, that NLRC5 is upregulated in response to viral infection, we wondered, whether NLRC5 is capable of inhibiting innate immune signalling pathways. To test our hypothesis, we transfected HEK293T cells with increasing amounts of NLRC5 and NF-κB or IFN-β reporter system. Additionally, cells were stimulated either with TNF to activate NF-κB or IFN-β was activated by overexpression of TBK1 or infection with SeV. Interestingly, overexpression of NLRC5 significantly impaired IFN-β reporter activation in HEK293T cells without affecting NF-κB, supporting a role for NLRC5 in type I interferon responses (Figure 3.4).
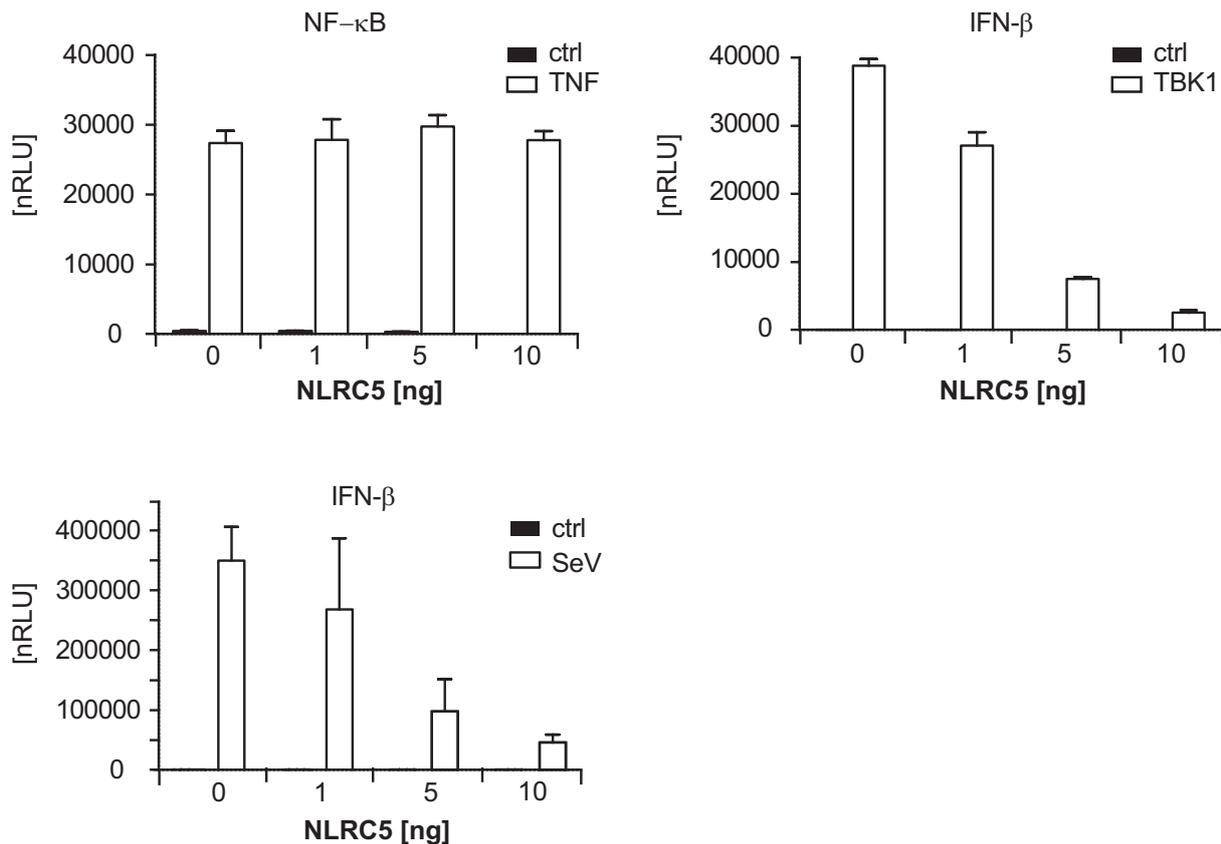
Figure 3.4 NLRC5 influences type I interferon signalling
Effect of NLRC5 overexpression on activated NF-κB or IFN-β signalling using HEK293T-based luciferase reporter assays. NF-κB signalling was activated using TNF, IFN-β signalling was activated using TBK1 overexpression or SeV infection. Read out was performed 16 h after transfection. Mean of three replicates indicated in normalized relative light units (nRLU) ± SD.

3.1.4 NLRC5 involvement in mounting interferon responses to viral infection

During our analysis, we observed that poly(I:C) and SeV induced NLRC5 expression (Figure 3.2). It is well established, that both poly(I:C) and SeV trigger type I IFN production, either by the TLR3 pathway (Alexopoulou *et al.*, 2001) or by the intracellular RLR RIG-I (Kato *et al.*, 2008). Furthermore, in our cell-based luciferase reporter assays, we detected an NLRC5-dependent in-hibition of the IFN-β promoter upon activation, either by overexpression of TBK1 or by SeV infection. Thus, we wanted to elucidate a possible role for NLRC5 in viral recognition. To ex-plore, whether endogenous NLRC5 might have an impact on SeV-mediated responses, we set up a system to conduct siRNA-mediated gene knock-down in phorbol 12-myristate 13-acetate (PMA) differentiated THP-1 cells, because these cells showed the highest basal expression of NLRC5 (Figure 3.1). siRNA transfected cells were treated for 16 h with SeV and supernatant and cells were collected. Type I interferons are predominately induced by SeV in human cells (Hua *et*

al., 1996). We therefore measured secreted IFN-α/β using a type I interferon-specific reporter cell line-based bioassay. NLRC5 knock-down reduced secretion of IFN-β compared to mock treatment with a nontargeting siRNA (control) (Figure 3.5 A).

NLRC5 knock-down efficiency was controlled in cell lysates of the same experiment and showed robust reduction of NLRC5 protein levels (Figure 3.5 B).

Moreover, we measured IFN-β mRNA levels by quantitative RT-PCR simultaneously from the same experiments. In correlation with the bioassay data, IFN-β mRNA levels were strongly induced by Sendai virus but showed a reduced induction in cells lacking NLRC5 (Figure 3.5 C). Although the results were highly reproducible, variances in the siRNA efficiency between experiments impaired the generation of highly significant results. Importantly, however, reduction of the cytokine responses correlated with the knock-down efficiency of the two siRNA duplexes used, making it unlikely that the effect was due to off-target effects of the used siRNAs.

To substantiate these results, we also assayed SeV-induced cytokines in THP-1 cells treated with the NLRC5 siRNA in comparison with mock treated cells. This showed a reduced release of RANTES (CCL5), MIP1α (CCL3), and IP-10, all cytokines well known to be induced by SeV in primary human cells (Matikainen *et al.*, 2000; Hua *et al.*, 1996) (Figure 3.5 D and E). The cytokine RANTES (CCL5) is highly inducible by type I IFN due to an IRF3-binding site in its promoter and plays an important role in viral recognition (Appay and Rowland-Jones, 2001; Song *et al.*, 2000). In particular together with the cytokines MIP1α (CCL3) and IP-10, it has been reported, that these cytokines were strongly upregulated upon SeV infection (Matikainen *et al.*, 2000; Hua *et al.*, 1996). Taken as a second read out, we performed an ELISA to detect RANTES release from NLRC5 knock-down cells upon SeV infection. Similar to type I IFN secretion (refer to Figure 3.5 A), also RANTES secretion was significantly reduced in NLRC5 knock-down cells (Figure 3.5 F). Moreover, RT-PCR confirmed reduced RANTES mRNA expression in cells lacking NLRC5 after SeV challenge (Figure 3.5 G).

A

B

C

D

E

F

G
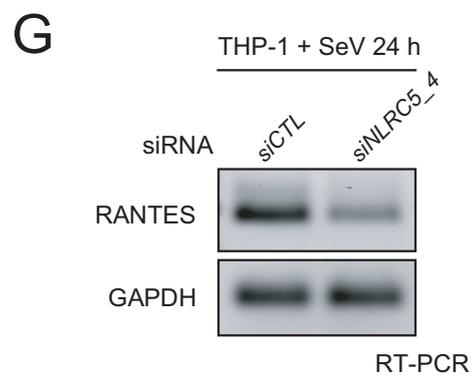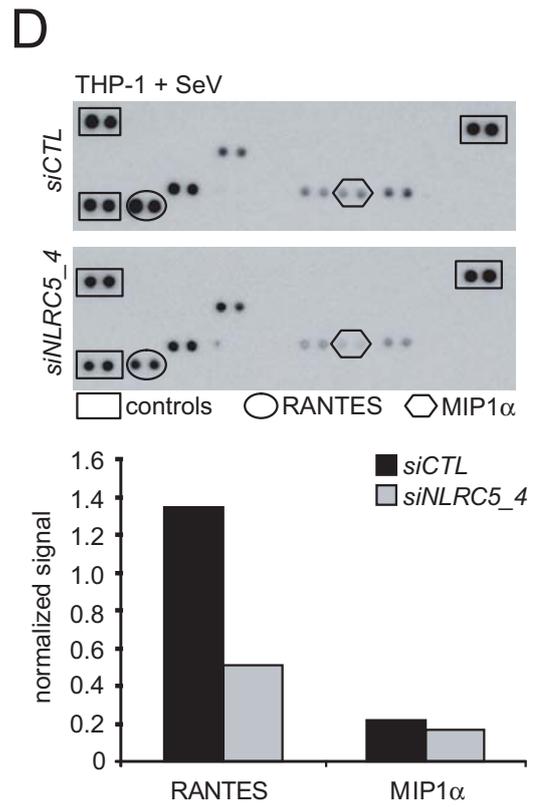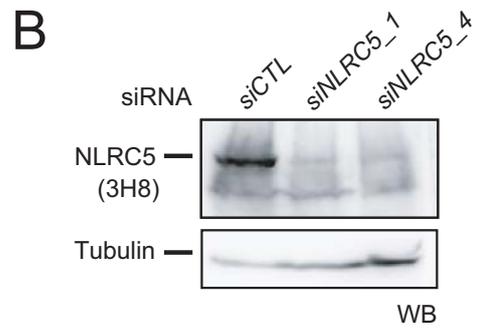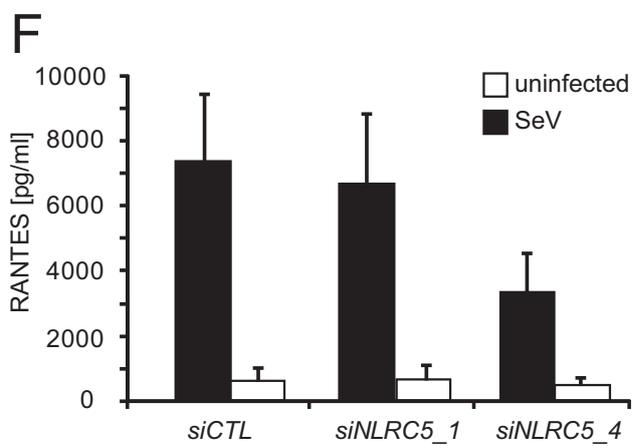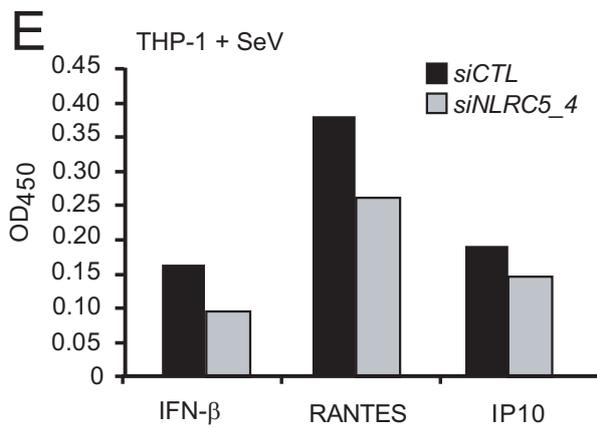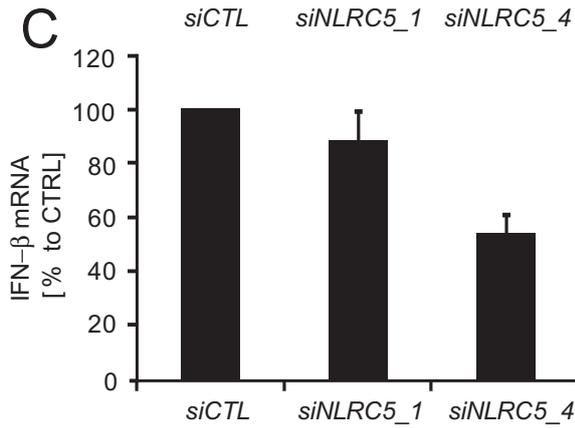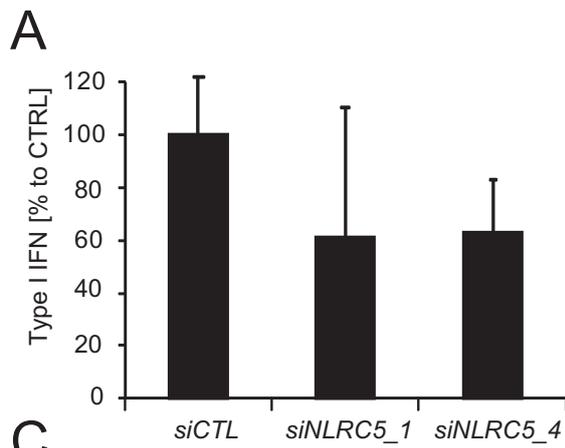
Figure 3.5 NLRC5 impacts on Sendai virus-mediated type I interferon repsonses
THP-1 cells were differentiated using PMA and afterwards treated with the indicated siRNAs for 72 h. After incubation, cells were stimulated with Sendai virus or left untreated as controls. A non-targeting siRNA was used as a control (siCTL).
A) Type I interferon release were assayed using a type I interferon secreted alkaline phosphatase reporter cell line (HEK-Blue™ IFN-α/β cells). The data are shown relative to control, with siCTL set to 100 %. Depicted are mean ± SD (n=3).
B) NLRC5 expression levels for siCTL and knock-down conditions were visualized on western blot using anti-NLRC5 3H8 antibody. Reprobing with anti-tubulin served as loading control.
C) IFN-β mRNA levels were assayed by quantitative RT-PCR from the same experiment, depicted in A. The data are normalized to GAPDH expression (n=2). siCTL expression levels were set to 100 %.
D) Analysis of the cytokine secretion profile after SeV infection of THP-1 cells treated with control siRNA (siCTL) or the NLRC5 specific siNLRC5_4 siRNA using a Western-based array. Densitometric quantification of the signals for RANTES and MIP1α, normalized to the controls are shown in the lower panel.
E) ELISA of the supernatants from A for IFN-β, RANTES and IP-10 protein levels.
F) RANTES cytokine secretion levels in the cell supernatant of THP-1 cells were measured by ELISA 16 h after Sendai virus infection (grey bars) or from untreated cells (white bars).
G) RANTES mRNA levels in THP-1 cells infected for 24 h with Sendai virus, either transfected with a non-targeting siRNA (siCTL) or siNLRC5_4 siRNA for 72 h. GAPDH levels served as a loading control.

To expand our results to primary cells, we used primary human dermal fibroblasts. First, we confirmed the expression of NLRC5 in these cells by RT-PCR. As observed for HeLa cells, treatment of human fibroblasts with 100 μg/ml poly(I:C) for 16 h led to significant induction of NLRC5 mRNA in cells derived from two different donors (male and female) (Figure 3.6 A). Next we conducted siRNA-mediated knock-down of NLRC5 in these cells for 72 h. Knock-down of NLRC5 with two different siRNA duplexes led to reduced type I IFN and RANTES release both after poly(I:C) and after SeV treatment (Figure 3.6 B and C). As seen in THP-1 cells both siRNA duplexes reduced the responses to different levels, correlating to their knock-down efficiency as evaluated by RT-PCR from the same experiment (Figure 3.6 D).

Although all donors showed slight variations in the response to poly(I:C) and SeV, the quality of the responses upon NLRC5 knock-down was comparable in all experiments. siNLRC5_4 was very potent in knocking down NLRC5 in donor 1 but less potent in donor 2, nevertheless, RANTES release was almost completely abolished in NLRC5 knock-down cells in response to both poly(I:C) and SeV. This led us to conclude that NLRC5 is needed for the efficient induction of anti-viral responses induced by the interferon pathway in human cells.
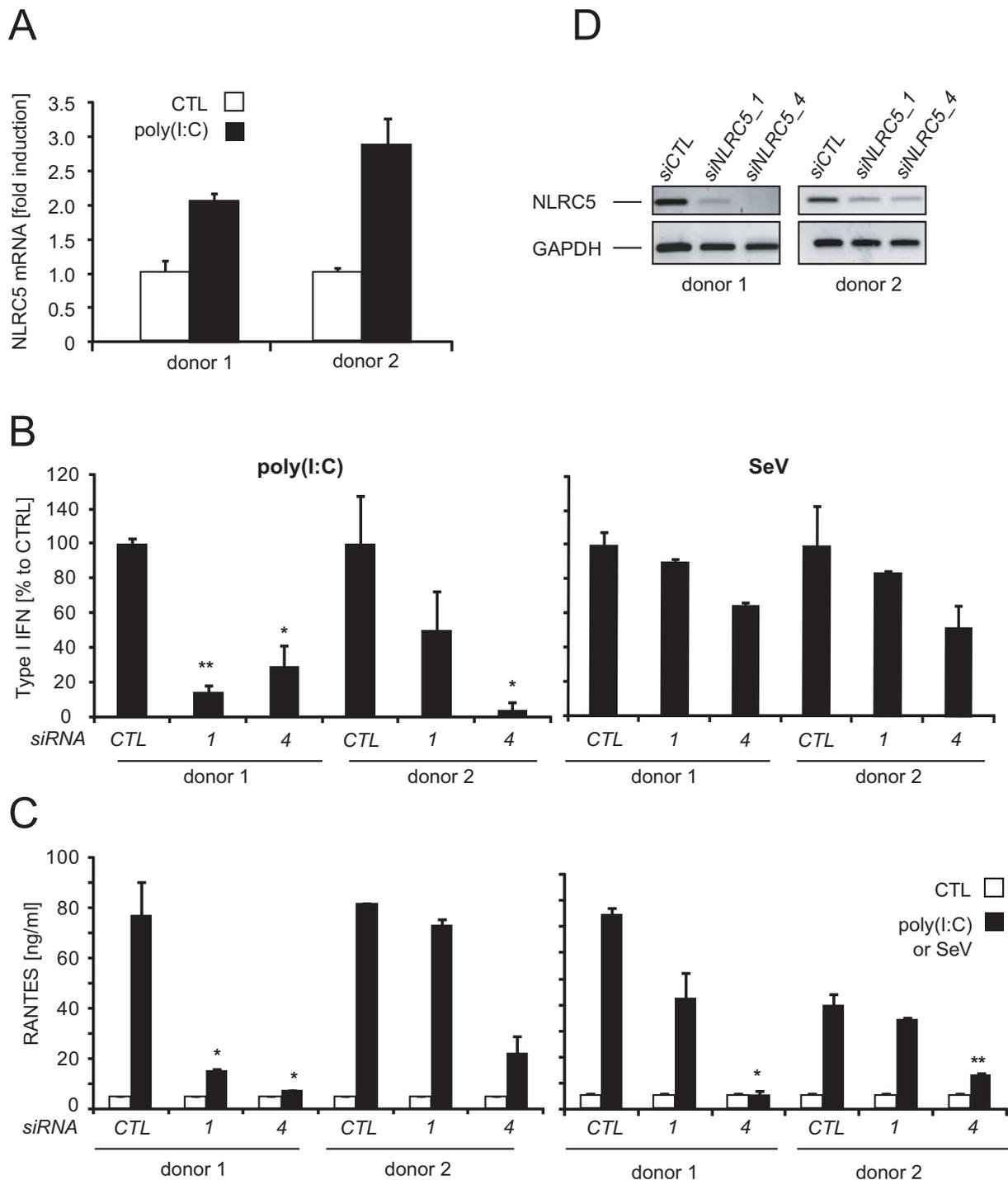
Figure 3.6 Influence of NLRC5 on type I interferon signalling in primary human dermal fibroblasts (hFibr)

A) NLRC5 mRNA levels measured using quantitative RT-PCR analysis after 24 h treatment with 100 µg/ml poly(I:C). The data is normalized to GAPDH expression and control conditions (CTL) were set to 100% for each donor.

B) Type I interferon secretion levels of hFibr, transfected with siRNA as indicated for 72 h. After transfection, cells were stimulated with 100 µg/ml poly(I:C) or infected with Sendai virus for 16h. Type I interferon levels were assayed using a type I interferon secreted alkaline phosphatase reporter cell line (HEK-Blue™ IFN-α/β cells). Data are relative to CTL, set to 100%.

C) RANTES secretion levels from the same supernatants used in B after 16h of poly(I:C) or Sendai virus treatment (grey bars) or mock treatment (white bars). Data were analysed using a two-sided student's *t* test. (*) p<0.05; (**) p<0.005

D) NLRC5 mRNA expression levels of the experiments, shown in B and C. GAPDH expression served as a loading control.

3.2 NLRC5 controls basal MHC class I gene expression in an MHC enhanceosome-dependent manner

3.2.1 NLRC5 contributes to MHC class I gene expression

During the first part of this thesis, several reports analysed NLRC5 with conflicting results for many of the reported functions, including its ability to activate MHC class I transcription and its accurate function in immune signalling pathways still remains unresolved. To address these unresolved issues, we first tested the ability of our NLRC5 constructs to activate MHC class I promoter regions in an HEK293T-based luciferase reporter assay (Zurek *et al.*, 2011). For that purpose, we cotransfected various amounts of an NLRC5 expression vector (1 to 10 ng plasmid) in HEK293T cells together with HLA class I A (HLA-A) and B (HLA-B) gene promoter reporter constructs (described in Gobin *et al.*, 2001). Expression of NLRC5 significantly activated HLA-A and HLA-B luciferase reporter expression in this system (Figure 3.7 A).

Moreover, overexpression of NLRC5 but not of NOD1 or NOD2 increased MHC class I protein levels in HEK293T cells (Figure 3.7 B). Thus, overexpression of NLRC5 significantly activates MHC class I promoter regions, resulting in an upregulation of MHC class I protein expression.
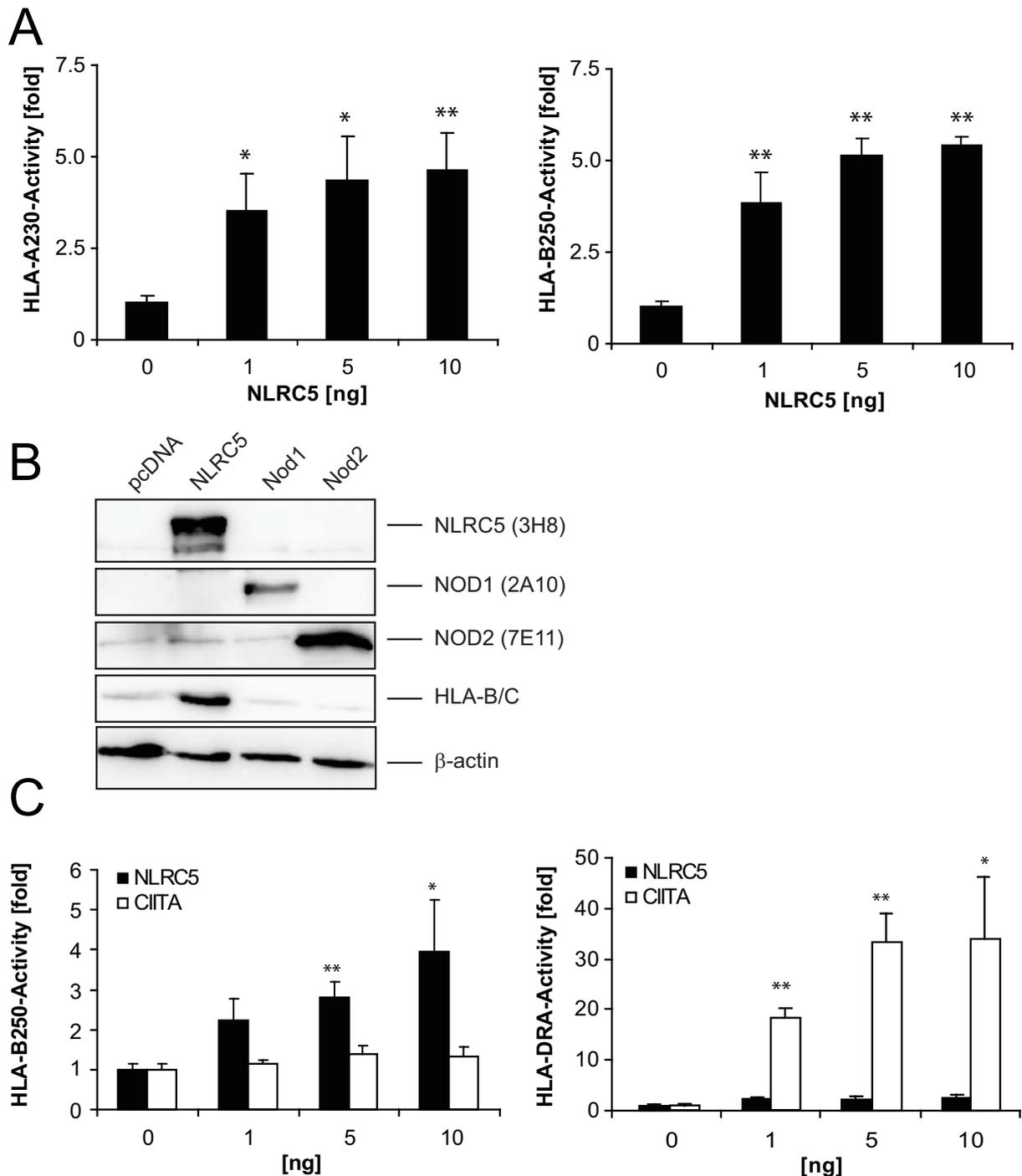
Figure 3.7 NLRC5 induces classical HLA class I promoter activation
A and C) HEK293T cells were transiently transfected with NLRC5 (A and C) or CIITA (C) in the presence of a HLA class I promoter driven luciferase expression plasmid (HLA-A or HLA-B) or a HLA-DRA class II promoter driven luciferase expression plasmid. Luciferase activity was measured 20 h after transfection and normalized to β-galactosidase expression. Depicted are mean (n=3) ± SD. Data were analysed using a two-sided student's *t* test. (*) p<0.05; (**) p<0.005
B) Western Blot analysis of HEK293T cells transiently transfected with empty vector, NLRC5, NOD1 or NOD2. Expression of endogenous MHC class I molecules was visualized using anti-HLA-B/C (HC10) antibody. Expression of NLR proteins was visualized using anti-NOD1 2A10, anti-NOD2 7E11 or anti-NLRC5 3H8 as indicated. Reprobing with anti-GAPDH served as loading control.

Although, NLRC5 is referred to be a member of the Nodosome containing NLR proteins (Kufer and Sansonetti, 2011), it shows the closest homology within the NLR gene family to the MHC class II transcriptional activator (CIITA) in their NACHT and LRR domain (Istomin and Godzik, 2009; Proell *et al.*, 2008). CIITA as an outstanding member of the NLR protein family does not play a role in pattern recognition, but its function is clearly defined as transcriptional activation (reviewed in Reith *et al.*, 2005). This makes a functional analogy between these two NLR proteins plausible. Therefore, we compared the ability of NLRC5 and CIITA to activate HLA class II and I reporter gene constructs in HEK293T cells, respectively. Whereas NLRC5 expression resulted in a significant and dose-dependent HLA class I induction, its effect on an HLA class II DRA promoter reporter construct was negligible. Vice versa, CIITA activated the HLA-DRA promoter strongly and showed a low, but reproducible activation of HLA-B promoter (Figure 3.7 C).

Overexpression of NLRC5 strongly activated MHC class I expression therefore knock-down of endogenous NLRC5 in THP-1 should result in a decrease in MHC class I expression. Indeed, knock-down of NLRC5 in the myeloid macrophage-like cell line using siRNA robustly reduced mRNA levels of endogenous NLRC5 (Figure 3.8 A) and led to a decreased expression of HLA-B mRNA and HLA class I cell surface expression (Figure 3.8 B).
Similar results were also obtained in HeLa cells (Figure 3.8 C). In all cases, transfection of control siRNA (siCTL) had no effect on NLRC5 or MHC class I gene expression as compared with untreated cells (Figure 3.8 A and C).

We also analysed nontransformed primary human dermal fibroblasts, in which we induced high levels of NLRC5 expression by treatment with poly(I:C) (refer to Figure 3.2 B). For both NLRC5-specific siRNA duplexes, knock-down of NLRC5 correlated with a reduction in endogenous HLA-B mRNA expression levels. Similar results were obtained in two different donors (male and female), independently. Moreover, knock-down of NLRC5 also diminished HLA-B expression triggered by SeV infection (Figure 3.8 D).

Taken together, this strongly suggests that NLRC5 is involved in the control of constitutive MHC class I gene expression.
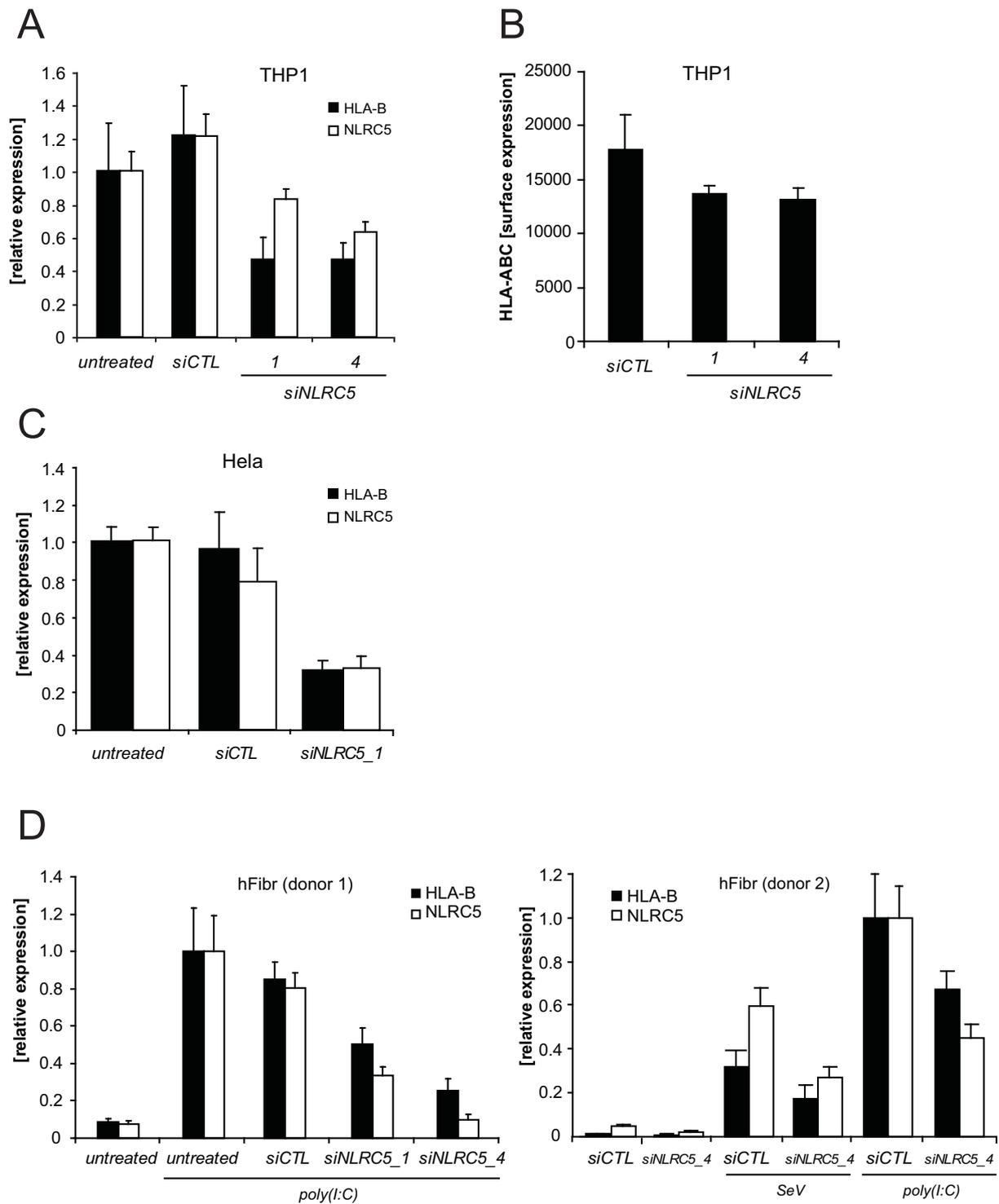
Figure 3.8 NLRC5 contributes to MHC class I expression

A) THP-1 cells were differentiated using PMA and afterwards treated with the indicated siRNAs for 72 h. HLA-B or NLRC5 mRNA expression was measured using quantitative RT-PCR. THP-1 cells were either left untreated (untreated), or treated with the siRNAs as indicated below. GAPDH expression was used as normalization control.

B) Same experimental setup as in A. HLA-A/B/C surface expression was measured in FACS analysis in the different knock-down conditions (indicated below). The experiment was performed in duplicates.

C) HeLa cells were transfected with a non-targeting siRNA (siCTL) or NLRC5-targeting siRNA (siNLRC5_1) for 72 h. HLA-B or NLRC5 mRNA expression was measured using quantitative RT-PCR.

D) Primary human dermal fibroblasts from two different donors (male and female) were transfected with a non-targeting siRNA (siCTL) or NLRC5-targeting siRNA (siNLRC5_4) for 72 h. HLA-B and NLRC5 expression levels were measured after 16h of poly(I:C) or Sendai virus treatment to induce HLA expression in control or NLRC5 knock-down conditions. The expression was normalized to GAPDH and poly(I:C) treated control conditions (untreated, left graph; siCTL, right graph) were set to 1.

3.2.2 MHC class I gene expression correlates with NLRC5 expression levels

Although, MHC class I expression is nearly ubiquitous on nucleated cells, strong differences can be found in expression levels between different cell types and tissues (van den Elsen *et al.*, 2004; Burke and Ozato, 1989). In previous experiments, we could clearly point out, that the expression profile of NLRC5 also shows strong differences between cell types and tissues (Figure 3.1 A).

Based on the previous findings, we asked whether NLRC5 levels correlate with basal HLA class I gene expression in human tissues. Comparison of HLA class I B mRNA expression levels with those of NLRC5 revealed a close correlation between the expression levels of both genes in tissues with non to very low (skeletal muscle and heart), intermediate (liver, kidney, prostate, thymus, and colon), or high expression (resting CD8$^+$ T cells). However, in some tissues, such as brain and lung, the expression levels were more disparate (Figure 3.9 A). These results are compatible with a positive role for NLRC5 in MHC class I gene expression but also suggest that, at least in certain tissues, other factors contribute to the overall expression levels.

Several tissues and cell lines show very low to undetectable MHC class I expression (van den Elsen *et al.*, 2004; Martin *et al.*, 1997). One example is the murine melanoma cell line B16 and its various sublines (Krawczyk *et al.*, 2008; Martin *et al.*, 1997). In collaboration with Viktor Steimle and Galaxia Rodriguez, B16F10 cells were transfected with an empty vector or with vectors expressing EGFP-NLRC5, EGFP-NLRC5 K234A or EGFP-CIITA. Analysis of transiently transfected cells showed that NLRC5 robustly induced MHC class I expression, whereas CIITA induced MHC class II expression. Expression of a Walker A mutant of NLRC5 (EGFP-NLRC5 K234A) had no effect on MHC class I expression (Figure 3.9 B).
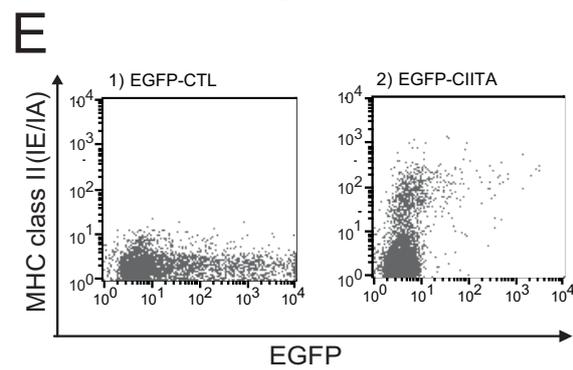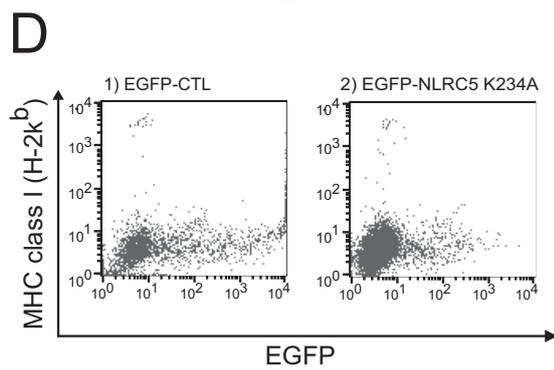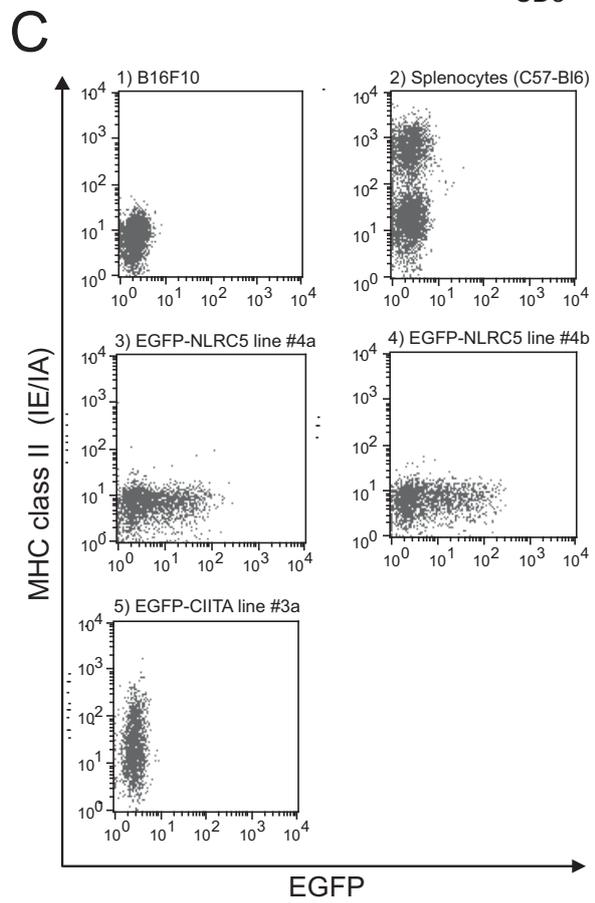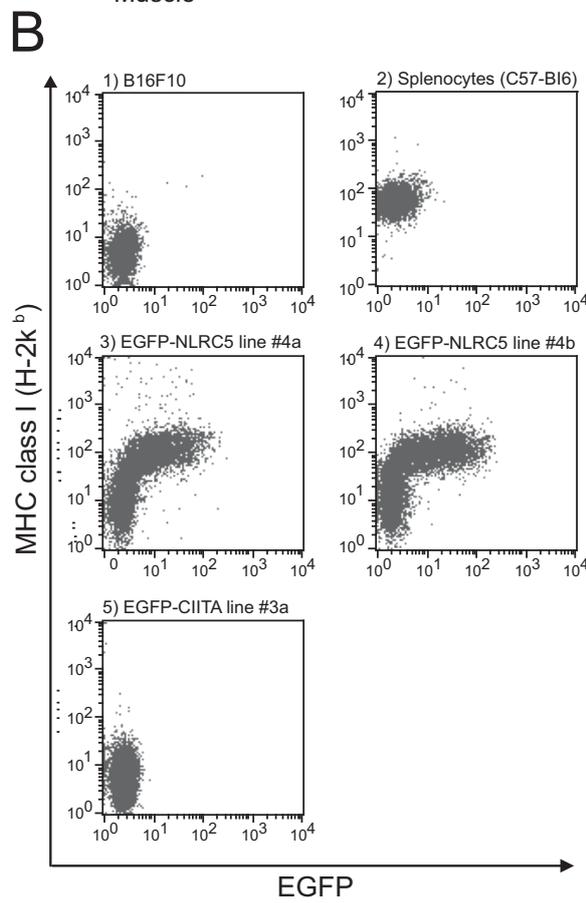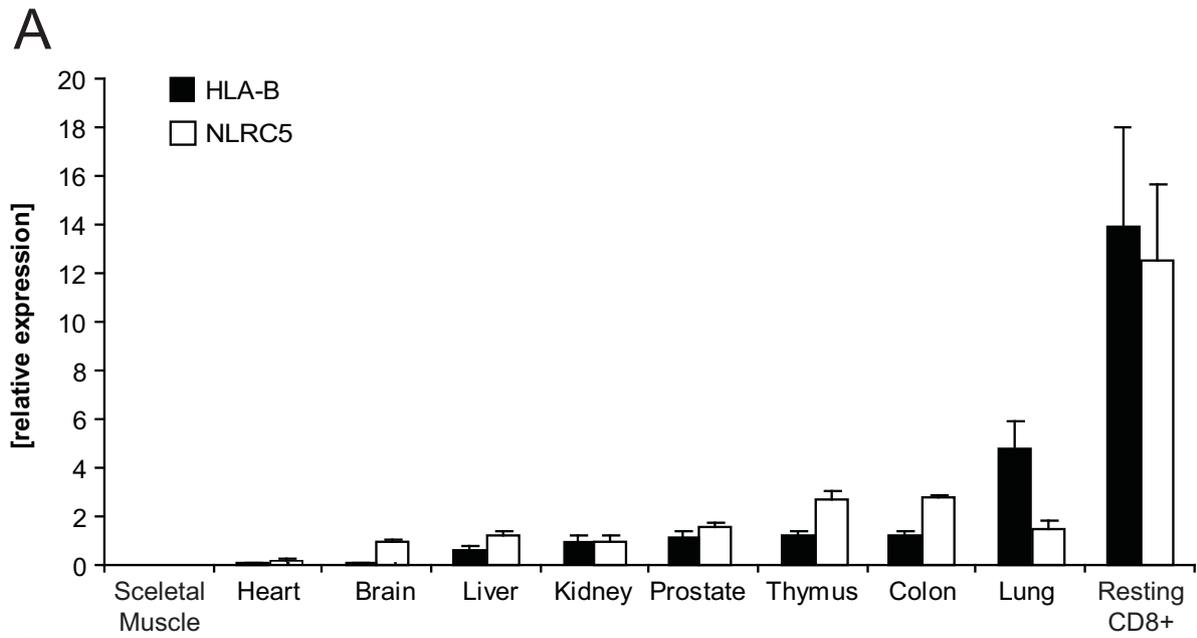
Figure 3.9 NLRC5 expression levels correlate with MHC class I expression levels.
A) Relative HLA-B (black bars) and NLRC5 (white bars) expression in selected human tissues and cells. HLA-B and NLRC5 expression normalized to GAPDH expression is shown. NLRC5 and HLA-B expression in kidney was set to 1. Bars represent means ± SD (n=3). Tissues were assigned according to increasing HLA-B expression levels.
B - C) Surface expression of MHC class I (H-2k^b) or MHC class II (IE/IA) molecules in the murine cell line B16F10. Cells were stably transfected with EGFP-NLRC5 or EGFP-CIITA constructs and cultivated for 4 weeks in selection medium prior FACS analysis. Murine splenocytes served as positive controls. Flow cytometry analysis for EGFP and MHC class II signals are shown.
D - E) Same experimental setup as in B and C. Flow cytometry analysis was performed after 5 days of transfection as indicated above.
The experiments were performed in collaboration with G. Rodriguez and V. Steimle.

After 2 weeks of selection with appropriate antibiotics, NLRC5-transfected B16F10 cells were sorted once with antibody and magnetic beads for MHC class I-positive cells, whereas CIITA-transfected cells were enriched for MHC class II-positive cells (Figure 3.9 B and C).

In parallel experiments, we were unable to enrich for MHC class I-positive or class II-positive cells in vector- or NLRC5-K234A–transfected cells, showing that B16F10 cells are negative or nearly negative for MHC class I and II and that EGFP-NLRC5 K234A does not activate MHC class I expression (Figure 3.9 D).

Stable expression of EGFP-NLRC5 induced endogenous MHC class I gene and protein expression levels very substantially in two independently transfected and selected cell populations (Fig. 3.9 B3 and B4). Remarkably, MHC class I levels in the EGFP-positive cells were comparable to those found on freshly isolated murine splenic lymphocytes (Fig. 3.9 B2). The distinctive kink in the dot plots showing EGFP-NLRC5 expression on the x-axis and MHC class I (H-2K^b) on the y-axis (Figure 3.9 B3 and B4) suggests a threshold mechanism, where only a limited amount of NLRC5 expression is needed to fully activate endogenous MHC class I gene expression. EGFP-CIITA also induced MHC class I expression in B16F10 cells, albeit less efficiently than NLRC5 (Figure 3.10). As expected, MHC class II expression was strongly induced by EGFP-CIITA in the same cells (Figure 3.9 C5). The level of EGFP-CIITA expression is very low in these stable transfectants, because EGFP expression could not be detected (Figure 3.9 B5 and C5). However, we did detect EGFP expression readily in the same cells 2 D and 5 D (Figure 3.9 E) after transfection, demonstrating the integrity of the construct (Figure 3.9 E).

EGFP-NLRC5 expression had no effect on MHC class II expression in B16F10 cells (Figure 3.9 C3 and C4).
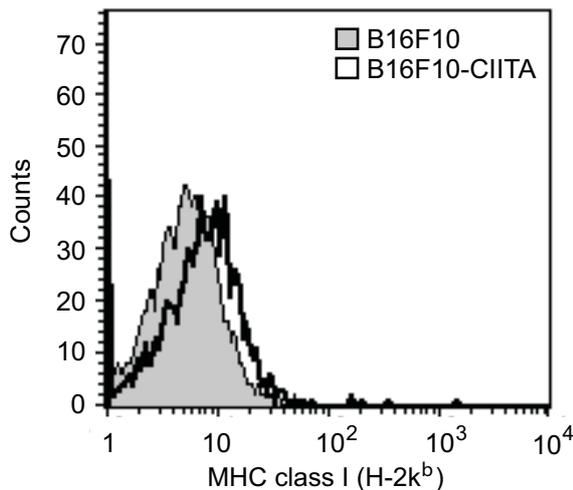
**Figure 3.10 CIITA slightly influences MHC class I levels in B16F10 cells**
Surface MHC class I expression of B16F10 control cells or B16F10 stably transfected with EGFP-CIITA.

These results show that endogenous NLRC5 and MHC class I mRNA expression levels are closely correlated in various cell lines and tissues and that NLRC5, on its own, is able to induce high levels of endogenous MHC class I gene expression in B16F10 cells.

3.2.3 NLRC5-mediated MHC class I expression is dependent on nuclear shuttling and the integral protein fold of NLRC5

NLRC5 shares the typical tripartite structure of NLR proteins, consisting of an N-terminal effector domain, a central nucleotide-binding domain (also called NACHT domain) and a C-terminal leucine-rich repeat (LRR) domain. However, our knowledge of the contribution of these domains to the subcellular localization, nuclear trafficking and MHC class I activation of NLRC5 remains fragmentary. Therefore, we generated various NLRC5 deletion and point mutants (Figure 3.11 D) and analysed their ability to shuttle to the nucleus by immunofluorescence analysis in HeLa cells, as well as their capacity to activate MHC class I transcription by HLA class I B promoter reporter assays in HeLa and HEK293T cells (Figure 3.11).

Wildtype (wt) NLRC5 was localized predominantly in the cytoplasm, but inhibition of Crm1-dependent nuclear export with LepB led to a strong nuclear accumulation of NLRC5 (Figure 3.11 A). These experiments show that NLRC5 transits through the cell nucleus, which is in agreement with recently reported findings (Benko *et al.*, 2010; Meissner *et al.*, 2010).
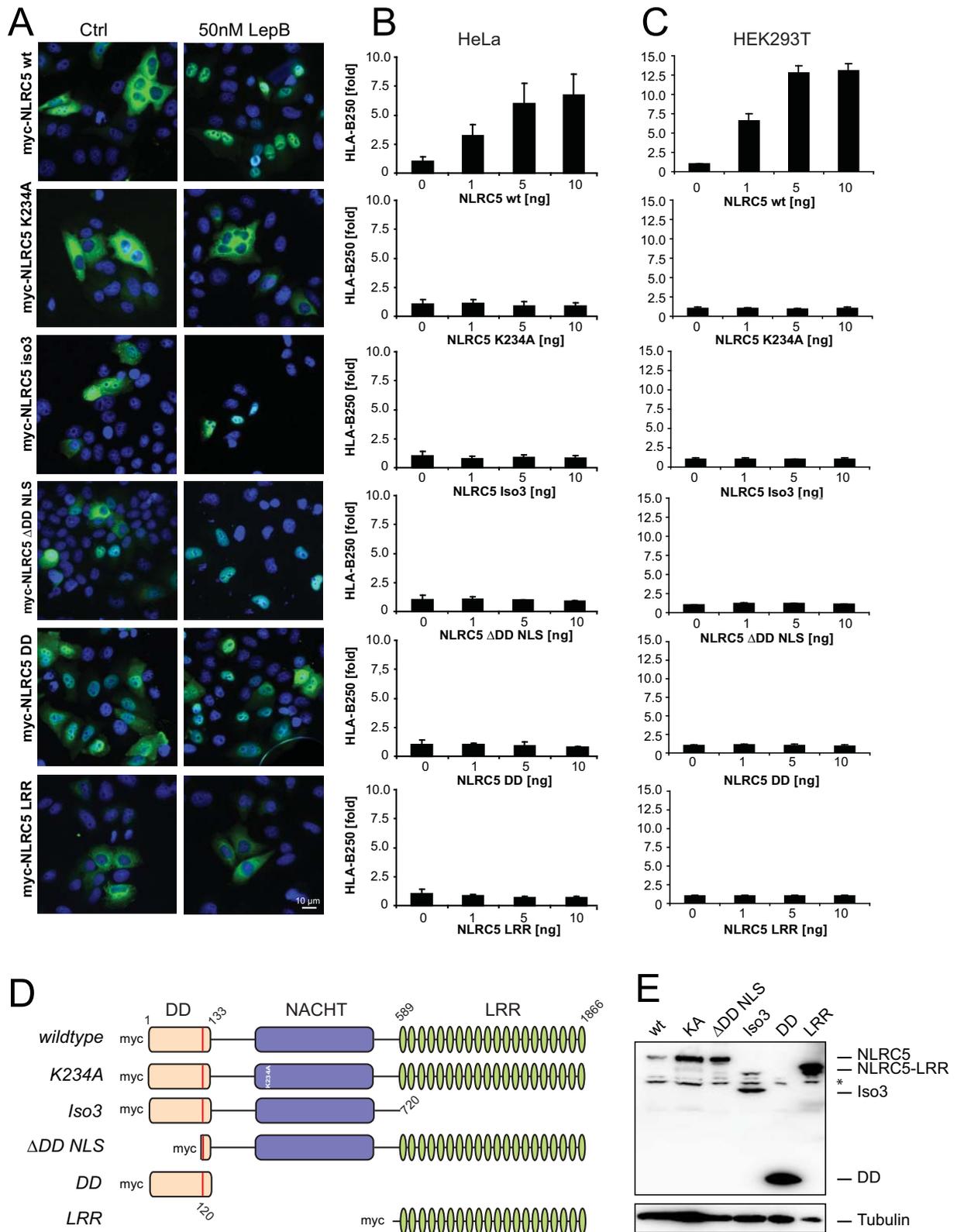
Figure 3.11 NLRC5 localization and domain structure that is required for MHC class I activation
A) Photomicrographs of indirect immunofluorescence of HeLa cells transiently transfected with myc-epitope tagged NLRC5 constructs (schematic overview in C) for 24h. Cells were fixed untreated or treated with 50 nM Leptomycin B (LepB) for 4 h prior to fixation. Signals obtained with anti-MYC 9E10 antibody are depicted in green; DAPI DNA staining is depicted in blue. Scale bar 10 μm.

B – C) Cell based luciferase reporter assay in HeLa cells (B) or HEK293T cells (C) with increasing amounts of NLRC5 in the presence of a HLA-B-promoter-driven luciferase construct. Luciferase activity was measured after 20 h of expression and normalized to β-galactosidase expression. The assay was performed in triplicates. Shown are means ± SD (n=3).

D) Schematic overview of the NLRC5 constructs. The endogenous NLRC5 nuclear localization signal (NLS) is depicted in red in the N-terminal death domain (DD). The numbers refer to specific amino acid positions.

E) Western blot expression analysis of myc-epitope tagged NLRC5 expression constructs in HEK293T cells. NLRC5 constructs are visualized using anti-MYC 9E10 antibody. Tubulin served as a loading control. Background signal is indicated by asterisk (*).

The requirement of a functional ATPase domain in NLRC5 for subcellular localization and transport and the ability to activate MHC class I transcription were analysed by mutating the conserved lysine residue (K234) in the predicted Walker A motif of NLRC5 to alanine (K234A) (Proell *et al.*, 2008) . In contrast to wt NLRC5, NLRC5 K234A was localized exclusively in the cytoplasm, even after LepB treatment (Figure 3.11 A). In agreement with the cytoplasmic localization, we found that NLRC5 K234A was unable to activate the HLA-B250 promoter in HeLa cells (Figure 3.11 B), which we also observed in HEK293T cells (Figure 3.11 C) and in B16F10 cells (Figure 3.9 D). This suggests that nuclear shuttling of NLRC5 is essential for its activity on MHC class I gene expression. We previously showed that NLRC5 is expressed in various isoforms (refer to Figure 3.1). In this part of the study, we focused our attention on isoform 3, which lacks the entire LRR domain and is expressed in several human tissues (Figure 3.1 E). NLRC5 isoform 3 localized predominantly in the nucleus, even in the absence of LepB (Figure 3.11 A), yet it completely failed to activate MHC class I transcription (Figure 3.11 B and C). This indicates that the C-terminal LRR domain is involved in nuclear export of NLRC5, as well as in transcriptional activation. CIITA contains, at its N-terminal end, a "classical" acidic activation domain that activates transcription in yeast when tethered to a promoter (Riley *et al.*, 1995; Zhou and Glimcher, 1995). CIITA is expressed from four independent promoters, generating four isoforms (FI, FII, FIII, and FIV) (Muhlethaler-Mottet *et al.*, 1997). Although CIITA-FII, FIII and FIV start at their N-terminal end with the acidic activation domain, CIITA-FI contains an additional domain N-terminal of the acidic domain, which has homology to a CARD domain. This CIITA-FI reported to contribute to MHC class II gene activation in vitro (Nickerson *et al.*, 2001), whereas it seems to be dispensable *in vivo* (Zinzow-Kramer *et al.*). Although NLRC5 lacks an N-terminal acidic activation domain found in CIITA, its N-terminal domain adopts a death domain fold. This death domain lacks obvious homology to the CARD and PYD found in other NLRs, including the CARD of CIITA-FI, or known transcriptional activation domains (refer to result

part 3.1.1 and figure 3.1 A). In contrast, the results shown above suggested that NLRC5 functions as a transcriptional activator. Accordingly, we investigated whether the N-terminal NLRC5 effector domain is necessary for MHC class I transcriptional activation. A truncated form of NLRC5, lacking the N-terminal part of the effector domain but still containing a recently identified nuclear localization signal at amino acid positions 122–134 (NLRC5ΔDD NLS) (Meissner *et al.*, 2010) was found in the nucleus in ~50% of HeLa cells in the absence of LepB. Nuclear localization of this construct was increased by inhibiting nuclear export (Fig. 3.11 A); however, it was unable to activate the MHC class I promoter neither in HeLa nor in HEK293T cells (Figure 3.11 B and C). These experiments show that the N-terminal death-fold domain, a functional ATPase domain, and the C-terminal LRR domain of NLRC5 are all required to induce MHC class I gene expression, whereas the requirements for nuclear shuttling are different. As expected from the previous experiments, the N-terminal death domain alone showed an exclusively nuclear localization in the absence of LepB, whereas the LRR region alone was completely cytoplasmic due to the absence of a NLS domain, irrespective of the presence or absence of LepB (Fig. 3.11 A). Neither construct was able to activate MHC class I transcription in HeLa or HEK293T cells (Figure 3.11 B and C). All constructs were expressed at comparable levels in HEK293T (Figure 3.11 E) and HeLa cells, showing that the differences in reporter gene activation reflect protein activity and not protein levels.

The previous experiments were carried out by ectopic expression of epitope tagged protein constructs under the control of a strong viral promoter. Thus, overexpression can easily lead to saturation of transport pathways and may yield artifactual results. Therefore, we also analysed the subcellular localization of endogenous NLRC5 in HeLa cells by cytoplasmic and nuclear protein fractionation and subsequent western blotting. To obtain detectable amounts of NLRC5 protein, cells were pretreated with poly(I:C) to induce NLRC5 expression (refer to Figure 3.1.6). This revealed a strong nuclear accumulation of endogenous NLRC5 after blocking of nuclear export by LepB, whereas NLRC5 was mainly cytoplasmic in untreated cells (Fig. 3. 12). Blotting for tubulin and lamin A/C demonstrated the absence of cross-contamination of cytoplasmic and nuclear fractions (Fig. 3.12, middle and lower panels). Of note, induction of NLRC5 expression by poly(I:C) treatment did not correlate with accumulation of NLRC5 in the nucleus. This is reminiscent of our observation that overexpressed NLRC5 strongly activated MHC class I gene expression, besides being mainly localized in the cytoplasm (Fig. 3.11 A).
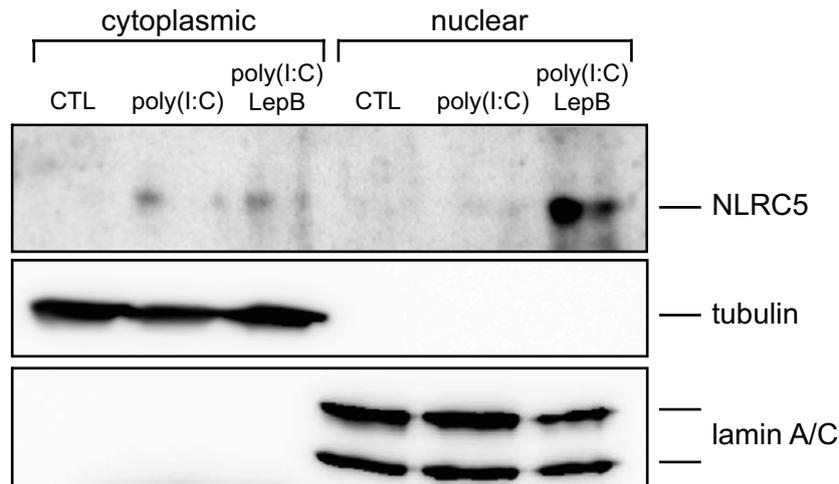
Figure 3.12 Endogenous NLRC5 shuttles to the nucleus
HeLa cells were induced for endogenous NLRC5 expression using 100 µg/ml poly(I:C) for 20 h. Cells were treated with 50 nM Leptomycin B (LepB) for 4 h, subsequently harvested and cytoplasm and nuclear proteins were extracted from about 1×10^7 cells. Endogenous NLRC5 was precipitated from cytoplasmic and nuclear extracts using anti-NLRC5 3H8 antibody (upper panel). Reprobing with anti-tubulin (cytoplasmic) and anti-lamin A/C served as loading and cross-contamination control. About 100 µg of protein was loaded on the gel. Immunoprecipitates correlate to ~10-fold enrichment over input.

Taken together, these results show that NLRC5 shuttles through the nucleus and that MHC class I promoter activation is dependent on a functional ATPase domain and on the presence of both the death domain and LRR region of NLRC5, suggesting that the integral NLRC5 fold is needed for subcellular transport and transactivation function.

3.2.4 Nuclear–cytoplasmic shuttling of NLRC5 enhances MHC class I promoter activation

In our previous experiments we found out that nuclear localization of NLRC5 is pivotal for activation of MHC class I signalling. In order to analyze the importance of nuclear shuttling in more detail, we asked whether forcing nuclear localization of NLRC5 would result in increased MHC class I promoter activation due to a faster and more efficient nuclear import. For that purpose, we generated NLRC5 constructs containing either a myc-epitope tag or a myc-epitope followed by a double SV40 NLS sequence at the N terminus (myc-2xNLS-NLRC5).

As depicted in figure 3.13 A, this construct showed a predominantly nuclear localization (right image) without LepB treatment, which is in contrast to wt NLRC5, with a predominantly cytoplasmic localization in untreated cells (left image) and NLRC5 K234A with an unfailingly cytoplasmic localization (centre image). Unexpectedly, myc-2xNLS-NLRC5 wt showed a reduced

capacity to activate the HLA class I A and B promoters and did not show a dose-dependent induction of the MHC class I promoter, as observed for wt myc-NLRC5 (Figure 3.13 B).
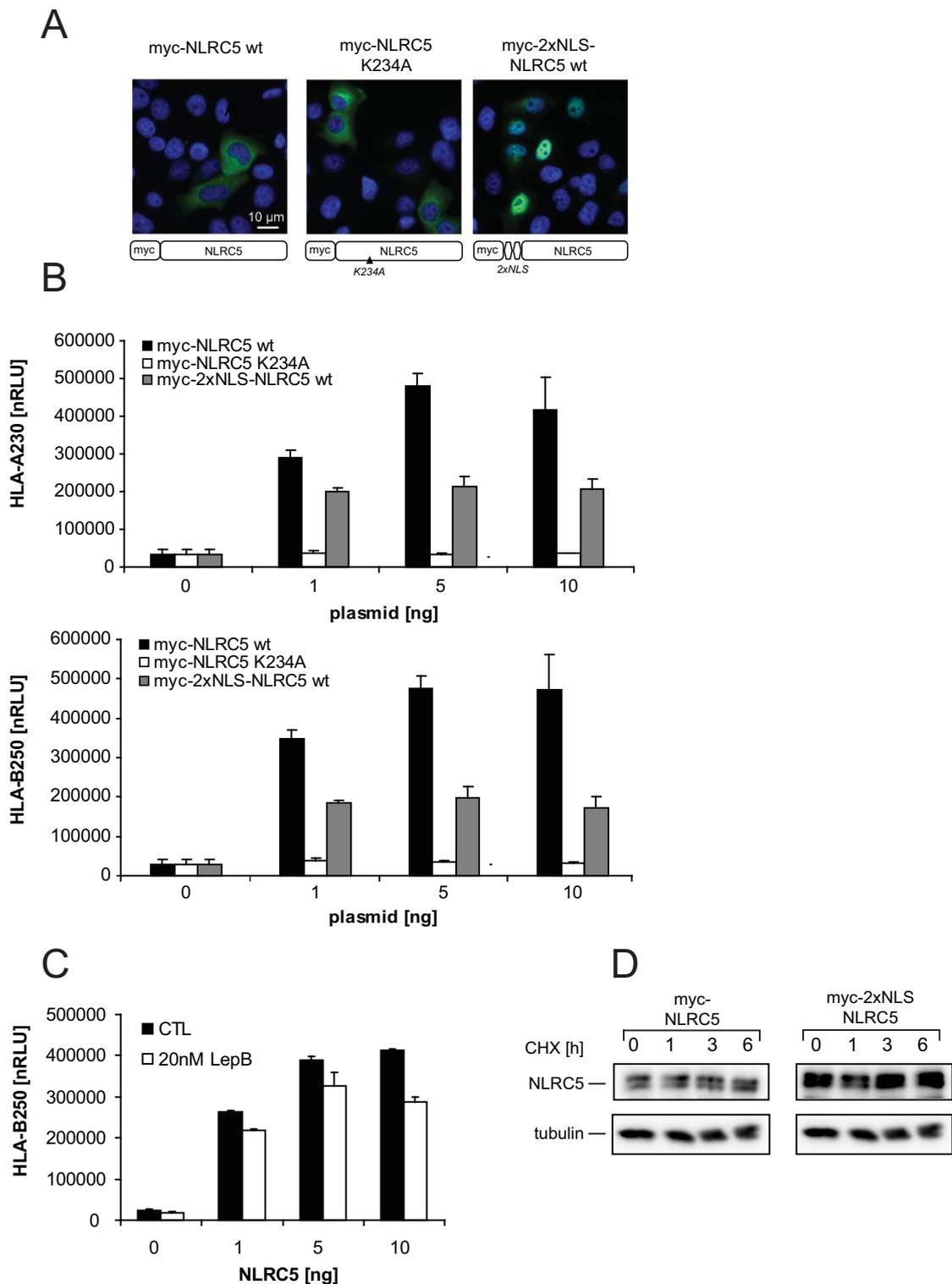
Figure 3.13 Nuclear/cytoplasmic shuttling is important for NLRC5 function
A) Photomicrographs of indirect immunofluorescence of HeLa cells transiently transfected with myc-epitope tagged NLRC5 wildtype (left), Walker A mutant (middle) and 2xNLS construct (left). Signals obtained with anti-MYC 9E10 antibody are depicted in green; DAPI DNA staining is depicted in blue. Scale bar 10 µm.

B) HEK293T-based luciferase reporter assay to address the signalling activity of NLRC5 constructs from A. Increasing amounts of NLRC5 constructs were transiently transfected in the presence of a HLA-A230 or HLA-B250-promoter-driven luciferase constructs. Luciferase activity was normalized to β-galactosidase. The readout was performed in triplicates (Mean ± SD).

C) HEK293T-based luciferase reporter assay with increasing amounts of NLRC5 either untreated or treated with 20 nM Leptomycin B (LepB) 4 h prior luciferase read out. Luciferase activity was normalized to β-galactosidase. The readout was performed in triplicates (Mean ± SD).

D) Western blot analysis of transiently transfected myc-epitope tagged NLRC5 wildtype (wt) or myc-epitope tagged 2xNLS NLRC5. After 24 h, protein stability was analysed by blockage of protein neo-synthesis with 30 µg/ml cycloheximide for the indicated time.

Notably, this was not due to a change in protein stability or turnover, as assessed by Western blotting after blocking of protein synthesis using cycloheximide (Figure 3.13 D). Although we cannot formally exclude that the introduction of the NLS sequences affected the protein function, blocking nuclear export by LepB also led to decreased MHC class I gene activation in HEK293T cells by wildtype NLRC5 (Figure 3.13 C).

This indicates that nuclear localization, as well as constant cytoplasmic/nuclear shuttling, is essential for full NLRC5 activity.

3.2.5 NLRC5-mediated MHC class I promoter activation is mediated by the MHC enhanceosome

To date, structure and activation of MHC class I promoter are well understood. Activation of MHC class I genes is dependent on a core promoter and upstream regulatory elements containing NF-κB- and ISRE-binding elements and a regulatory region originally called site-α (Gobin *et al.*, 1997). This site-α was shown to contain a region homologous to the S/X/Y composite *cis*-acting crucial for MHC class II gene activation (Gobin *et al.*, 1998b; Gobin *et al.*, 1997; Martin *et al.*, 1997). The MHC enhanceosome complex, and in particular the RFX complex, was shown to be required both for basal MHC class I expression (in absence of CIITA) and for CIITA-dependent activated MHC class I expression (Gobin *et al.*, 1997). Given the close homology of NLRC5 and CIITA, we anticipated that the site-α/S/X/Y element is also involved in NLRC5-mediated MHC class I promoter activation. In their previous study, Gobin and co-workers found a 5 nucleotide motif inside the X1 box element, which was crucial for both basal (CIITA-independent) and CIITA-dependent MHC class I expression (Gobin *et al.*, 1998b).

A

B

C

D
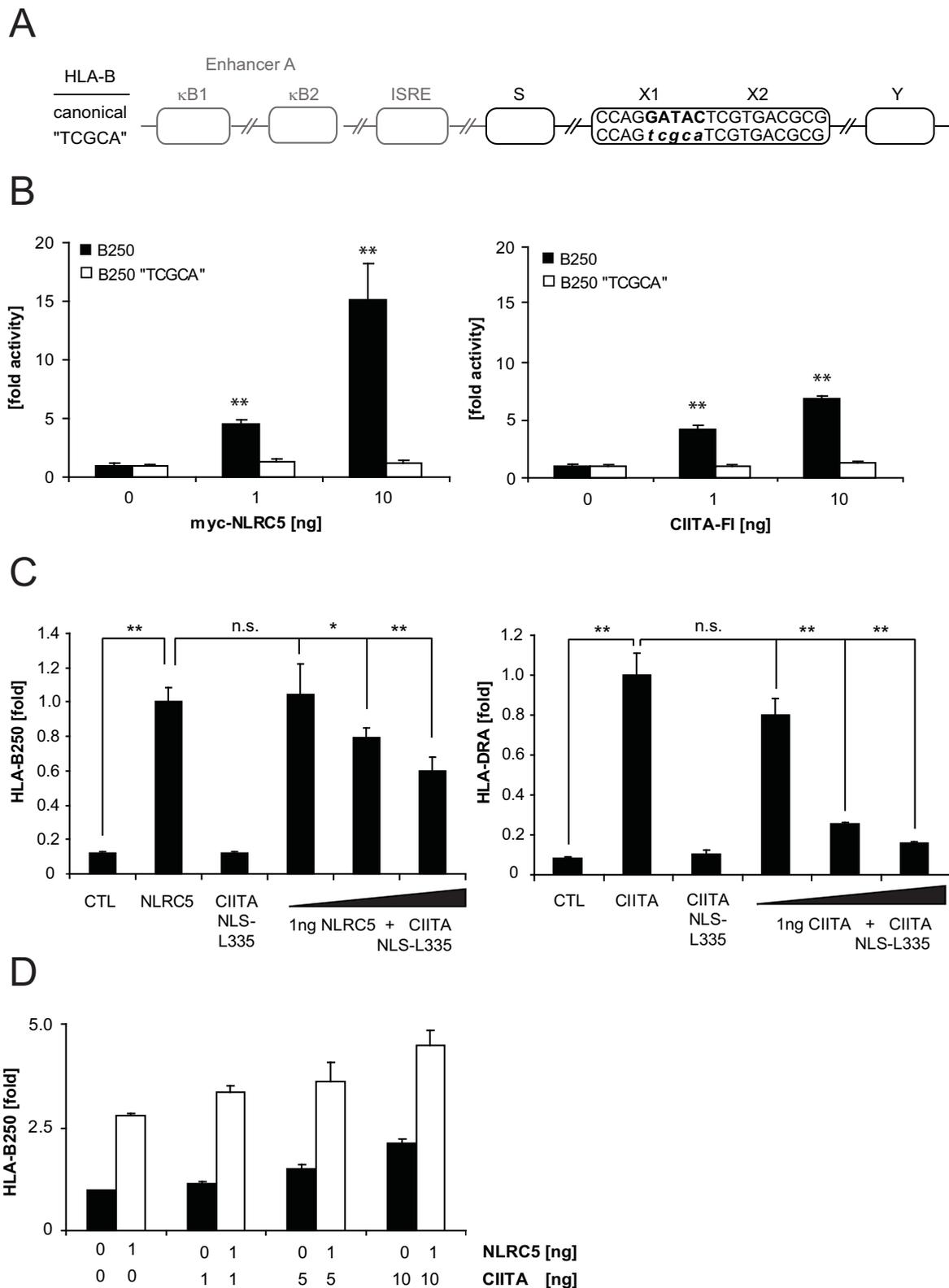
Figure 3.14 Involvement of the X-box motif in NLRC5-driven MHC class I activation
A) Schematic overview of the classical MHC class I promoter elements, responsible for inducible MHC class I expression. Sequence comparison between classical MHC class I promoter (canonical) and X1-box mutation ("TCGCA").
B) HEK293T-based luciferase reporter assay with increasing amounts of NLRC5 or CIITA-FI in the presence of canonical (B250) X1-box mutated (B250"TCGCA") MHC class I promoter driven luciferase.

Luciferase activity was normalized to β-galactosidase. The readout was performed in triplicates (Mean ± SD). Data were analysed using a two-sided student's *t* test. (*) p<0.05; (**) p<0.005

C) HEK293T cells were transfected with 1 ng NLRC5 or 1 ng CIITA alone or together with the CIITA-deletion construct CIITA NLS-L335. B250 (left panel) and DRA (right panel) luciferase activity, normalized to β-galactosidase activity, is shown as fold activation to mock-transfected cells (set to 1). The readout was performed in triplicates (Mean ± SD). Data were analysed using a two-sided student's *t* test. (*) p<0.05; (**) p<0.005; n.s. = not significant

D) HEK293T cells were transfected with CIITA alone or with CIITA in the presence of NLRC5. HLA-B250-driven luciferase activity normalized to β-galactosidase is shown. Mock transfected activity was set to 1. Data represents mean ± SD, performed in triplicates.

Therefore, we tested whether NLRC5 could activate an HLA class I B promoter reporter construct containing a mutated X1 box element ("TCGCA"; Figure 3.14 A). Testing the defective X1-Box HLA class I B250 "TCGCA" constructs in our HEK293T-based luciferase assay revealed an inability for overexpressed NLRC5 to activate this defective "TCGCA" construct, whereas NLRC5 robustly turned on the wt B250-luciferase construct in the same experiment (Figure 3.14 B; left panel). The parallel experiment with CIITA confirmed the results of Gobin and colleagues (Figure 3.14 B; right panel) (Gobin *et al.*, 1998b).

Interestingly, we found in this and similar experiments that the CARD-containing CIITA isoform I activated MHC class I expression more efficiently compared with isoform III (compare Figure 3.14, right panel with Figure 3.7 C, left panel and Figure 3.14 D). Taken together, these findings suggest that MHC class I activation by both NLRC5 and CIITA is dependent on a functional X1 box.

To date, the recruitment of CIITA to the MHC enhanceosome through multiple protein–protein interactions with RFX5, RFXAP, RFX-ANK, CREB and NF-Y is pretty well understood (Figure 1.5) (DeSandro *et al.*, 2000; Hake *et al.*, 2000; Zhu *et al.*, 2000; Scholl *et al.*, 1997). Interestingly, most of the interaction surfaces in CIITA were mapped to the NACHT and LRR regions (reviewed in Reith and Mach, 2001), since these regions show the highest sequence similarity between NLRC5 and CIITA (Istomin and Godzik, 2009; Proell *et al.*, 2008). Thus, we reasoned that NLRC5 and CIITA might share, at least in part, similar interaction surfaces and, therefore, might be able to compete with each other for binding to the MHC enhanceosome. To test this hypothesis, we used a strongly dominant-negative N-terminally truncated CIITA mutant called CIITA-NLS-L335. CIITA-NLS-L335 is expressed at 30–50-fold higher levels compared with wt CIITA because of its greatly increased stability, and it displaces CIITA efficiently from the MHC class II promoter (Schnappauf *et al.*, 2003; Masternak *et al.*, 2000a; Bontron *et al.*, 1997). In agreement with Camacho-Carvajal and colleagues, overexpression of CIITA-NLS-L335 efficiently

suppresses CIITA dependent MHC class II gene expression in a dose-dependent manner (Figure 3.14 C, right panel and Camacho-Carvajal *et al.*, 2004).

Interestingly, we also observed a strong dose-dependent reduction in NLRC5-dependent MHC class I promoter activation when CIITA-NLS-L335 was coexpressed with NLRC5, suggesting a competition between the two factors for the same binding sites (Figure 3.14 C, left panel). The previous experiments indicated that both NLRC5 and CIITA act via site-α/S/X/Y and the MHC enhanceosome in the MHC class I promoters, thus we wanted to test for a possible cross-talk between these two factors. To elucidate this, we cotransfected a constant amount of NLRC5 with increasing amounts of CIITA and measured the activation of the HLA class I B reporter construct. As shown in Figure 3.14 D, we observed an additive effect of CIITA on NLRC5-dependent MHC class I expression. This further supports the hypothesis that NLRC5 and CIITA occupy the same binding interface.

Taken together, these results show that NLRC5 activates MHC class I gene expression via MHC enhanceosome binding to the site-α/S/X/Y element and also suggest that NLRC5 interacts, at least in part, with the same protein partners as does CIITA via overlapping interaction sites.

3.3 Domain Mapping of NLRC5 and CIITA

3.3.1 NLRC5/CIITA chimeric proteins are able to activate both MHC class I and II transcription

In paragraph 3.2, we figured out that MHC class I transcriptional activation by NLRC5 depends on a functional enhanceosome complex, similar to the activation of MHC class II by CIITA. Of note, similar results were obtained in a study from Meissner and co-workers (Meissner *et al.* 2012c). Although, we provided evidence that NLRC5 mainly acts to drive MHC I expression whereas CIITA induces MHC II expression (Figure in 3.7 C), the underlying mechanism for this discrimination of MHC class I or MHC class II promoter sites by NLRC5 or CIITA remains largely elusive. To gain insight into the discrimination of MHC I and II promoters by NLRC5 and CIITA, we generated a series of chimeric constructs containing combinations of different domains of NLRC5 and CIITA. First we started to swap the N-terminal effector domains leaving the NACHT-LRR C-terminus of CIITA or NLRC5 intact (Figure 3.15 A).

Based on modelling of the structures and secondary structural database information (psipred v3.0) we defined the N-terminal domain of NLRC5 comprising amino acids 1 to 142

(according to NP_115582). For CIITA, it was reported that deletion of the acidic domain (aa 1-163) alone or the acidic and the proline/serine/threonine domain (aa 1-335) both resulted in dominant negative phenotypes (Camacho-Carvajal *et al.*, 2004; Bontron *et al.*, 1997; Chin *et al.*, 1997; Yun *et al.*, 1997; Zhou *et al.*, 1997).
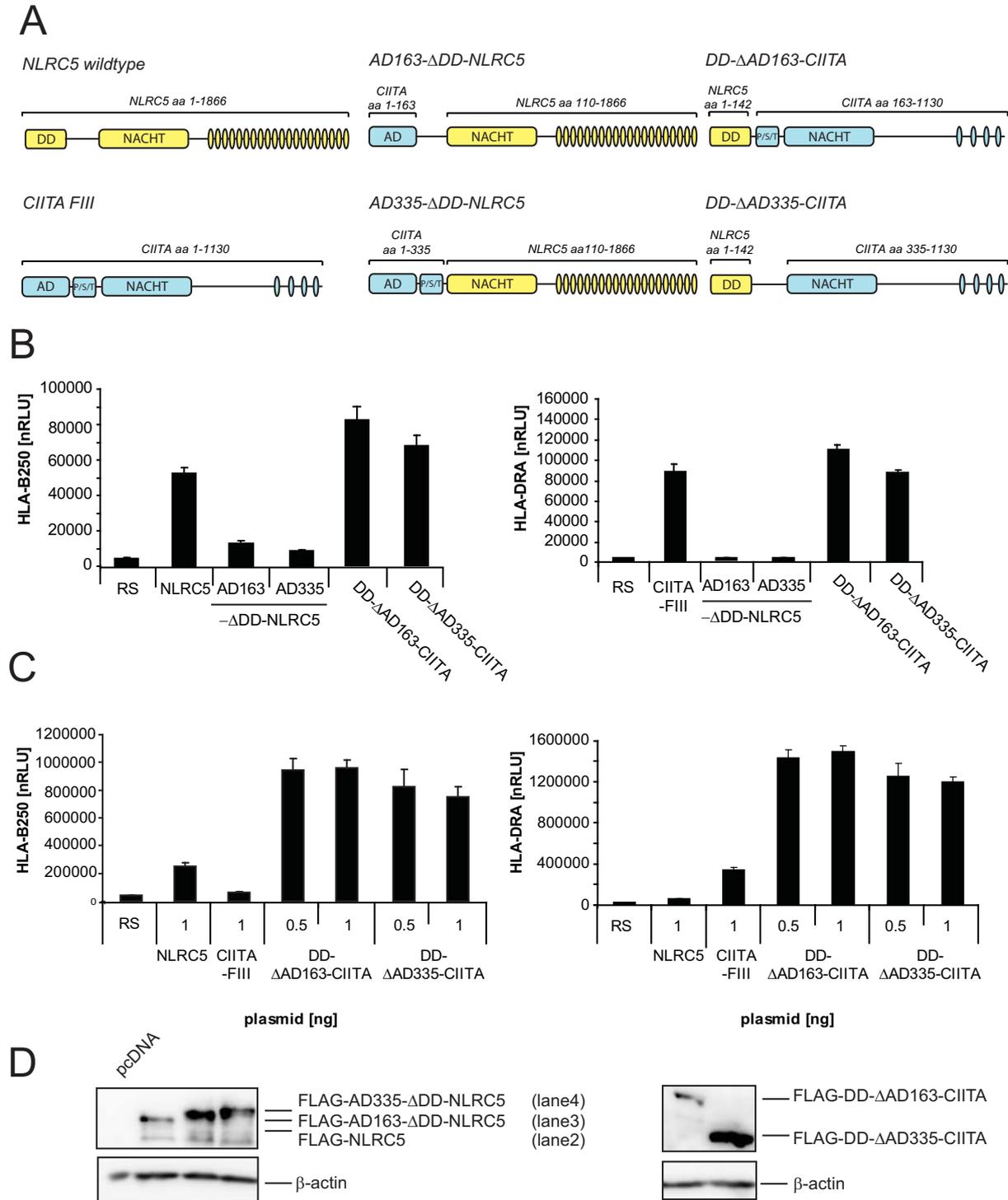
Figure 3.15 Contribution of the N-terminal effector domains of NLRC5 and CIITA to MHC activation
A) Schematic overview of wildtype NLRC5 and CIITA (left part) in comparison to the effector domain chimeric proteins (middle and right part). Note that in DD-ΔAD163-CIITA, V165 is missing.

B) HEK293T cells were transfected with 5 ng of indicated plasmid together with a luciferase reporter construct, as indicated on the y axis. The readout was performed 24 hours after transfection. Luciferase activity was normalized to β-galactosidase activity. The readout was performed in triplicates (Mean ± SD).
C) Similar experimental setup as in B with different amounts of transfected plasmid, as indicated on the x axis.
D) Western Blot analysis of transiently transfected chimeric proteins. 6 wells of a 96 well plate transiently transfected with 5 ng of plasmid were pooled and analysed for protein expression using the indicated antibodies. GAPDH serves as a loading control.

We thus used two constructs of the N-terminal domain of CIITA; the acidic domain alone (aa 1-163) and the acidic and P/S/T domain (aa 1-335) (according to NP_000237; refer to Krawczyk and Reith, 2006). These N-terminal domains were fused to the remaining C-terminal part of NLRC5 or CIITA as summarized in Figure 3.15 A.

In a first set of experiments, we tested the ability of our chimeric fusion constructs to differentially activate MHC class I or II promoters in HEK293T cells that do not express endogenous NLRC5 (refer to figure 3.1) or CIITA (Hake *et al.*, 2000), using luciferase gene-reporter assays. As expected, expression of 5 ng NLRC5 or 5 ng CIITA led to significant activation of the MHC I or MHC II reporter, respectively (Figure 3.15). NLRC5 with its effector domain (aa 1-142) replaced by the CIITA N-terminal domain with (AD335-ΔDD-NLRC5) or without the P/S/T-domain (AD163-ΔDD-NLRC5) did neither significantly activate the HLA-B nor the HLA-DRA promoter (Figure 3.15 B).

Interestingly, vice versa, after replacement of the N-terminal part of CIITA by the N-terminal effector domain of NLRC5 (aa 1-142), we observed a potent activation of both the HLA-B250 and the HLA-DRA reporters (Figure 3.15). Activation of MHC class I and class II promoters by these chimeric constructs thereby was at least as potent as with NLRC5 or CIITA wildtype constructs. Moreover, even at concentrations of 0.5 ng plasmid per well, both constructs were sufficient for full blown reporter activation (Figure 3.15 C).

Interestingly, the construct still harbouring the P/S/T-domain of CIITA (DD-ΔAD163-CIITA) showed a somewhat higher activity as compared to DD-ΔAD335-CIITA in all assays (Figure 3.15 B and C). Comparable expression levels of the used constructs in the assays were verified by Western blot analysis (Figure 3.15 D).
Of note, CIITA-L335, lacking the acidic domain and the P/S/T-domain was completely signalling inactive (Figure 3.14 C) suggesting that MHC class I and II activation of this chimera was dependent on the effector domain of NLRC5. Nevertheless, the effector domain of NLRC5 is not sufficient to trigger MHC class I activation on its own (Figure 3.11 B and C).
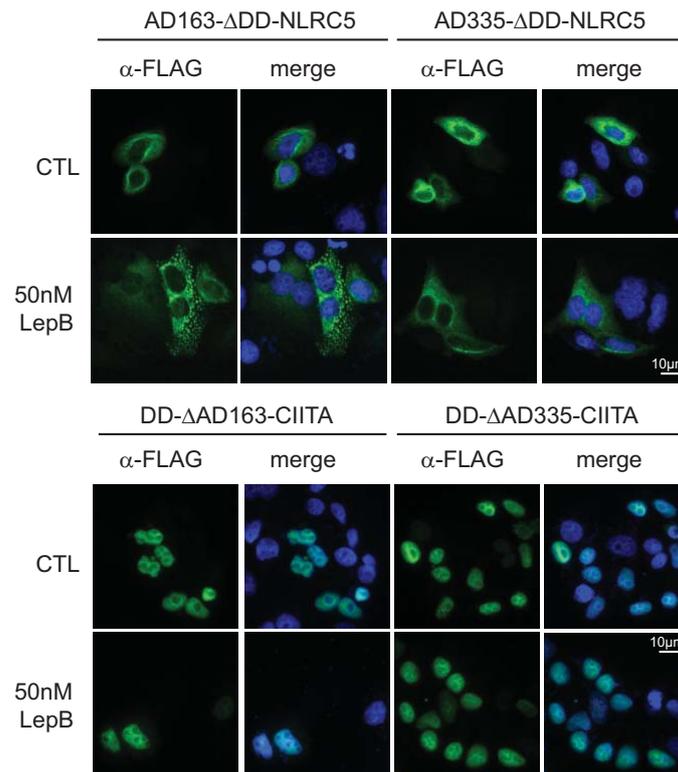
Figure 3.16 Nuclear shuttling determines MHC activation in NLRC5-CIITA-chimeric constructs
Photomicrographs of indirect immunofluorescence of HeLa cells transiently transfected with FLAG-epitope tagged AD163-ΔDD-NLRC5, AD335-ΔDD-NLRC5, DD-ΔAD163-CIITA and DD-ΔAD335-CIITA as indicated. Cells were either treated with 50 nM LepB or left untreated prior fixation. Signals obtained with anti-FLAG M2 are depicted in green, DAPI staining is depicted in blue.

In this work we established, that NLRC5 needs to shuttle to the nucleus in order to activate MHC class I gene expression (Figure 3.11 and Meissner *et al.*, 2012c; Meissner *et al.*, 2010) and similar results are reported for CIITA (Camacho-Carvajal *et al.*, 2004; Hake *et al.*, 2000). To address if lack of promoter activation of the AD335-ΔDD-NLRC5 and AD163-ΔDD-NLRC5 constructs is a result of mislocalized protein, we expressed our collection of chimeras in HeLa cells and blocked nuclear export with 50 nM Leptomycin B (LepB) to force nuclear localization. In line with the results obtained in the reporter assays, AD335-ΔDD-NLRC5 and AD163-ΔDD-NLRC5 were not detected inside the nucleus after LepB treatment (Figure 3.16, upper panels). In contrast, DD-ΔAD163-CIITA and DD-ΔAD335-CIITA were able to shuttle to the nucleus and showed a pronounced nuclear localization even without LepB treatment (Figure 3.16, lower panels). The latter results fit well with the identification of a NLS in the effector domain of NLRC5 (aa 121-122; aa 132-134) (Meissner *et al.*, 2010).

Reasoning, that perturbed nuclear shuttling might be responsible for the lack of potent MHC activation of AD335-ΔDD-NLRC5 and AD163-ΔDD-NLRC5, we fused a double SV40 NLS sequence at the N terminus of these constructs. However, we were not able to obtain nuclear shuttling of the NLS-tagged constructs, and accordingly observed no activation of either MHC class I or MHC class II promoter (Figure 3.17).
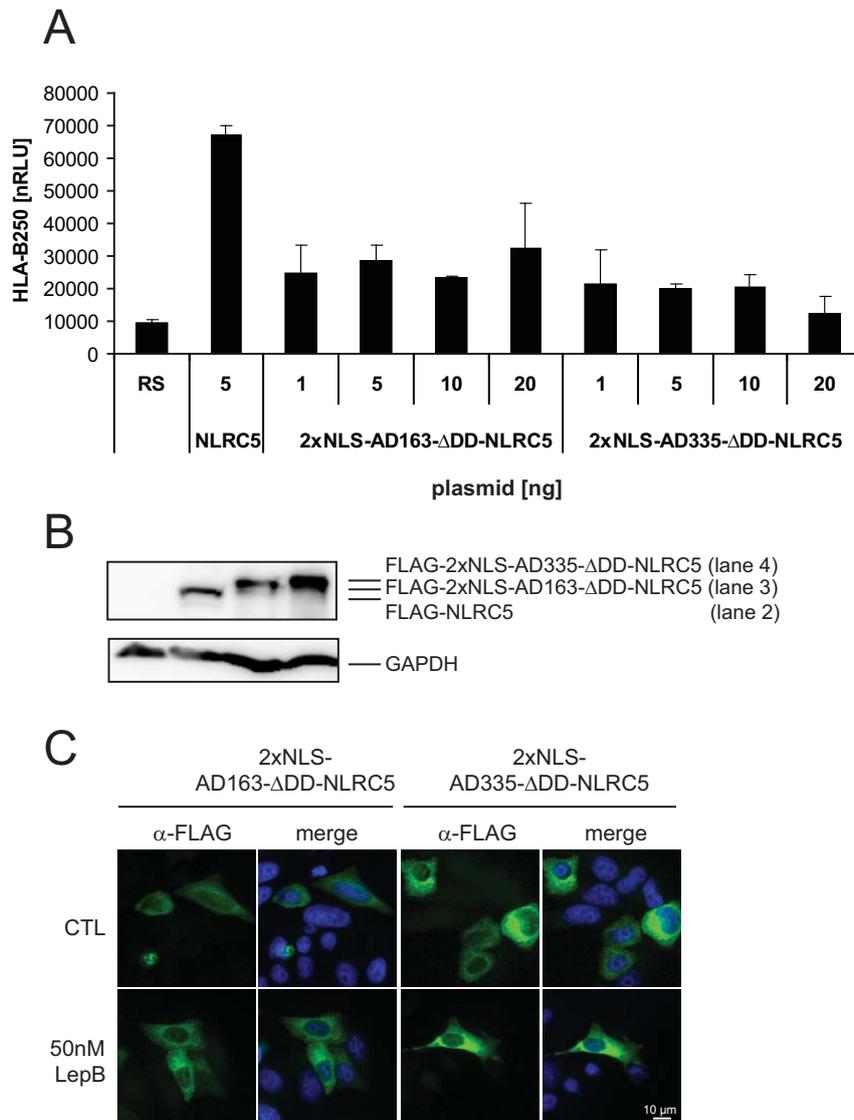
Figure 3.17 Fusion of N-terminal SV40 NLS is not sufficient to drive nuclear localization of AD163-ΔDD-NLRC5 and AD335-ΔDD-NLRC5.

A) HEK293T cells were transiently transfected with increasing amounts of AD163-ΔDD-NLRC5 and AD335-ΔDD-NLRC5 constructs in the presence of MHC class I promoter luciferase. The readout was performed 24 h after transfection. HLA-B250-driven luciferase normalized to β-galactosidase is shown. The readout was performed in triplicates (Mean ± SD).

B) Western Blot analysis of transiently transfected proteins. 6 wells of a 96 well plate transiently transfected with 5 ng of plasmid were pooled and analysed for protein expression using the indicated antibodies. GAPDH served as a loading control.

C) Photomicrographs of indirect immunofluorescence of HeLa cells transiently transfected with FLAG-epitope tagged 2xNLS-AD163-ΔDD-NLRC5 and 2xNLS-AD335-ΔDD-NLRC5. Cells were either treated

with 50 nM LepB or left untreated prior fixation. Signals obtained with anti-FLAG M2 are depicted in green, DAPI staining is depicted in blue.

Finally, in order to validate the effect of our constructs on endogenous MHC class I and II protein expression, we expressed wildtype NLRC5, wildtype CIITA and our chimeric DD-ΔAD335-CIITA construct in HEK293T cells and analysed MHC class I and class II protein levels in whole cell lysates by immunoblot analysis. As depicted in Figure 3.18, overexpression of wildtype NLRC5 and DD-ΔAD335-CIITA strongly induced endogenous MHC class I protein expression, whereas the inactive K234A Walker A mutant of NLRC5 (NLRC5 K234A; Figure 3.11 B and C) or CIITA failed to induce MHC class I expression (Figure 3.18). In agreement, both DD-ΔAD335-CIITA and CIITA induced MHC class II proteins expression.
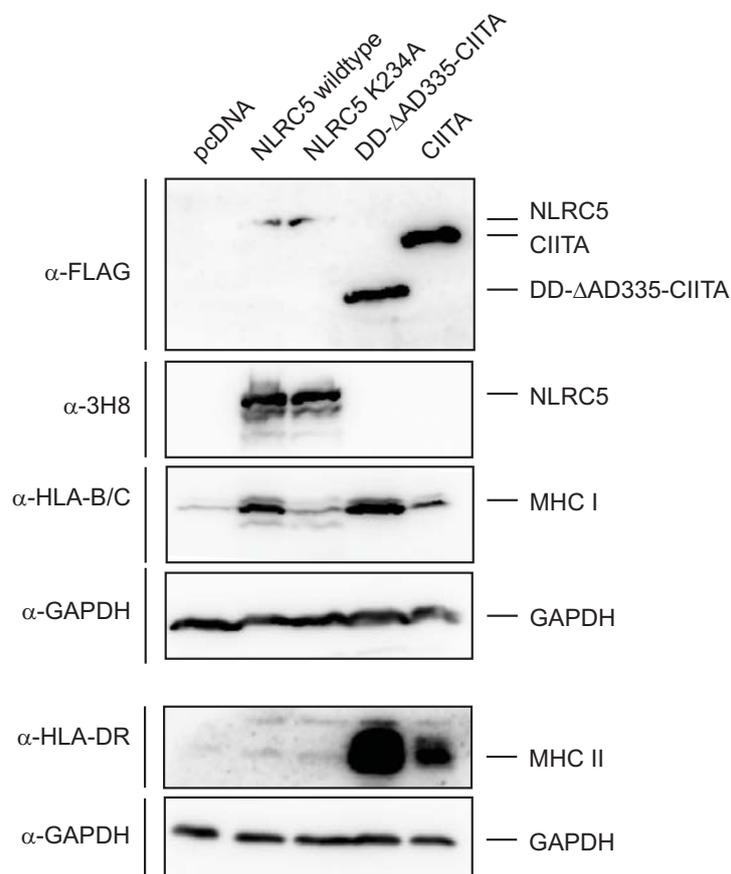
Figure 3.18 Contribution of the N-terminal effector domains of NLRC5 to endogenous MHC activation in HEK293T cells
HEK293T cells were transiently transfected with 3 µg of FLAG-epitope tagged NLRC5 wildtype, NLRC5 K234A mutant, DD-ΔAD335-CIITA or CIITA plasmid per 15 cm dish for 24 h. Protein expression was analysed using the specific antibodies indicated on the left. Detected proteins were indicated on the right. A second gel was prepared using half of the protein amount, to detect MHC class II expression. Reprobing with anti-GAPDH antibody served as a loading control.

We wondered, whether the signalling activity of the NLRC5 effector domain can be maintained, when fused to other NLR protein backbones related to CIITA. To this end, we also generated a fusion protein of the NLRC5 effector domain to NOD1 lacking the CARD domain, termed DD-ΔDD-NOD1 (Figure 3.19 A).
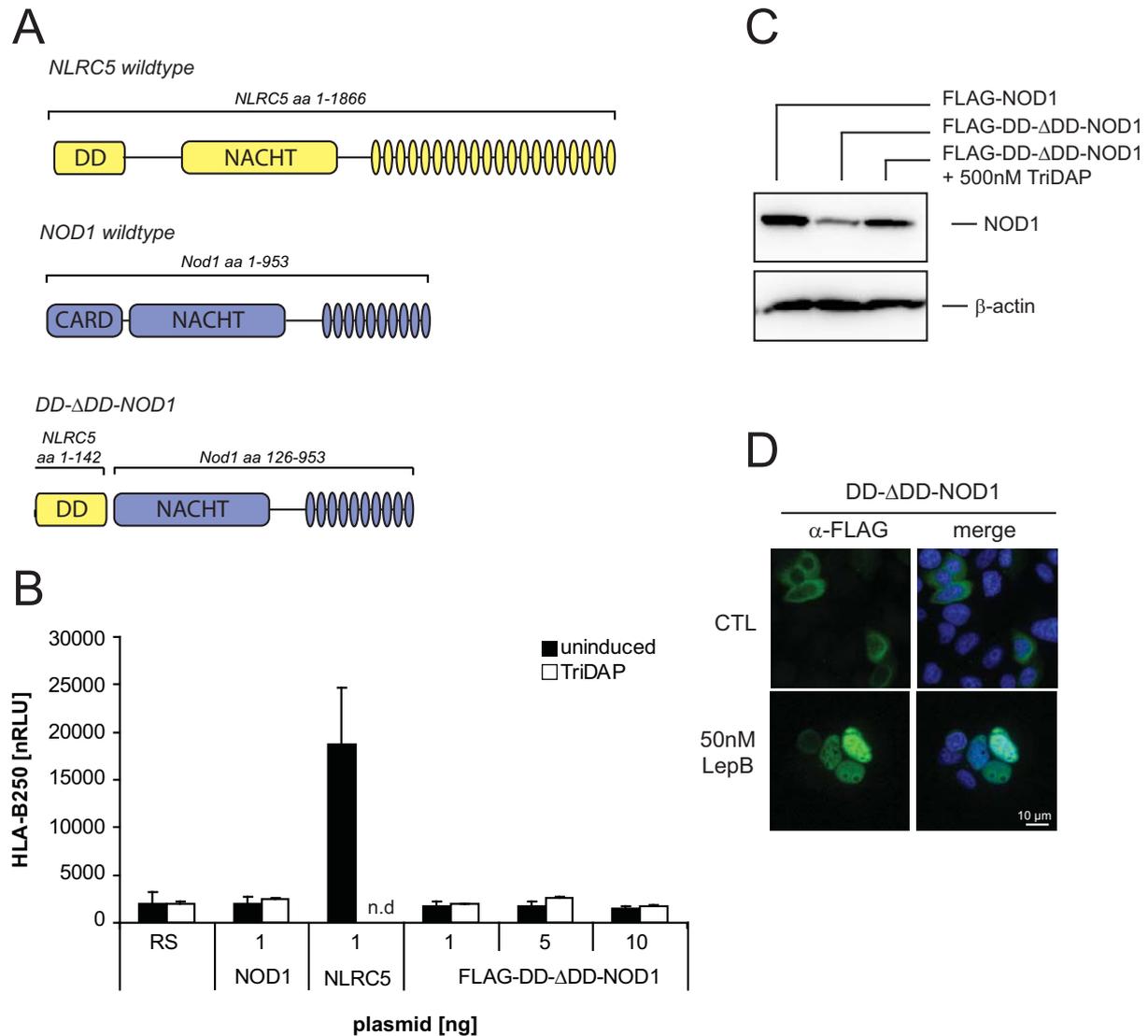
Figure 3.19 The N-terminal effector domain of NLRC5 alone is not sufficient to trigger MHC class I promoter activation.

A) Schematic overview of NLRC5 wildtype, NOD1 wildtype and DD-ΔDD-NOD1, the latter of which was created by replacement of the NOD1 CARD domain (aa 1-125) with the NLRC5 effector domain (aa 1-142).

B) HEK293T cells were transiently transfected with NLRC5, NOD1 or DD-ΔDD-NOD1 in the presence of MHC class I driven luciferase. NOD1 constructs were left unstimulated or stimulated with 500 nM TriDAP. Luciferase expression was measured 24 h post transfection and normalized to β-galactosidase expression. The experiment was performed in triplicates (Mean ± SD).

C) Western blot analysis of FLAG-epitope tagged NOD1 wildtype and DD-ΔDD-NOD1 (6 wells pooled; each transfected with 5 ng of plasmid). Proteins were visualized with anti-FLAG M2 antibody, reprobing with anti-β-actin served as a loading control.

C) Photomicrographs of indirect immunofluorescence of HeLa cells transiently transfected with FLAG-epitope tagged DD-ΔDD-NOD1. Cells were either left untreated or treated with 50 nM LepB prior fixation. Signals obtained with anti-FLAG M2 are depicted in green, DAPI staining is depicted in blue.

NOD1 was chosen, since its function in pathogen recognition is already established and it has no transactivator activity (Kufer and Sansonetti, 2011; Kufer *et al.*, 2006). Moreover, NOD1 is strongly activated by the peptidoglycan fragment TriDAP (Girardin *et al.*, 2003b) and a working model for NOD1 was already proposed (Zurek *et al.*, 2012a). Whereas NLRC5 potently activates HLA-B250-luciferase expression, NOD1 overexpression alone fails to induce HLA-B250-luciferase expression (Figure 3.19 B). Moreover, overexpression of DD-ΔDD-NOD1 did not activate HLA-B250-luciferase, neither in a control assay, nor with TriDAP induction (Figure 3.19 B). Expression of DD-ΔDD-NOD1 was verified by western blot analysis (Figure 3.19 C) and nuclear localization was controlled (Fig. 3.19 D). Although, the construct was well expressed and showed nuclear localization, no HLA-B250 promoter activation was detected with this chimeric NLR (Figure 3.19 B), strongly suggesting that particularities in the NACHT-LRR of CIITA are responsible for the transcriptional activity.

3.3.2 Generation of LRR domain chimeric NLR proteins

In case of NOD1 and NOD2, the leucine-rich-repeat domain has been reported to be essential to mediate activation of these NLRs and to drive NF-κB activation by TriDAP or MDP, respectively (Girardin *et al.*, 2005; Tanabe *et al.*, 2004). Furthermore, LRR swap experiments indicate that the sensing specificity of NOD1 and NOD2 can be interchanged by swap of their LRR domains (Girardin *et al.*, 2005). In CIITA, the LRR domain is strongly implicated in nuclear transport and MHC class II activation (Ting and Trowsdale, 2002; Hake *et al.*, 2000; Bontron *et al.*, 1997), whereas in NLRC5, the LRR domain plays a pivotal role in MHC class I activation and is involved in nuclear export.

In order to test, if the LRR domains of NLRC5 and CIITA confer specificity for MHC class I versus MHC class II activation, we generated two LRR chimeric proteins, containing either the NLRC5 N-terminus and the CIITA LRRs (NLRC5_562_LRR_762) or vice versa (CIITA_762_LRR_562) (Figure 3.20 A).

In a first set of experiments, these LRR chimera constructs were tested in HEK293T-based luciferase reporter assays. As depicted in Figure 3.20 B, neither the NLRC5_562_LRR_762 nor the CIITA_762_LRR_562 construct did activate the MHC class I (upper left) or II (lower left) reporter, although the constructs were well expressed (Figure 3.20 C).

In indirect immunofluorescence experiments, NLRC5_562_LRR_762 was found to be able to localize to the nucleus even without LepB treatment, in agreement with the NLS in the N-terminal effector domain of NLRC5 (Meissner *et al.*, 2010) and the lack of the NLRC5 LRR region, which plays a role in nuclear export (Figure 3.11). Vice versa, CIITA_762_LRR_562 was not able to shuttle to the nucleus, even after LepB treatment

Taken together, although in principle, NLRC5_562_LRR_762 is able to shuttle to the nucleus, it is not capable to activate either MHC class I or MHC class II promoter, showing that the used LRR domain of CIITA is not sufficient to compensate the function of the NLRC5 LRRs. In contrast, CIITA_762_LRR_562 is not able to shuttle to the nucleus, most likely, due to the lack of the CIITA LRR sequence, which is reported to be involved in nuclear shuttling (Camacho-Carvajal *et al.*, 2004; Hake *et al.*, 2000).

Figure 3.20 Contribution of C-terminal LRR region to NLRC5 and CIITA signalling
A) Schematic overview of NLRC5_562_CIITA_762 and CIITA_762_LRR_562.
B) HEK293T-driven luciferase assay with MHC class I (upper) or MHC class II (lower) luciferase constructs in the presence of NLRC5_562_CIITA_762 or CIITA_762_LRR_562 constructs. Luciferase expression was measured 24h post transfection and normalized to β-galactosidase expression. The experiment was perfomed in triplicates (Mean ± SD).
C) Western blot analysis of FLAG-epitope tagged NLRC5_562_CIITA_762 and CIITA_762_LRR_562 (6 wells pooled; each transfected with 5 ng of plasmid). Proteins were visualized with anti-FLAG M2 antibody, reprobing with anti-β-actin served as a loading control.
D) Photomicrographs of indirect immunofluorescence of HeLa cells transiently transfected with NLRC5_562_CIITA_762 or CIITA_762_LRR_562. Cells were either left untreated or treated for 4 h with 50 nM LepB, prior fixation. Signals obtained with anti-FLAG M2 are depicted in green, DAPI staining is depicted in blue.

A

NLRC5_562_LRR_762

| *NLRC5 aa 1-561* | *CIITA aa 762-1130* |

DD | NACHT

CIITA_762_LRR_562

| *CIITA aa 1-761* | *NLRC5 aa 562-1866* |

AD | P/S/T | NACHT

B

C

170 —
130 —

— FLAG-CIITA_762_LRR_562

— FLAG-NLRC5_562_LRR_762

— β-actin

D

| | NLRC5_562_LRR_762 | | CIITA_762_LRR_562 | |
| | α-FLAG | merge | α-FLAG | merge |

CTL

50nM
LepB

10 μm
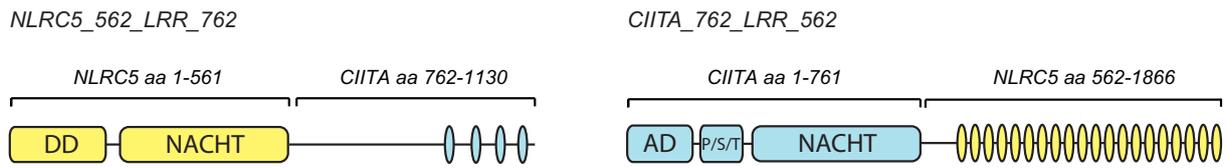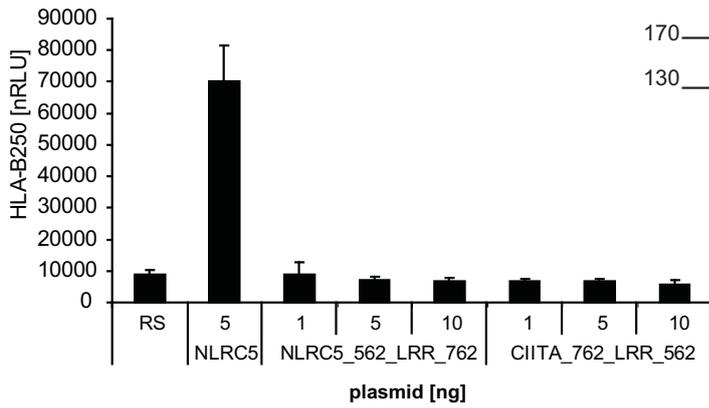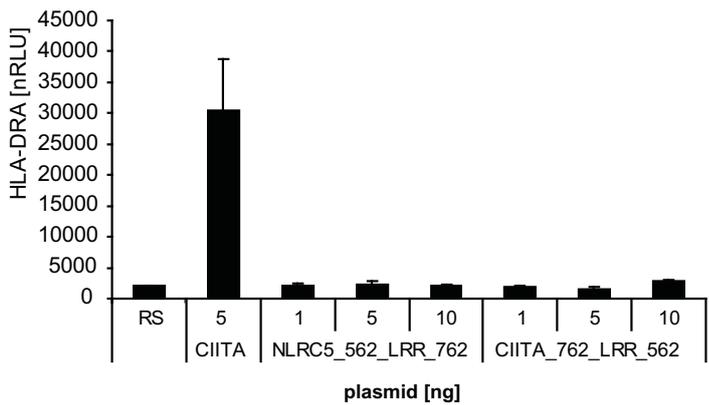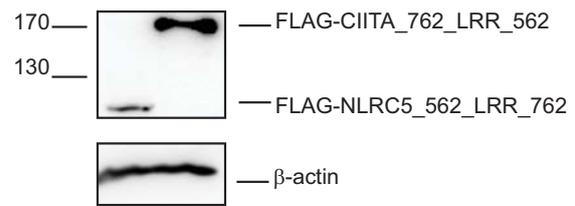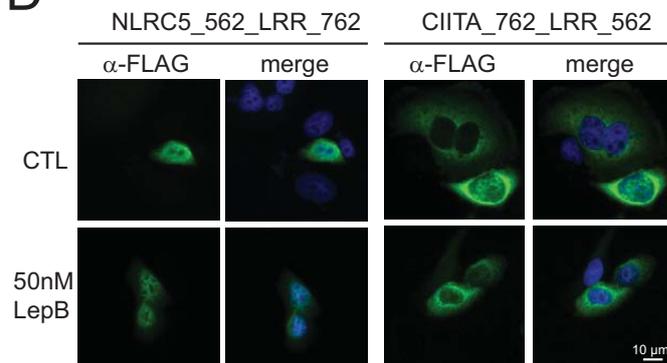
In the final part of the study, we analysed the specificity of the effector domain, the NACHT domain and the LRR domain of NLRC5 and CIITA in activation of MHC class I versus MHC class II expression. By generation of chimeric proteins, we observed, that the NLRC5 N-terminal effector domain fused to the CIITA C-terminus, including NACHT and LRR domain, completely restores MHC class I and, surprisingly, MHC class II activation. Although we could work out, that the NLRC5 effector domain induces MHC gene activation, the accurate underlying mechanism still remains unknown and has to be analysed in future experiments.

4 Discussion

4.1 A Role for the human nucleotide-binding domain, leucine-rich repeat-containing family member NLRC5 in antiviral responses

NLR proteins play pivotal roles as PRRs mediating detection of invading pathogens and triggering innate immune responses. In this study, we analysed the function of the NLR protein NLRC5. We started our enquiry with a detailed investigation of the expression pattern of NLRC5 in several human tissues and cell lines. We observed highest expression of human NLRC5 (hNLRC5) mRNA in hematopoietic cells, including monocytes, B cells and T cells. In line with that, immune related tissues, including spleen and lymph node showed higher expression than non-immune related tissue, including muscle tissue. Basal hNLRC5 expression in cell lines was restricted to myeloid (THP-1) and lymphoid (Jurkat) cells but was interestingly also found in the epithelial cell line HeLa (Figure 3.1). A similar expression analysis from Benko *et al.* supported our findings showing that hNLRC5 expression was mainly restricted to immune specific cells and tissues, including lymph node, lymphocytes and spleen (Benko *et al.*, 2010). Nonetheless, contrary results concerning the mRNA levels of NLRC5 in some human tissues were reported by Kuenzel and co-workers (Kuenzel *et al.*, 2010). Other NLR proteins as for example the well-established PRRs NOD1 and NOD2, which are closely related to NLRC5, were previously reported to be also expressed in APCs, as well as in hematopoietic cells (reviewed in Elinav *et al.*, 2011), thus we hypothesized an immune related function for NLRC5 being likely.

Six different isoforms of NLRC5 have been reported in databases (Figure 3.1). These isoforms differ from each other in their C-terminal LRR formation. For some NLR proteins, such as NOD1 and NOD2 a clear involvement of the LRR region in elicitor sensing was shown (Girardin *et al.*, 2005; Tanabe *et al.*, 2004), thus different LRR region compositions could enhance the variety of potential interacting elicitors or even change the conformation of the LRR region. We identified NLRC5 isoform 3 and isoform 4 and observed that isoform 3 is mainly expressed in $CD8^+$ and $CD4^+$, whereas isoform 4/5 is expressed at low levels in THP-1. Nevertheless, whether these NLRC5 mRNAs have biological relevance remains to be established.

We found a poly(I:C)- and Sendai Virus (SeV)-dependent upregulation of hNLRC5 mRNA and protein in non-hematopoietic cells, including HeLa cells and human primary dermal fibroblasts (hFibr). The induction by poly(I:C) was dependent on the TLR3/TBK1-signalling pathway, as verified in HeLa cells using siRNA (Figure 3.2). Recognition of SeV in human cells is independent of TLR3, but relies mainly on the cytoplasmic PRR RIG-I (Kato *et al.*, 2006). Nevertheless, both TLR3 and RIG-I activation resulted in type I IFN induction in a TBK1-dependent

manner (refer to figure 1.1 and 1.3). Moreover, Kuenzel and colleagues reported increased hNLRC5 mRNA and protein levels upon IFN-γ treatment in HeLaS3 cells and THP-1 cells, but also in colon carcinoma cell lines, such as CaCo2 and HT29 (Kuenzel *et al.*, 2010). Murine NLRC5 (mNLRC5) was found to be inducible by IFN-γ (Benko *et al.*, 2010), poly(I:C) (Benko *et al.*, 2010) and LPS (Benko *et al.*, 2010; Cui *et al.*, 2010). Also LPS was reported to augment NLRC5 expression, however this seems to be cell type specific (Benko *et al.*, 2010; Cui *et al.*, 2010). Notably, we were not able to detect increased levels of hNLRC5 mRNA levels in THP-1 cells after LPS stimulation, which was independently confirmed by Kuenzel *et al.* (Kuenzel *et al.*, 2010). A comprehensive analysis of mNLRC5 in BMDMs was provided by Staehli *et al.*, clearly shows that poly(I:C)/TLR3-dependent and LPS/TLR4-dependent upregulation of mNLRC5 is mediated by type I IFN through STAT1 activation (Staehli *et al.*, 2012) (also refer to figure 1.1and 4.1). This is in line with our observations that hNLRC5 induction by poly(I:C) and SeV is a mechanism dependent on type I IFN release, rather than being directly dependent on TBK1 (Figure 3.2).

To elucidate a potential connection of hNLRC5 to innate immune signalling pathways, we further aimed to identify the signalling pathways linked to hNLRC5. Unlike other NLR proteins such as NOD1, NOD2 and NLRP3, overexpression of NLRC5 did not activate the classical pro-inflammatory pathways including NF-κB, MAPK or type I IFN (Figure 3.3). In contrast to our results, Kuenzel and colleagues reported that hNLRC5 activates ISRE- and INF-γ activating sequence (GAS)-containing promoters in HeLaS3 cells. They further provided evidence that this induction depends on dimerization of the N-terminal effector domain of NLRC5 (Kuenzel *et al.*, 2010). Since we used HEK293T cells, whereas Kuenzel and colleagues used HeLaS3 cells, a cell type specific activation of different pathways might explain this discrepancy. Even though, overexpression of hNLRC5 did not result in activation of immune pathways, it inhibited TBK1- and SeV-mediated IFN-β promoter activation (Figure 3.4). Noteworthy, also studies performed by Benko *et al.* and Cui *et al.* support an inhibitory function of NLRC5 in type I IFN signalling in similar experiments. Surprisingly, an inhibitory effect was also reported for NF-κB signalling in cell-based reporter assays (Benko *et al.*, 2010; Cui *et al.*, 2010), which is in contrast to our observations in a similar experimental setup (Figure 3.4). Cui *et al.* further provided a model for the inhibition of NF-κB and IFN-β by NLRC5. They reported an interaction of NLRC5 with IKK-α and IKK-β that inhibits their kinase activity. Additional interactions of NLRC5 with RIG-I and MDA5 were shown, blocking their signalling activity (Cui *et al.*, 2010).

However, in our hands, knock-down of NLRC5 decreased type I IFN expression and release in THP-1 cells upon SeV infection (Figure 3.5). Additional experiments in primary human dermal fibroblasts (hFibr), which are known to produce high levels of type I IFN (Sehgal and

Gupta, 1980; Sehgal *et al.*, 1978), revealed an even more pronounced decrease of type I IFN expression upon poly(I:C) induction and SeV infection (Figure 3.6). In agreement with our findings, similar results were obtained by Kuenzel *et al.* using a CMV-based infection model. NLRC5 knock-down resulted in a decrease of CMV-induced type I IFN release (Kuenzel *et al.*, 2010). Although these results are in contrast to previous experiments using overexpressed NLRC5 in HEK293T cells (Figure 3.3), we assumed that overexpression in HEK293T cells resulted in titration of a factor, which is pivotal for IFN-β induction. Such a scenario is very likely as shown by a recent study from Ling *et al.* that indicate that luciferase assays used for the analysis of NLR signalling are prone to such effects (Ling *et al.*, 2012). Co-immunoprecipitation experiments performed with TBK1, SINTBAD, TANK1, NAP1, IKK-ε, and IRF3, 7, and 5, as well as unbiased yeast two-hybrid screening of NLRC5 and its effector domain were conducted to address this observation in more detail (data not shown). Unfortunately, the results did not allow us to link NLRC5 to any known component of the type I IFN pathway yet, although as previously mentioned, Cui *et al.* were able to detect interactions between NLRC5 and IKK-α and IKK-β (Cui *et al.*, 2010).

Very recently, NLRC5-deficient mice were generated by different groups, which might help to clarify the implication of NLRC5 in immune signalling. Currently, five different full-body knock-out mice have been characterized (Biswas *et al.*, 2012; Robbins *et al.*, 2012; Staehli *et al.*, 2012; Tong *et al.*, 2012; Yao *et al.*, 2012; Kumar *et al.*, 2011b). In line with their previous observation of hNLRC5 as an inhibitor of type I IFN and NF-κB signalling (Cui *et al.*, 2010), Tong and colleagues observed a strong increase in type I IFN and NF-κB signalling upon TLR- and RIG-I activation in NLRC5-deficient mouse embryonic fibroblasts (MEFs) and peritoneal macrophages (PMMs) and to a lesser extent in bone marrow derived macrophages (BMDMs) (Tong *et al.*, 2012). Interestingly, no effect was observed in bone marrow-derived dendritic cells (BMDCs) deficient for NLRC5, which is in line with Kumar and co-workers, who were not able to detect altered type I IFN or NF-κB signalling in their NLRC5-deficient mice (Kumar *et al.*, 2011b). Thus, a cell type specific involvement of mNLRC5 in TLR and RIG-I signalling pathways seems to exist.

Furthermore, a contribution of murine NLRC5 to inflammasome signalling was reported by Yao *et al.* (Yao *et al.*, 2012), showing a moderate but significant effect on NLRP3 signalling but not on inflammasomes in general, although Kumar *et al.* did not observe a similar phenotype (Kumar *et al.*, 2011b). Nonetheless, Kumar *et al.* provided evidence, that human NLRC5 is able to activate caspase-1, resulting in IL-1β maturation, which was supported by similar findings from Davis *et al.*, reporting an involvement of human NLRC5 in inflammasome formation upon a broad variety of stimuli (Davis *et al.*, 2010).

Still, fundamental differences in human and murine NLRC5 might account for the discrepancies between our results and the phenotype of the knock-out mice (Tong *et al.*, 2012; Kumar *et al.*, 2011b).

4.2 NLRC5 controls basal MHC class I gene expression in an MHC enhanceosome-dependent manner

NLR proteins are mainly responsible for cytosolic pathogen recognition, but additional functions have been reported for some NLR proteins. The most prominent example is the transcriptional activator CIITA, which was shown to control the expression of MHC class II molecules *in vitro* and *in vivo* (Reith *et al.*, 2005). Alignment studies of the human NLR family performed for the nucleotide-binding domain and for the LRR region revealed a close homology between human CIITA (hCIITA) and human NLRC5 (hNLRC5) (Istomin and Godzik, 2009; Proell *et al.*, 2008). Taking this into consideration, Meissner and co-workers analysed the capability of hNLRC5 to activate MHC molecule expression. They found out, that NLRC5 is able to induce the classical MHC class I molecules (HLA-A/B/C) as well as MHC class I presentation associated proteins (β_2-microglobulin, TAP1, MLP2) in HEK293T and in Jurkat cells. Whereas we and other groups reported a predominantly cytoplasmic localization of overexpressed NLRC5 under steady-state conditions, they could further show, that blocking of Crm1-dependent nuclear export by Leptomycin B (LepB), resulted in nuclear accumulation of overexpressed hNLRC5 in HEK293T cells (Meissner *et al.*, 2010). Benko *et al.* also detected nuclear shuttling of hNLRC5 in HeLa cells, however in contrast to Meissner *et al.* they observed enhanced basal and inducible MHC class I surface expression in murine RAW264.7 cells after lentiviral-mediated knock-down of mNLRC5 (Benko *et al.*, 2010).

To clarify this discrepancy, we tested our hNLRC5 construct for the ability to activate MHC class I promoter in HEK293T-based luciferase reporter assays. In agreement with Meissner and colleagues, we were able to detect that NLRC5 induced both MHC class I promoter activation (Figure 3.7 A) as well as MHC class I expression on the protein level (Figure 3.7 B) in HEK293T cells, which originally display low basal MHC class I expression. In agreement with Martin and colleagues (Martin *et al.*, 1997), Meissner and coworkers were able to detect high levels of MHC class I after hCIITA overexpression *in vitro* (Meissner *et al.*, 2010), whereas our CIITA construct failed to robustly activate the MHC class I promoter. Although we do not have an explanation for this contradiction, CIITA-deficient mice display normal MHC class I surface expression levels, debilitating a regulatory function of CIITA for MHC class I expression *in vivo* (Itoh-Lindstrom *et al.*, 1999). In agreement with Meissner *et al.*, hNLRC5 was not able to activate MHC class II expression in our studies (Figure 3.7 C) and also NLRC5-deficient mice do not

display altered MHC class II expression levels (Biswas *et al.*, 2012; Staehli *et al.*, 2012; Tong *et al.*, 2012; Yao *et al.*, 2012). Knock-down experiments in THP-1 cells, basally expressing high levels of hNLRC5, or in poly(I:C)-induced HeLa cells supported a role for hNLRC5 in MHC class I expression, both on mRNA and on surface expression level (Figure 3.8). This finding was further expanded to primary human dermal fibroblasts, where HLA-B mRNA levels correlated with hNLRC5 expression levels.

As previously mentioned, MHC class I molecules are expressed on almost all nucleated cells, although differences in their expression levels are detectable among different tissues (van den Elsen *et al.*, 2004). Thus we compared the expression of HLA-B and hNLRC5 in several human tissues (Figure 3.9 A). As expected, we found a quite good correlation between HLA-B expression and hNLRC5 in several tissues, but also differences, for example lung tissue, indicating additional expression control mechanisms. We further analysed the contribution of hNLRC5 to MHC class I expression in the murine melanoma cell line B16F10, which is deficient for MHC class I expression. We could work out, that MHC class I expression was completely restored after stable transfection of B16F10 cells with hNLRC5 (Figure 3.9 B-E). Similar findings were also observed with MHC class I expression upon CIITA transfection in a study performed by Martin and colleagues (Martin *et al.*, 1997), although we were not able to detect CIITA-dependent MHC class I expression. Of note, these results also show that human NLRC5 can functionally compensate murine NLRC5 for its role in MHC class I gene expression.

The involvement of NLRC5 in MHC class I regulation was further verified in mice by several independent studies (Biswas *et al.*, 2012; Robbins *et al.*, 2012; Staehli *et al.*, 2012; Tong *et al.*, 2012; Yao *et al.*, 2012; Kumar *et al.*, 2011b). Most of these studies reported reduced MHC class I levels in immune-related tissues and cells of NLRC5-deficient mice, including CD4$^+$ T cells, CD8$^+$ T cells and DCs, supporting our and Meissner's *in vitro* findings (Meissner *et al.*, 2010). As a consequence of reduced MHC class I surface expression resulting in decreased antigen presentation, Staehli and colleagues reported less efficient killing of NLRC5-deficient target cells by CD8$^+$ T cells (Staehli *et al.*, 2012). Nevertheless, MHC class I molecule expression does not completely rely on NLRC5 (also refer to figure 3.9 A), rather, it was shown to be inducible by IFN-γ in both control (NLRC5$^{fl/fl}$) and NLRC5-deficient mice (Staehli *et al.*, 2012), which was further confirmed by Biswas and colleagues (Biswas *et al.*, 2012). This goes in line with our finding, that certain tissues with low NLRC5 expression still show high amounts of MHC class I (Figure 3.9 A), supporting the presence of additional regulatory elements of MHC class I expression.

MHC class I molecules are responsible for cytoplasmic antigen presentation to CD8$^+$ T cells also in positive selection – in line with that, Staehli and colleagues detected slightly reduced CD8$^+$ T

cell levels in the spleen of NLRC5-deficient mice. Evidence for *in vivo* relevance was given by Biswas and colleagues and Yao and colleagues, both independently describing severely reduced levels of CD8$^+$ T cells and thus IFN-γ release in NLRC5-deficient mice after *L. monocytogenes* infection. Conform to that, bacterial clearance was affected, indicated by increased bacterial burden in liver and spleen, clearly showing that NLRC5 in these studies is not a negative regulator of inflammatory responses (Biswas *et al.*, 2012; Yao *et al.*, 2012)

Although Tong *et al.* detected decreased MHC class I surface expression in NLRC5-deficient B and T cells, they concentrated on TLR signalling in these mice and were able to detect increased TLR responses in mice lacking NLRC5 (Tong *et al.*, 2012), which goes in line with their first publication, revealing NLRC5 as a negative regulator of NF-κB and type I IFN responses (Cui *et al.*, 2010). Noteworthy, the phenotype was cell type specific and could not be observed in a similar study from Kumar *et al.* (Kumar *et al.*, 2011b). Of note, the coherence of MHC class I expression and TLR signalling was addressed by a recent publication from Xu and co-workers (Xu *et al.*, 2012). They proposed a working model, in which activation of TLRs leads to an MHC class I molecule-dependent activation of the phosphatase SHP2, which in term inhibits NF-κB or type I IFN signalling (Xu *et al.*, 2012). Although, this study needs further confirmation, these results provide a plausible explanation how NLRC5 might indirectly affect TLR and eventually also other immune signalling pathways, at least in selected cell types.

During the first part of this study, we created deletion-constructs of NLRC5 (depicted in figure 3.11 D) to elucidate the mechanism of NLRC5 signalling in more detail. We tested HLA-B-promoter activation as well as nuclear localization of these constructs. We found out, that NLRC5-dependent MHC class I activation relies on the complete domain structure of the protein (Figure 3.11), as well as on shuttling of the protein into the nucleus. Responsible for nuclear shuttling is an N-terminally located NLS (Meissner *et al.*, 2010), as well as the NACHT ATPase activity (Figure 3.11; in terms of MHC class I activation also refer to Figure 3.9 D). Accordingly, NLRC5 constructs harbouring the N-terminal effector domain including NLRC5 wildtype, iso3 and DD, were able to shuttle to the nucleus and accumulated after LepB stimulation (refer to figure 3.11). Interestingly, constructs lacking the LRR region showed nuclear localization even in the absence of LepB, including NLRC5 iso3 and DD. Thus the LRR region appears to be involved in nuclear export. Although, NLRC5 and CIITA show close homology in their LRR region (Istomin and Godzik, 2009), differences in LRR function concerning subcellular localization are obvious. For CIITA it has been shown, that several structural features of the LRR region are important for nuclear import (Camacho-Carvajal *et al.*, 2004; Harton *et al.*, 2002; Hake *et al.*, 2000), whereas the LRR region of NLRC5 seems to be dispensable for nuclear import (Figure 3.11). Additionally for CIITA, a functional nucleotide binding domain is crucial for MHC class II

activation. Interestingly, in contrast to other NLR proteins analysed so far, CIITA was reported to harbour a GTP-binding motif, rather than an ATP-binding motif (Chin *et al.*, 1997). Although, the detailed role for GTP-binding in transcriptional activation of MHC class II by CIITA remains fragmentary (Bewry *et al.*, 2007), it has been proposed, that reduced transactivator function in GTP-binding deficient CIITA constructs is rather a result of increased nuclear export, than of reduced transactivator function (Raval *et al.*, 2003). Nevertheless, in contrast to NLRC5, disruption of the Walker A motif in CIITA abolished MHC transactivator activity without affecting nuclear shuttling (Bewry *et al.*, 2007; Raval *et al.*, 2003). A strong dominant negative effect was also observed for a CIITA construct lacking the acidic- and P/S/T-domain, indicating that this construct still was able to bind the enhanceosome, but was inable to recruit the transcription machinery (Camacho-Carvajal *et al.*, 2004; Yun *et al.*, 1997; Zhou *et al.*, 1997). Unlike other NLR proteins, the activity of CIITA completely relies on its transcriptional control, for example via IFN-γ induction of CIITA transcription. This means, CIITA is directly capable of MHC class II induction without any further stimuli, which is in contrast to NOD1, NOD2 or NLRP3 for example, which need a stimulus resulting in a conformational change for complete activation. Whether this is also the case for NLRC5 remains to be elucidated. To conclude, although the principle of action seems to be comparable for CIITA and NLRC5, the domains involved in nuclear transport differ among both proteins, indicating further differences in the exact mechanism of MHC activation.

Overexpression of proteins is prone to false positive results, in particular for studies on subcellular localization. To exclude false positive artefacts, we analysed the ability of endogenous NLRC5 in HeLa cells to shuttle to the nucleus. We boosted the expression of NLRC5 in HeLa cells using poly(I:C) and precipitated NLRC5 from the cytosolic and nuclear cell extracts. Using this technique we were able to detect endogenous NLRC5 inside the nucleus for the first time, a result that further supports ours and others findings regarding nuclear localization of NLRC5 (Meissner *et al.*, 2012c; Benko *et al.*, 2010; Meissner *et al.*, 2010).

Both NLRC5- and CIITA-dependent MHC activation relies on nuclear shuttling. In contrast to NLRC5, which is mainly present in the cytoplasm in untreated cells (Figure 3.11), CIITA is predominantly localized inside the nucleus even under steady-state conditions (Hake *et al.*, 2000). Controversy, N-terminally NLS-tagged NLRC5, which is exclusively nuclear, showed a reduced MHC class I activation potential (Figure 3.13). Similar findings were reported by Meissner and colleagues, who obtained decreased MHC class I activation activity for nuclear forced NLRC5 (Meissner *et al.*, 2012b). Although we cannot formally exclude that the added 2xNLS form SV40 disturbed the integrity of the N-terminal domain of NLRC5, we do not think that this is very likely, because N-terminal addition of the FLAG-epitope tag, the myc-epitope tag or even

EGFP did not appear to have an effect on the activity and transport behaviour of NLRC5 (Figure 3.9). Rather, we could also detect decreased MHC class I activation after 4h of LepB stimulation in HEK293T-based luciferase assays (Figure 3.13 C). There are several possible explanations for this complex transport behaviour, which are not mutually exclusive. Transactivation potential might be dependent on cytoplasmic modifications of the proteins that are not carried out correctly if nuclear import is mediated via a "classical" importin-α–dependent pathway. Noteworthy to mention here is the appearance of a double band in SDS-gel electrophoresis upon overexpression of NLRC5 or NLRC5-LRR, indicating of such modifications. It is possible that nuclear import of NLRC5 depends on the interaction with protein partners in the cytoplasm. The involvement of the LRR domain in this process makes this plausible, because LRR domains are best known as protein-interaction domains (Kobe and Kajava, 2001). Lastly, it is possible that nuclear export is somehow linked to the transactivation function of NLRC5 and CIITA.

A working model for our findings concerning NLRC5 signalling in correlation with other studies is depicted in figure 4.1.

Figure 4.1 Working model for NLRC5 signalling.
NLRC5 is induced by both type I and type II IFNs through canonical IFN pathways (Staehli *et al.*, 2012) (left part).
MHC class I activation by NLRC5 requires nuclear presence as well as the complete integral fold of NLRC5. MHC class I activation by NLRC5 relies on the enhanceosome complex and is further enhanced by cytoplasmic-nuclear-shuttling, most likely due to posttranslational modifications (middle part).
We and Kuenzel (Kuenzel *et al.*, 2010) could further provide evidence, that NLRC5 plays a role in mounting type I IFN responses upon poly(I:C) treatment and viral infection, whereas the detailed mechanism remains unresolved (right part) (based on Krawczyk and Reith, 2006; Akira and Takeda, 2004; van den Elsen *et al.*, 2004).

Working model for NLRC5 signalling

Induction   MHC class I activation   Contribution to type I IFN signalling
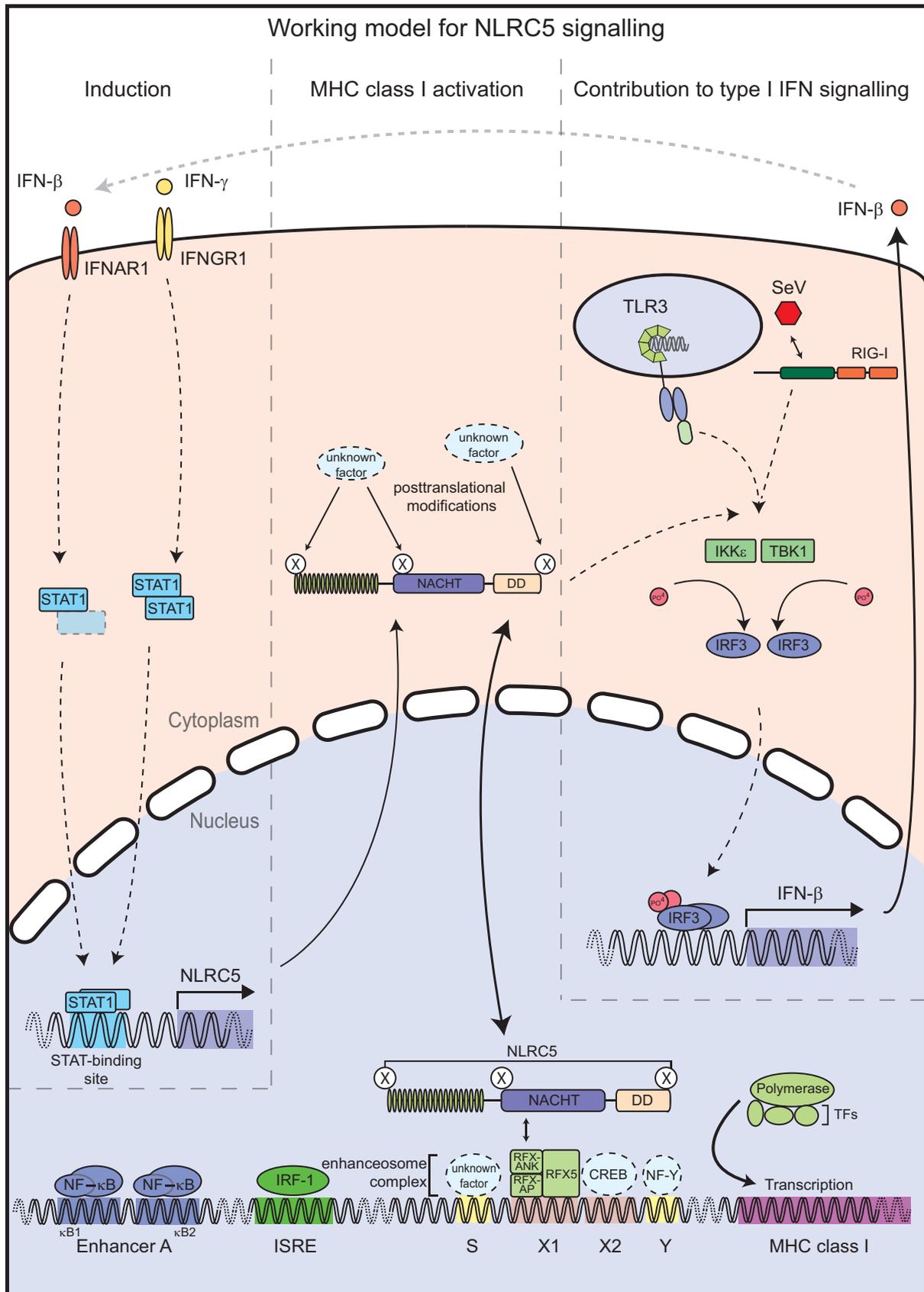
4.3 Detailed function of NLRC5 in MHC transcriptional regulation

CIITA-dependent MHC class II activation relies on the enhanceosome complex, which binds mainly to the X1, X2-motif of the MHC class II promoter region (reviewed in Krawczyk and Reith, 2006; Reith *et al.*, 2005). A similar region in the MHC class I promoter was shown to be important for enhanceosome-dependent MHC class I activation as well (Gobin *et al.*, 1998b). Mutation of this X1, X2-motif completely abolished NLRC5-dependent MHC class I activation, demonstrating the dependency on the enhanceosome complex (Figure 3.14).

This was further independently validated by Meissner *et al.*, showing that NLRC5-mediated MHC class I activation is dependent on the complete enhanceosome complex, consisting of RFX-5, RFX-ANK and RFX-AP. Interestingly, Meissner and colleagues identified the S-motif as an important motif for NLRC5-dependent MHC class I activation (refer to figure 1.5 and figure 3.14), but dispensable for CIITA-dependent MHC class I activation in this study (Meissner *et al.*, 2012c). To date, the role of the S-motif is not entirely clear, but an intact integrity of the S-motif is pivotal for the recruitment of CIITA to the MHC class II promoter in an enhanceosome-dependent manner (Muhlethaler-Mottet *et al.*, 2004). Nonetheless, involvement of the S-motif in different regulatory mechanisms and specificity concerning the mode of action between NLRC5 and CIITA remain conceivable.

Interaction between RFX-ANK and NLRC5 was reported by Meissner *et al.*, by which binding to the enhanceosome complex is mediated. This interaction was depending on the ankyrin repeats of RFX-ANK, although this interaction has to be analysed in further detail (Meissner *et al.*, 2012c).

Interestingly, whereas CIITA-FIII only marginally activated MHC class I promoter in our hands, the dendritic isoform FI showed a much stronger MHC class I activation (compare figure 3.14 D or 3.14 B). To date, the function of the N-terminal CARD domain of CIITA-FI remains to be elucidated, however, a recent publication reported that CIITA-FI could not be linked to any critical function in antigen presentation and immune responses (Zinzow-Kramer *et al.*, 2012). Thus, it remains unclear whether CIITA-FI can compensate for MHC class I expression in the absence of NLRC5.

NLRC5 and CIITA both function as a transcriptional activator for MHC class I and II induction, respectively, which is mediated by the enhanceosome complex. To find out, which domain structure is important for specific recruitment of NLRC5 or CIITA, we generated chimeric constructs of NLRC5 and CIITA. In an earlier report from Girardin *et al.*, fusion of the NOD2 LRR region to the NOD1 CARD and NACHT region resulted in a functional protein, which could be specifically induced by the NOD2 elicitor MDP, showing functionality of domain swapping between two related NLR proteins (Girardin *et al.*, 2005). Based on these finding, we

generated constructs of NLRC5 containing only the effector domain (DD), or lacking the effector domain (ΔDD) but including the NLS site, respectively. These constructs were fused to the CIITA C-terminus or N-terminus, respectively (refer to figure 3.15 A). CIITA AD (AD163-ΔDD-NLRC5) or AD and P/S/T (AD335-ΔDD-NLRC5) domains fused to NLRC5-NACHT-LRR region are completely signalling inactive in HEK293T-based luciferase reporter assays. Camacho-Carvajal and co-workers identified a CIITA-mutant lacking AD and P/S/T (aa 1 to 335; termed CIITA-L335) harbouring a strong dominant negative effect on CIITA signalling when fused to an NLS (CIITA-NLS-L335) (Camacho-Carvajal *et al.*, 2004). Unexpectedly, we were able to restore MHC class II activation of the CIITA-L335 constructs as well as MHC class I activation potential by N-terminal fusing of the NLRC5 death domain-fold domain to this construct (DD-ΔAD335-CIITA) (Figure 3.15 B; right). To date, the exact function of the P/S/T domain remains unresolved (Boss and Jensen, 2003) and it was also dispensable for MHC activation in our constructs, since both constructs either harbouring the P/S/T (DD-ΔAD163-CIITA) or lacking the P/S/T (DD-ΔAD335-CIITA) offered similar signalling activities. These findings were further verified in HEK293T cells with comparable induction for endogenous MHC class I and class II expression levels (Figure 3.18).

Similar to wildtype NLRC5 and CIITA, both DD-ΔAD163-CIITA and DD-ΔAD335-CIITA were able to shuttle to the nucleus, whereas AD163-ΔDD-NLRC5 and AD335-ΔDD-NLRC5 remained entirely cytoplasmic, most likely due to the lack of the N-terminal NLS of NLRC5, which promotes nuclear import. However, nuclear accumulation could not be achieved for AD163-ΔDD-NLRC5 and AD335-ΔDD-NLRC5 by fusion to a double SV40 NLS, although small background activation of MHC class I promoter luciferase remained detectable (Figure 3.17).

The molecular mechanism involving MHC class II activation by CIITA has been analysed in great detail and it has been established, that enhanceosome-binding of CIITA is mediated by the LRR and NACHT region (also refer to the dominant negative function of CIITA-L335), whereas the N-terminal transcription activation domain (AD) mediates transcription machinery recruitment (reviewed in Krawczyk and Reith, 2006; Ting and Trowsdale, 2002; Reith and Mach, 2001). The fact, that DD-ΔAD163-CIITA and DD-ΔAD335-CIITA activate both MHC class I and MHC class II expression, even without the AD of CIITA leads to the conclusion, that the effector domain of NLRC5 is sufficient to recruit components of the transcription machinery, which drive both MHC class I and MHC class II transcription. To maintain specificity for MHC class I transcription by NLRC5, recruitment of additional regulatory factors seems likely. Initial experiments from Meissner *et al.* show, that the S-box motif is important for NLRC5-mediated

MHC class I induction, but not for CIITA-mediated MHC class I induction in luciferase reporter assays (Meissner *et al.*, 2012b).

The effector domain of NLRC5 completely restores the activity of CIITA-L335 to induce MHC class II expression and also activates MHC class I expression (Figure 3.15). To analyse, whether the effector domain of NLRC5 is also capable of MHC class I activation fused onto the NACHT-LRR region of other related NLR proteins, we fused the effector domain of NLRC5 to the NACHT-LRR region of the PRR NOD1, which itself is neither able to shuttle to the nucleus, nor activate MHC expression (Zurek *et al.*, 2012b and Figure 3.19). Fusion of the effector domain to the NOD1-NACHT-LRR region benefits nuclear import, most likely due to the N-terminal NLS of NLRC5. However, nuclear DD-ΔDD-NOD1 did not maintain MHC class I promoter activation in our experimental setup, most likely because of the inability of the NOD1 NACHT-LRR region to interact with components of the enhanceosome complexes. To conclude, although the NLRC5 effector domain is pivotal for MHC class I activation and also capable of MHC class II activation to a certain extend in a NLRC5-CIITA-chimeric protein, most likely due to beneficial recruitment of additional factors by the NACHT-LRR region of CIITA, it is not sufficient to trigger MHC expression, when these factors are missing.

Finally, we addressed the contribution of the LRR region of NLRC5 and CIITA to MHC promoter activation. Distinct analyses of the LRR of CIITA revealed pivotal functions in nuclear shuttling and activation of MHC class II promoter (Camacho-Carvajal *et al.*, 2004; Hake *et al.*, 2000). Although detailed analyses are missing so far for NLRC5, increase in nuclear accumulation of NLRC5 constructs lacking the LRR was observed. Thus a contribution of the LRR of NLRC5 in nuclear export seems conceivable. Nevertheless, fusion of NLRC5 N-terminus and CIITA-LRR as well as CIITA-N-terminus and NLRC5-LRR neither activated MHC class I promoter constructs nor MHC class II promoter constructs.

5 Conclusion

The results obtained in this thesis cover two different roles for the NLR protein NLRC5. On the one hand, we show that NLRC5 is inducible upon TLR3 and RIG-I stimulation, both triggering different pathways, resulting in type I IFN production. Interestingly, also NLRC5 itself contributes to type I IFN expression upon TLR3 and RIG-I stimulation, verified by knock-down experiments in the lymphoid cell line THP-1 as well as in human primary dermal fibroblasts (hFibr). On the other hand, we show that NLRC5 can shuttle to the nucleus and activates MHC class I gene expression. Moreover, we provided evidence, that the mechanism of MHC class I activation is similar to MHC class II activation, which is mediated by the closely related NLR protein CIITA. We identified the enhanceosome complex as crucial component of NLRC5-dependent MHC class I activation. Furthermore, we obtained first insights into the contribution of the N-terminal effector domain to trigger MHC class I activation as well as in exceptional circumstances also MHC class II activation.

MHC class I surface expression plays an important role in clearance of cytoplasmic pathogens, for example viruses and bacteria, since pathogen-derived cytoplasmic antigens are presented to the cell surface via the MHC class I pathway (refer to figure 1.4). In the present work, we could demonstrate that NLRC5 is upregulated upon different viral PAMPs, including poly(I:C) and SeV resulting in increased MHC class I levels. In particular after viral infections, the host organism profits from enhanced antigen presentation in infected cells, resulting in cytotoxic T cell mediated killing and restriction of local infections. Interestingly, NLRC5 itself contributes to antiviral immunity by maintaining type I IFN responses in human. Thus, due to its bifurcate function, NLRC5 is a promising candidate for antiviral immune therapy.

Importantly to mention, cancer therapy greatly profits from a better understanding of MHC class I regulation. It is known for a long time, that many tumors show reduced or impaired MHC class I surface expression, which provides a mechanism for tumors to escape immunosurveillance, although the detailed mechanism remains to be elucidated (Reinis, 2011). Moreover, cancer database records link the upregulation of classical MHC class I surface molecules (HLA-A/B/C) in cancer cell lines also to upregulation of NLRC5 protein (http://www.broadinstitute.org/ccle/home).

Although the detailed mechanism of NLRC5 in MHC class I regulation still remains to be elucidated, we identified an NLRC5-CIITA chimeric protein, which potently activates MHC class I and MHC class II expression and could demonstrate the contribution of the N-terminal effector domain in this process. The use of this chimeric protein can further lead to a better understanding of the discrimination between MHC class I and MHC class II transcriptional regulation.

The identification of NLRC5 as the MHC class I transactivator as well as our identification of an NLRC5-CIITA-chimeric protein that activates both MHC class I and class II expression further contributes to the understanding of MHC regulation and to the development of new techniques for immunotherapy of MHC class I deficient tumors.

6 References

Abbott, D.W., Yang, Y., Hutti, J.E., Madhavarapu, S., Kelliher, M.A. and Cantley, L.C. (2007) Coordinated regulation of Toll-like receptor and NOD2 signaling by K63-linked polyubiquitin chains. *Mol Cell Biol.* **27**: 6012-6025.

Ablasser, A., Bauernfeind, F., Hartmann, G., Latz, E., Fitzgerald, K.A. and Hornung, V. (2009) RIG-I-dependent sensing of poly(dA:dT) through the induction of an RNA polymerase III-transcribed RNA intermediate. *Nat Immunol.* **10**: 1065-1072.

Accolla, R.S. (1983) Human B cell variants immunoselected against a single Ia antigen subset have lost expression of several Ia antigen subsets. *J Exp Med.* **157**: 1053-1058.

Akashi-Takamura, S. and Miyake, K. (2008) TLR accessory molecules. *Curr Opin Immunol.* **20**: 420-425.

Akira, S. and Takeda, K. (2004) Toll-like receptor signalling. *Nat Rev Immunol.* **4**: 499-511.

Akira, S., Uematsu, S. and Takeuchi, O. (2006) Pathogen recognition and innate immunity. *Cell.* **124**: 783-801.

Alexopoulou, L., Holt, A.C., Medzhitov, R. and Flavell, R.A. (2001) Recognition of double-stranded RNA and activation of NF-kappaB by Toll-like receptor 3. *Nature.* **413**: 732-738.

Allen, I.C., Moore, C.B., Schneider, M., Lei, Y., Davis, B.K., Scull, M.A.*, et al* (2011) NLRX1 protein attenuates inflammatory responses to infection by interfering with the RIG-I-MAVS and TRAF6-NF-kappaB signaling pathways. *Immunity.* **34**: 854-865.

Anand, P.K., Malireddi, R.K., Lukens, J.R., Vogel, P., Bertin, J., Lamkanfi, M. and Kanneganti, T.D. (2012) NLRP6 negatively regulates innate immunity and host defence against bacterial pathogens. *Nature.* **488**: 389-393.

Appay, V. and Rowland-Jones, S.L. (2001) RANTES: a versatile and controversial chemokine. *Trends Immunol.* **22**: 83-87.

Bao, Q., Riedl, S.J. and Shi, Y. (2005) Structure of Apaf-1 in the auto-inhibited form: a critical role for ADP. *Cell Cycle.* **4**: 1001-1003.

Bauernfeind, F.G., Horvath, G., Stutz, A., Alnemri, E.S., MacDonald, K., Speert, D.*, et al* (2009) Cutting edge: NF-kappaB activating pattern recognition and cytokine receptors license NLRP3 inflammasome activation by regulating NLRP3 expression. *J Immunol.* **183**: 787-791.

Benko, S., Magalhaes, J.G., Philpott, D.J. and Girardin, S.E. (2010) NLRC5 limits the activation of inflammatory pathways. *J Immunol.* **185**: 1681-1691.

Bertrand, M.J., Doiron, K., Labbe, K., Korneluk, R.G., Barker, P.A. and Saleh, M. (2009) Cellular inhibitors of apoptosis cIAP1 and cIAP2 are required for innate immunity signaling by the pattern recognition receptors NOD1 and NOD2. *Immunity.* **30**: 789-801.

Bewry, N.N., Bolick, S.C., Wright, K.L. and Harton, J.A. (2007) GTP-dependent recruitment of CIITA to the class II major histocompatibility complex promoter. *J Biol Chem.* **282**: 26178-26184.

Bielig, H., Zurek, B., Kutsch, A., Menning, M., Philpott, D.J., Sansonetti, P.J. and Kufer, T.A. (2009) A function for AAMP in Nod2-mediated NF-kappaB activation. *Mol Immunol.* **46**: 2647-2654.

Biswas, A., Meissner, T.B., Kawai, T. and Kobayashi, K.S. (2012) Cutting edge: impaired MHC class I expression in mice deficient for Nlrc5/class I transactivator. *J Immunol.* **189**: 516-520.

Bontron, S., Ucla, C., Mach, B. and Steimle, V. (1997) Efficient repression of endogenous major histocompatibility complex class II expression through dominant negative CIITA mutants isolated by a functional selection strategy. *Mol Cell Biol.* **17**: 4249-4258.

Boothby, M., Gravallese, E., Liou, H.C. and Glimcher, L.H. (1988) A DNA binding protein regulated by IL-4 and by differentiation in B cells. *Science.* **242**: 1559-1562.

Boss, J.M. and Jensen, P.E. (2003) Transcriptional regulation of the MHC class II antigen presentation pathway. *Curr Opin Immunol.* **15**: 105-111.

Bousfiha, A., Picard, C., Boisson-Dupuis, S., Zhang, S.Y., Bustamante, J., Puel, A*., et al* (2010) Primary immunodeficiencies of protective immunity to primary infections. *Clin Immunol.* **135**: 204-209.

Bucher, P., Karplus, K., Moeri, N. and Hofmann, K. (1996) A flexible motif search technique based on generalized profiles. *Comput Chem.* **20**: 3-23.

Burckstummer, T., Baumann, C., Bluml, S., Dixit, E., Durnberger, G., Jahn, H*., et al* (2009) An orthogonal proteomic-genomic screen identifies AIM2 as a cytoplasmic DNA sensor for the inflammasome. *Nat Immunol.* **10**: 266-272.

Burke, P.A. and Ozato, K. (1989) Regulation of major histocompatibility complex class I genes. *Year Immunol.* **4**: 23-40.

Camacho-Carvajal, M.M., Klingler, S., Schnappauf, F., Hake, S.B. and Steimle, V. (2004) Importance of class II transactivator leucine-rich repeats for dominant-negative function and nucleo-cytoplasmic transport. *Int Immunol.* **16**: 65-75.

Casanova, J.L., Abel, L. and Quintana-Murci, L. (2012) Human TLRs and IL-1Rs in host defense: natural insights from evolutionary, epidemiological, and clinical genetics. *Annu Rev Immunol.* **29**: 447-491.

Chamaillard, M., Hashimoto, M., Horie, Y., Masumoto, J., Qiu, S., Saab, L*., et al* (2003) An essential role for NOD1 in host recognition of bacterial peptidoglycan containing diamino-pimelic acid. *Nat Immunol.* **4**: 702-707.

Chen, G.Y., Liu, M., Wang, F., Bertin, J. and Nunez, G. (2011) A functional role for Nlrp6 in intestinal inflammation and tumorigenesis. *J Immunol.* **186**: 7187-7194.

Chin, K.C., Li, G.G. and Ting, J.P. (1997) Importance of acidic, proline/serine/threonine-rich, and GTP-binding regions in the major histocompatibility complex class II transactivator: generation of transdominant-negative mutants. *Proc Natl Acad Sci U S A.* **94**: 2501-2506.

Chiu, Y.H., Macmillan, J.B. and Chen, Z.J. (2009) RNA polymerase III detects cytosolic DNA and induces type I interferons through the RIG-I pathway. *Cell.* **138**: 576-591.

Cohen, G.M. (1997) Caspases: the executioners of apoptosis. *Biochem J.* **326 (Pt 1)**: 1-16.

Correa, R.G., Milutinovic, S. and Reed, J.C. (2012) Roles of NOD1 (NLRC1) and NOD2 (NLRC2) in innate immunity and inflammatory diseases. *Biosci Rep.*

Cui, J., Zhu, L., Xia, X., Wang, H.Y., Legras, X., Hong, J*., et al* (2010) NLRC5 negatively regulates the NF-kappaB and type I interferon signaling pathways. *Cell.* **141**: 483-496.

D'Osualdo, A. and Reed, J.C. (2012) NLRP1, a regulator of innate immunity associated with vitiligo. *Pigment Cell Melanoma Res.* **25**: 5-8.

D'Osualdo, A., Weichenberger, C.X., Wagner, R.N., Godzik, A., Wooley, J. and Reed, J.C. (2011) CARD8 and NLRP1 undergo autoproteolytic processing through a ZU5-like domain. *PLoS One.* **6**: e27396.

Damgaard, R.B., Nachbur, U., Yabal, M., Wong, W.W., Fiil, B.K., Kastirr, M., *et al* (2012) The ubiquitin ligase XIAP recruits LUBAC for NOD2 signaling in inflammation and innate immunity. *Mol Cell.* **46**: 746-758.

Danot, O., Marquenet, E., Vidal-Ingigliardi, D. and Richet, E. (2009) Wheel of Life, Wheel of Death: A Mechanistic Insight into Signaling by STAND Proteins. *Structure.* **17**: 172-182.

Davis, B.K., Roberts, R.A., Huang, M.T., Willingham, S.B., Conti, B.J., Brickey, W.J., *et al* (2010) Cutting edge: NLRC5-dependent activation of the inflammasome. *J Immunol.* **186**: 1333-1337.

DeSandro, A.M., Nagarajan, U.M. and Boss, J.M. (2000) Associations and interactions between bare lymphocyte syndrome factors. *Mol Cell Biol.* **20**: 6587-6599.

Durand, B., Sperisen, P., Emery, P., Barras, E., Zufferey, M., Mach, B. and Reith, W. (1997) RFXAP, a novel subunit of the RFX DNA binding complex is mutated in MHC class II deficiency. *Embo J.* **16**: 1045-1055.

Elinav, E., Strowig, T., Henao-Mejia, J. and Flavell, R.A. (2011) Regulation of the antimicrobial response by NLR proteins. *Immunity.* **34**: 665-679.

Faustin, B., Lartigue, L., Bruey, J.M., Luciano, F., Sergienko, E., Bailly-Maitre, B., *et al* (2007) Reconstituted NALP1 inflammasome reveals two-step mechanism of caspase-1 activation. *Mol Cell.* **25**: 713-724.

Fernandes-Alnemri, T., Yu, J.W., Datta, P., Wu, J. and Alnemri, E.S. (2009) AIM2 activates the inflammasome and cell death in response to cytoplasmic DNA. *Nature.* **458**: 509-513.

Fitzgerald, K.A., Rowe, D.C., Barnes, B.J., Caffrey, D.R., Visintin, A., Latz, E., *et al* (2003a) LPS-TLR4 signaling to IRF-3/7 and NF-kappaB involves the toll adapters TRAM and TRIF. *J Exp Med.* **198**: 1043-1055.

Fitzgerald, K.A., McWhirter, S.M., Faia, K.L., Rowe, D.C., Latz, E., Golenbock, D.T., *et al* (2003b) IKKepsilon and TBK1 are essential components of the IRF3 signaling pathway. *Nat Immunol.* **4**: 491-496.

Franchi, L., Warner, N., Viani, K. and Nunez, G. (2009) Function of Nod-like receptors in microbial recognition and host defense. *Immunol Rev.* **227**: 106-128.

Fritz, J.H., Ferrero, R.L., Philpott, D.J. and Girardin, S.E. (2006) Nod-like proteins in immunity, inflammation and disease. *Nat Immunol.* **7**: 1250-1257.

Gasse, P., Riteau, N., Charron, S., Girre, S., Fick, L., Petrilli, V., *et al* (2009) Uric acid is a danger signal activating NALP3 inflammasome in lung injury inflammation and fibrosis. *Am J Respir Crit Care Med.* **179**: 903-913.

Gee, P., Chua, P.K., Gevorkyan, J., Klumpp, K., Najera, I., Swinney, D.C. and Deval, J. (2008) Essential role of the N-terminal domain in the regulation of RIG-I ATPase activity. *J Biol Chem.* **283**: 9488-9496.

Girardin, S.E., Jehanno, M., Mengin-Lecreulx, D., Sansonetti, P.J., Alzari, P.M. and Philpott, D.J. (2005) Identification of the critical residues involved in peptidoglycan detection by Nod1. *J Biol Chem.* **280**: 38648-38656.

Girardin, S.E., Boneca, I.G., Viala, J., Chamaillard, M., Labigne, A., Thomas, G., *et al* (2003a) Nod2 is a general sensor of peptidoglycan through muramyl dipeptide (MDP) detection. *J Biol Chem.* **278**: 8869-8872.

Girardin, S.E., Boneca, I.G., Carneiro, L.A., Antignac, A., Jehanno, M., Viala, J., *et al* (2003b) Nod1 detects a unique muropeptide from gram-negative bacterial peptidoglycan. *Science.* **300**: 1584-1587.

Gobin, S.J., Peijnenburg, A., Keijsers, V. and van den Elsen, P.J. (1997) Site alpha is crucial for two routes of IFN gamma-induced MHC class I transactivation: the ISRE-mediated route and a novel pathway involving CIITA. *Immunity*. **6**: 601-611.

Gobin, S.J., Keijsers, V., van Zutphen, M. and van den Elsen, P.J. (1998a) The role of enhancer A in the locus-specific transactivation of classical and nonclassical HLA class I genes by nuclear factor kappa B. *J Immunol*. **161**: 2276-2283.

Gobin, S.J., van Zutphen, M., Woltman, A.M. and van den Elsen, P.J. (1999) Transactivation of classical and nonclassical HLA class I genes through the IFN-stimulated response element. *J Immunol*. **163**: 1428-1434.

Gobin, S.J., van Zutphen, M., Westerheide, S.D., Boss, J.M. and van den Elsen, P.J. (2001) The MHC-specific enhanceosome and its role in MHC class I and beta(2)-microglobulin gene transactivation. *J Immunol*. **167**: 5175-5184.

Gobin, S.J., Peijnenburg, A., van Eggermond, M., van Zutphen, M., van den Berg, R. and van den Elsen, P.J. (1998b) The RFX complex is crucial for the constitutive and CIITA-mediated transactivation of MHC class I and beta2-microglobulin genes. *Immunity*. **9**: 531-541.

Gong, Y.N. and Shao, F. (2012) Sensing bacterial infections by NAIP receptors in NLRC4 inflammasome activation. *Protein Cell*. **3**: 98-105.

Gorelik, E., Peppoloni, S., Overton, R. and Herberman, R.B. (1985) Increase in H-2 antigen expression and immunogenicity of BL6 melanoma cells treated with N-methyl-N'-nitronitrosoguanidine. *Cancer Res*. **45**: 5341-5347.

Gorelik, E., Jay, G., Kim, M., Hearing, V.J., DeLeo, A. and McCoy, J.P., Jr. (1991) Effects of H-2Kb gene on expression of melanoma-associated antigen and lectin-binding sites on BL6 melanoma cells. *Cancer Res*. **51**: 5212-5218.

Grenier, J.M., Wang, L., Manji, G.A., Huang, W.J., Al-Garawi, A., Kelly, R., *et al* (2002) Functional screening of five PYPAF family members identifies PYPAF5 as a novel regulator of NF-kappaB and caspase-1. *FEBS Lett*. **530**: 73-78.

Grimes, C.L., Ariyananda Lde, Z., Melnyk, J.E. and O'Shea, E.K. (2012) The innate immune protein Nod2 binds directly to MDP, a bacterial cell wall fragment. *J Am Chem Soc*. **134**: 13535-13537.

Gross, O., Thomas, C.J., Guarda, G. and Tschopp, J. (2011) The inflammasome: an integrated view. *Immunol Rev*. **243**: 136-151.

Hake, S.B., Masternak, K., Kammerbauer, C., Janzen, C., Reith, W. and Steimle, V. (2000) CIITA leucine-rich repeats control nuclear localization, in vivo recruitment to the major histocompatibility complex (MHC) class II enhanceosome, and MHC class II gene transactivation. *Mol Cell Biol*. **20**: 7716-7725.

Halle, A., Hornung, V., Petzold, G.C., Stewart, C.R., Monks, B.G., Reinheckel, T., *et al* (2008) The NALP3 inflammasome is involved in the innate immune response to amyloid-beta. *Nat Immunol*. **9**: 857-865.

Hanson, P.I. and Whiteheart, S.W. (2005) AAA+ proteins: have engine, will work. *Nat Rev Mol Cell Biol*. **6**: 519-529.

Harton, J.A., Cressman, D.E., Chin, K.C., Der, C.J. and Ting, J.P. (1999) GTP binding by class II transactivator: role in nuclear import. *Science*. **285**: 1402-1405.

Harton, J.A., O'Connor, W., Jr., Conti, B.J., Linhoff, M.W. and Ting, J.P. (2002) Leucine-rich repeats of the class II transactivator control its rate of nuclear accumulation. *Hum Immunol*. **63**: 588-601.

Hasegawa, M., Fujimoto, Y., Lucas, P.C., Nakano, H., Fukase, K., Nunez, G. and Inohara, N. (2008) A critical role of RICK/RIP2 polyubiquitination in Nod-induced NF-kappaB activation. *Embo J.* **27**: 373-383.

Hayashi, F., Smith, K.D., Ozinsky, A., Hawn, T.R., Yi, E.C., Goodlett, D.R*., et al* (2001) The innate immune response to bacterial flagellin is mediated by Toll-like receptor 5. *Nature.* **410**: 1099-1103.

Heil, F., Hemmi, H., Hochrein, H., Ampenberger, F., Kirschning, C., Akira, S*., et al* (2004) Species-specific recognition of single-stranded RNA via toll-like receptor 7 and 8. *Science.* **303**: 1526-1529.

Hemmi, H., Takeuchi, O., Kawai, T., Kaisho, T., Sato, S., Sanjo, H*., et al* (2000) A Toll-like receptor recognizes bacterial DNA. *Nature.* **408**: 740-745.

Hofmann, K., Bucher, P. and Tschopp, J. (1997) The CARD domain: a new apoptotic signalling motif. *Trends Biochem Sci.* **22**: 155-156.

Hornung, V. and Latz, E. (2010) Intracellular DNA recognition. *Nat Rev Immunol.* **10**: 123-130.

Hornung, V., Ablasser, A., Charrel-Dennis, M., Bauernfeind, F., Horvath, G., Caffrey, D.R*., et al* (2009) AIM2 recognizes cytosolic dsDNA and forms a caspase-1-activating inflammasome with ASC. *Nature.* **458**: 514-518.

Hornung, V., Ellegast, J., Kim, S., Brzozka, K., Jung, A., Kato, H*., et al* (2006) 5'-Triphosphate RNA is the ligand for RIG-I. *Science.* **314**: 994-997.

Howcroft, T.K., Raval, A., Weissman, J.D., Gegonne, A. and Singer, D.S. (2003) Distinct transcriptional pathways regulate basal and activated major histocompatibility complex class I expression. *Mol Cell Biol.* **23**: 3377-3391.

Hsu, L.C., Ali, S.R., McGillivray, S., Tseng, P.H., Mariathasan, S., Humke, E.W*., et al* (2008) A NOD2-NALP1 complex mediates caspase-1-dependent IL-1beta secretion in response to Bacillus anthracis infection and muramyl dipeptide. *Proc Natl Acad Sci U S A.* **105**: 7803-7808.

Hua, J., Liao, M.J. and Rashidbaigi, A. (1996) Cytokines induced by Sendai virus in human peripheral blood leukocytes. *J Leukoc Biol.* **60**: 125-128.

Hume, C.R. and Lee, J.S. (1989) Congenital immunodeficiencies associated with absence of HLA class II antigens on lymphocytes result from distinct mutations in trans-acting factors. *Hum Immunol.* **26**: 288-309.

Inohara, N., Koseki, T., Lin, J., del Peso, L., Lucas, P.C., Chen, F.F*., et al* (2000) An induced proximity model for NF-kappa B activation in the Nod1/RICK and RIP signaling pathways. *J Biol Chem.* **275**: 27823-27831.

Inohara, N., Koseki, T., del Peso, L., Hu, Y., Yee, C., Chen, S*., et al* (1999) Nod1, an Apaf-1-like activator of caspase-9 and nuclear factor-kappaB. *J Biol Chem.* **274**: 14560-14567.

Inohara, N., Ogura, Y., Fontalba, A., Gutierrez, O., Pons, F., Crespo, J*., et al* (2003) Host recognition of bacterial muramyl dipeptide mediated through NOD2. Implications for Crohn's disease. *J Biol Chem.* **278**: 5509-5512.

Ishikawa, H. and Barber, G.N. (2008) STING is an endoplasmic reticulum adaptor that facilitates innate immune signalling. *Nature.* **455**: 674-678.

Istomin, A.Y. and Godzik, A. (2009) Understanding diversity of human innate immunity receptors: analysis of surface features of leucine-rich repeat domains in NLRs and TLRs. *BMC Immunol.* **10**: 48.

Itoh-Lindstrom, Y., Piskurich, J.F., Felix, N.J., Wang, Y., Brickey, W.J., Platt, J.L.*, et al* (1999) Reduced IL-4-, lipopolysaccharide-, and IFN-gamma-induced MHC class II expression in mice lacking class II transactivator due to targeted deletion of the GTP-binding domain. *J Immunol.* **163**: 2425-2431.

Iwasaki, A. and Medzhitov, R. (2010) Regulation of adaptive immunity by the innate immune system. *Science.* **327**: 291-295.

Jin, C. and Flavell, R.A. (2010) Molecular mechanism of NLRP3 inflammasome activation. *J Clin Immunol.* **30**: 628-631.

Jin, M.S., Kim, S.E., Heo, J.Y., Lee, M.E., Kim, H.M., Paik, S.G.*, et al* (2007) Crystal structure of the TLR1-TLR2 heterodimer induced by binding of a tri-acylated lipopeptide. *Cell.* **130**: 1071-1082.

Johnson, D.R. (2003) Locus-specific constitutive and cytokine-induced HLA class I gene expression. *J Immunol.* **170**: 1894-1902.

Karin, M. and Ben-Neriah, Y. (2000) Phosphorylation meets ubiquitination: the control of NF-[kappa]B activity. *Annu Rev Immunol.* **18**: 621-663.

Karre, K. (2002) NK cells, MHC class I molecules and the missing self. *Scand J Immunol.* **55**: 221-228.

Kato, H., Takahasi, K. and Fujita, T. (2011) RIG-I-like receptors: cytoplasmic sensors for non-self RNA. *Immunol Rev.* **243**: 91-98.

Kato, H., Takeuchi, O., Mikamo-Satoh, E., Hirai, R., Kawai, T., Matsushita, K.*, et al* (2008) Length-dependent recognition of double-stranded ribonucleic acids by retinoic acid-inducible gene-I and melanoma differentiation-associated gene 5. *J Exp Med.* **205**: 1601-1610.

Kato, H., Takeuchi, O., Sato, S., Yoneyama, M., Yamamoto, M., Matsui, K.*, et al* (2006) Differential roles of MDA5 and RIG-I helicases in the recognition of RNA viruses. *Nature.* **441**: 101-105.

Kawai, T. and Akira, S. (2010) The role of pattern-recognition receptors in innate immunity: update on Toll-like receptors. *Nat Immunol.* **11**: 373-384.

Kawai, T., Takahashi, K., Sato, S., Coban, C., Kumar, H., Kato, H.*, et al* (2005) IPS-1, an adaptor triggering RIG-I- and Mda5-mediated type I interferon induction. *Nat Immunol.* **6**: 981-988.

Kerur, N., Veettil, M.V., Sharma-Walia, N., Bottero, V., Sadagopan, S., Otageri, P. and Chandran, B. (2011) IFI16 acts as a nuclear pathogen sensor to induce the inflammasome in response to Kaposi Sarcoma-associated herpesvirus infection. *Cell Host Microbe.* **9**: 363-375.

Kobe, B. and Kajava, A.V. (2001) The leucine-rich repeat as a protein recognition motif. *Curr Opin Struct Biol.* **11**: 725-732.

Kofoed, E.M. and Vance, R.E. (2011) Innate immune recognition of bacterial ligands by NAIPs determines inflammasome specificity. *Nature.* **477**: 592-595.

Komuro, A. and Horvath, C.M. (2006) RNA- and virus-independent inhibition of antiviral signaling by RNA helicase LGP2. *J Virol.* **80**: 12332-12342.

Koonin, E.V. and Aravind, L. (2000) The NACHT family - a new group of predicted NTPases implicated in apoptosis and MHC transcription activation. *Trends Biochem Sci.* **25**: 223-224.

Kowalinski, E., Lunardi, T., McCarthy, A.A., Louber, J., Brunel, J., Grigorov, B.*, et al* (2011) Structural basis for the activation of innate immune pattern-recognition receptor RIG-I by viral RNA. *Cell.* **147**: 423-435.

Krawczyk, M. and Reith, W. (2006) Regulation of MHC class II expression, a unique regulatory system identified by the study of a primary immunodeficiency disease. *Tissue Antigens*. **67**: 183-197.

Krawczyk, M., Seguin-Estevez, Q., Leimgruber, E., Sperisen, P., Schmid, C., Bucher, P. and Reith, W. (2008) Identification of CIITA regulated genetic module dedicated for antigen presentation. *PLoS Genet*. **4**: e1000058.

Krieg, A., Correa, R.G., Garrison, J.B., Le Negrate, G., Welsh, K., Huang, Z.*, et al* (2009) XIAP mediates NOD signaling via interaction with RIP2. *Proc Natl Acad Sci U S A*. **106**: 14524-14529.

Kuenzel, S., Till, A., Winkler, M., Hasler, R., Lipinski, S., Jung, S.*, et al* (2010) The nucleotide-binding oligomerization domain-like receptor NLRC5 is involved in IFN-dependent antiviral immune responses. *J Immunol*. **184**: 1990-2000.

Kufer, T.A. (2008) Signal transduction pathways used by NLR-type innate immune receptors. *Mol Biosyst*. **4**: 380-386.

Kufer, T.A. and Sansonetti, P.J. (2011) NLR functions beyond pathogen recognition. *Nat Immunol*. **12**: 121-128.

Kufer, T.A., Kremmer, E., Banks, D.J. and Philpott, D.J. (2006) Role for erbin in bacterial activation of Nod2. *Infect Immun*. **74**: 3115-3124.

Kufer, T.A., Kremmer, E., Adam, A.C., Philpott, D.J. and Sansonetti, P.J. (2008) The pattern-recognition molecule Nod1 is localized at the plasma membrane at sites of bacterial interaction. *Cell Microbiol*. **10**: 477-486.

Kumar, H., Kawai, T. and Akira, S. (2011a) Pathogen recognition by the innate immune system. *Int Rev Immunol*. **30**: 16-34.

Kumar, H., Pandey, S., Zou, J., Kumagai, Y., Takahashi, K., Akira, S. and Kawai, T. (2011b) NLRC5 deficiency does not influence cytokine induction by virus and bacteria infections. *J Immunol*. **186**: 994-1000.

Kumar, V. and McNerney, M.E. (2005) A new self: MHC-class-I-independent natural-killer-cell self-tolerance. *Nat Rev Immunol*. **5**: 363-374.

Laemmli, U.K. (1970) Cleavage of structural proteins during the assembly of the head of bacteriophage T4. *Nature*. **227**: 680-685.

Laroui, H., Yan, Y., Narui, Y., Ingersoll, S.A., Ayyadurai, S., Charania, M.A.*, et al* (2011) L-Ala-gamma-D-Glu-meso-diaminopimelic acid (DAP) interacts directly with leucine-rich region domain of nucleotide-binding oligomerization domain 1, increasing phosphorylation activity of receptor-interacting serine/threonine-protein kinase 2 and its interaction with nucleotide-binding oligomerization domain 1. *J Biol Chem*. **286**: 31003-31013.

Lemaitre, B., Nicolas, E., Michaut, L., Reichhart, J.M. and Hoffmann, J.A. (1996) The dorsoventral regulatory gene cassette spatzle/Toll/cactus controls the potent antifungal response in Drosophila adults. *Cell*. **86**: 973-983.

Li, K., Chen, Z., Kato, N., Gale, M., Jr. and Lemon, S.M. (2005) Distinct poly(I-C) and virus-activated signaling pathways leading to interferon-beta production in hepatocytes. *J Biol Chem*. **280**: 16739-16747.

Li, M., Muller, J., Rao, V., Hearing, V., Lueders, K. and Gorelik, E. (1996) Loss of intracisternal A-type retroviral particles in BL6 melanoma cells transfected with MHC class I genes. *J Gen Virol*. **77 (Pt 11)**: 2757-2765.

Ling, A., Soares, F., Croitoru, D.O., Tattoli, I., Carneiro, L.A., Boniotto, M*., et al* (2012) Post-transcriptional Inhibition of Luciferase Reporter Assays by the Nod-like Receptor Proteins NLRX1 and NLRC3. *J Biol Chem.* **287**: 28705-28716.

Long, E.O., Mach, B. and Accolla, R.S. (1984) Ia-negative B-cell variants reveal a coordinate regulation in the transcription of the HLA class II gene family. *Immunogenetics.* **19**: 349-353.

Luo, D., Ding, S.C., Vela, A., Kohlway, A., Lindenbach, B.D. and Pyle, A.M. (2011) Structural insights into RNA recognition by RIG-I. *Cell.* **147**: 409-422.

Maekawa, T., Kufer, T.A. and Schulze-Lefert, P. (2012) NLR functions in plant and animal immune systems: so far and yet so close. *Nat Immunol.* **12**: 817-826.

Mariathasan, S., Newton, K., Monack, D.M., Vucic, D., French, D.M., Lee, W.P*., et al* (2004) Differential activation of the inflammasome by caspase-1 adaptors ASC and Ipaf. *Nature.* **430**: 213-218.

Mariathasan, S., Weiss, D.S., Newton, K., McBride, J., O'Rourke, K., Roose-Girma, M*., et al* (2006) Cryopyrin activates the inflammasome in response to toxins and ATP. *Nature.* **440**: 228-232.

Martin, B.K., Chin, K.C., Olsen, J.C., Skinner, C.A., Dey, A., Ozato, K. and Ting, J.P. (1997) Induction of MHC class I expression by the MHC class II transactivator CIITA. *Immunity.* **6**: 591-600.

Martinon, F., Burns, K. and Tschopp, J. (2002) The inflammasome: a molecular platform triggering activation of inflammatory caspases and processing of proIL-beta. *Mol Cell.* **10**: 417-426.

Masternak, K., Muhlethaler-Mottet, A., Villard, J., Peretti, M. and Reith, W. (2000a) Molecular genetics of the Bare lymphocyte syndrome. *Rev Immunogenet.* **2**: 267-282.

Masternak, K., Muhlethaler-Mottet, A., Villard, J., Zufferey, M., Steimle, V. and Reith, W. (2000b) CIITA is a transcriptional coactivator that is recruited to MHC class II promoters by multiple synergistic interactions with an enhanceosome complex. *Genes Dev.* **14**: 1156-1166.

Masternak, K., Barras, E., Zufferey, M., Conrad, B., Corthals, G., Aebersold, R*., et al* (1998) A gene encoding a novel RFX-associated transactivator is mutated in the majority of MHC class II deficiency patients. *Nat Genet.* **20**: 273-277.

Matikainen, S., Pirhonen, J., Miettinen, M., Lehtonen, A., Govenius-Vintola, C., Sareneva, T. and Julkunen, I. (2000) Influenza A and sendai viruses induce differential chemokine gene expression and transcription factor activation in human macrophages. *Virology.* **276**: 138-147.

Matsukura, S., Kokubu, F., Kubo, H., Tomita, T., Tokunaga, H., Kadokura, M*., et al* (1998) Expression of RANTES by normal airway epithelial cells after influenza virus A infection. *Am J Respir Cell Mol Biol.* **18**: 255-264.

McDonald, C., Chen, F.F., Ollendorff, V., Ogura, Y., Marchetto, S., Lecine, P*., et al* (2005) A role for Erbin in the regulation of Nod2-dependent NF-kappaB signaling. *J Biol Chem.* **280**: 40301-40309.

Medzhitov, R., Preston-Hurlburt, P. and Janeway, C.A., Jr. (1997) A human homologue of the Drosophila Toll protein signals activation of adaptive immunity. *Nature.* **388**: 394-397.

Meissner, T.B., Li, A., Liu, Y.J., Gagnon, E. and Kobayashi, K.S. (2012b) The nucleotide-binding domain of NLRC5 is critical for nuclear import and transactivation activity. *Biochem Biophys Res Commun.* **418**: 786-791.

Meissner, T.B., Liu, Y.J., Lee, K.H., Li, A., Biswas, A., van Eggermond, M.C.*, et al* (2012c) NLRC5 cooperates with the RFX transcription factor complex to induce MHC class I gene expression. *J Immunol.* **188**: 4951-4958.

Meissner, T.B., Li, A., Biswas, A., Lee, K.H., Liu, Y.J., Bayir, E.*, et al* (2010) NLR family member NLRC5 is a transcriptional regulator of MHC class I genes. *Proc Natl Acad Sci U S A.* **107**: 13794-13799.

Mercer, E.A., Korhonen, L., Skoglosa, Y., Olsson, P.A., Kukkonen, J.P. and Lindholm, D. (2000) NAIP interacts with hippocalcin and protects neurons against calcium-induced cell death through caspase-3-dependent and -independent pathways. *Embo J.* **19**: 3597-3607.

Meylan, E., Curran, J., Hofmann, K., Moradpour, D., Binder, M., Bartenschlager, R. and Tschopp, J. (2005) Cardif is an adaptor protein in the RIG-I antiviral pathway and is targeted by hepatitis C virus. *Nature.* **437**: 1167-1172.

Miao, E.A., Mao, D.P., Yudkovsky, N., Bonneau, R., Lorang, C.G., Warren, S.E.*, et al* (2010) Innate immune detection of the type III secretion apparatus through the NLRC4 inflammasome. *Proc Natl Acad Sci U S A.* **107**: 3076-3080.

Mizel, S.B., West, A.P. and Hantgan, R.R. (2003) Identification of a sequence in human toll-like receptor 5 required for the binding of Gram-negative flagellin. *J Biol Chem.* **278**: 23624-23629.

Mo, J., Boyle, J.P., Howard, C.B., Monie, T.P., Davis, B.K. and Duncan, J.A. (2012) Pathogen sensing by nucleotide-binding oligomerization domain-containing protein 2 (NOD2) is mediated by direct binding to muramyl dipeptide and ATP. *J Biol Chem.* **287**: 23057-23067.

Moreno, C.S., Beresford, G.W., Louis-Plence, P., Morris, A.C. and Boss, J.M. (1999) CREB regulates MHC class II expression in a CIITA-dependent manner. *Immunity.* **10**: 143-151.

Moreno, C.S., Emery, P., West, J.E., Durand, B., Reith, W., Mach, B. and Boss, J.M. (1995) Purified X2 binding protein (X2BP) cooperatively binds the class II MHC X box region in the presence of purified RFX, the X box factor deficient in the bare lymphocyte syndrome. *J Immunol.* **155**: 4313-4321.

Muhlethaler-Mottet, A., Otten, L.A., Steimle, V. and Mach, B. (1997) Expression of MHC class II molecules in different cellular and functional compartments is controlled by differential usage of multiple promoters of the transactivator CIITA. *Embo J.* **16**: 2851-2860.

Muhlethaler-Mottet, A., Di Berardino, W., Otten, L.A. and Mach, B. (1998) Activation of the MHC class II transactivator CIITA by interferon-gamma requires cooperative interaction between Stat1 and USF-1. *Immunity.* **8**: 157-166.

Muhlethaler-Mottet, A., Krawczyk, M., Masternak, K., Spilianakis, C., Kretsovali, A., Papamatheakis, J. and Reith, W. (2004) The S box of major histocompatibility complex class II promoters is a key determinant for recruitment of the transcriptional co-activator CIITA. *J Biol Chem.* **279**: 40529-40535.

Munoz, E., Courtois, G., Veschambre, P., Jalinot, P. and Israel, A. (1994) Tax induces nuclear translocation of NF-kappa B through dissociation of cytoplasmic complexes containing p105 or p100 but does not induce degradation of I kappa B alpha/MAD3. *J Virol.* **68**: 8035-8044.

Nagarajan, U.M., Louis-Plence, P., DeSandro, A., Nilsen, R., Bushey, A. and Boss, J.M. (1999) RFX-B is the gene responsible for the most common cause of the bare lymphocyte syndrome, an MHC class II immunodeficiency. *Immunity.* **10**: 153-162.

Neefjes, J., Jongsma, M.L., Paul, P. and Bakke, O. (2011) Towards a systems understanding of MHC class I and MHC class II antigen presentation. *Nat Rev Immunol.* **11**: 823-836.

Neerincx, A., Lautz, K., Menning, M., Kremmer, E., Zigrino, P., Hosel, M.*, et al* (2010) A role for the human nucleotide-binding domain, leucine-rich repeat-containing family member NLRC5 in antiviral responses. *J Biol Chem.* **285**: 26223-26232.

Netea, M.G., Wijmenga, C. and O'Neill, L.A. (2012) Genetic variation in Toll-like receptors and disease susceptibility. *Nat Immunol.* **13**: 535-542.

Nickerson, K., Sisk, T.J., Inohara, N., Yee, C.S., Kennell, J., Cho, M.C.*, et al* (2001) Dendritic cell-specific MHC class II transactivator contains a caspase recruitment domain that confers potent transactivation activity. *J Biol Chem.* **276**: 19089-19093.

Ninomiya-Tsuji, J., Kishimoto, K., Hiyama, A., Inoue, J., Cao, Z. and Matsumoto, K. (1999) The kinase TAK1 can activate the NIK-I kappaB as well as the MAP kinase cascade in the IL-1 signalling pathway. *Nature.* **398**: 252-256.

Normand, S., Delanoye-Crespin, A., Bressenot, A., Huot, L., Grandjean, T., Peyrin-Biroulet, L.*, et al* (2011) Nod-like receptor pyrin domain-containing protein 6 (NLRP6) controls epithelial self-renewal and colorectal carcinogenesis upon injury. *Proc Natl Acad Sci U S A.* **108**: 9601-9606.

O'Neill, L.A. and Bowie, A.G. (2011) The powerstroke and camshaft of the RIG-I antiviral RNA detection machine. *Cell.* **147**: 259-261.

Ogura, Y., Inohara, N., Benito, A., Chen, F.F., Yamaoka, S. and Nunez, G. (2001) Nod2, a Nod1/Apaf-1 family member that is restricted to monocytes and activates NF-kappaB. *J Biol Chem.* **276**: 4812-4818.

Oh, H.M., Lee, H.J., Seo, G.S., Choi, E.Y., Kweon, S.H., Chun, C.H.*, et al* (2005) Induction and localization of NOD2 protein in human endothelial cells. *Cell Immunol.* **237**: 37-44.

Pai, R.K., Askew, D., Boom, W.H. and Harding, C.V. (2002) Regulation of class II MHC expression in APCs: roles of types I, III, and IV class II transactivator. *J Immunol.* **169**: 1326-1333.

Park, B.S., Song, D.H., Kim, H.M., Choi, B.S., Lee, H. and Lee, J.O. (2009) The structural basis of lipopolysaccharide recognition by the TLR4-MD-2 complex. *Nature.* **458**: 1191-1195.

Peri, F. and Piazza, M. (2012) Therapeutic targeting of innate immunity with Toll-like receptor 4 (TLR4) antagonists. *Biotechnol Adv.* **30**: 251-260.

Pichlmair, A., Schulz, O., Tan, C.P., Naslund, T.I., Liljestrom, P., Weber, F. and Reis e Sousa, C. (2006) RIG-I-mediated antiviral responses to single-stranded RNA bearing 5'-phosphates. *Science.* **314**: 997-1001.

Proell, M., Riedl, S.J., Fritz, J.H., Rojas, A.M. and Schwarzenbacher, R. (2008) The Nod-like receptor (NLR) family: a tale of similarities and differences. *PLoS ONE.* **3**: e2119.

Rathinam, V.A., Vanaja, S.K. and Fitzgerald, K.A. (2012) Regulation of inflammasome signaling. *Nat Immunol.* **13**: 333-332.

Raval, A., Weissman, J.D., Howcroft, T.K. and Singer, D.S. (2003) The GTP-binding domain of class II transactivator regulates its nuclear export. *J Immunol.* **170**: 922-930.

Reinis, M. (2011) Immunotherapy of MHC class I-deficient tumors. *Future Oncol.* **6**: 1577-1589.

Reith, W. and Mach, B. (2001) The bare lymphocyte syndrome and the regulation of MHC expression. *Annu Rev Immunol.* **19**: 331-373.

Reith, W., LeibundGut-Landmann, S. and Waldburger, J.M. (2005) Regulation of MHC class II gene expression by the class II transactivator. *Nat Rev Immunol.* **5**: 793-806.

Reits, E.A., Vos, J.C., Gromme, M. and Neefjes, J. (2000) The major substrates for TAP in vivo are derived from newly synthesized proteins. *Nature.* **404**: 774-778.

Riedl, S.J. and Salvesen, G.S. (2007) The apoptosome: signalling platform of cell death. *Nat Rev Mol Cell Biol.* **8**: 405-413.

Riedl, S.J., Li, W., Chao, Y., Schwarzenbacher, R. and Shi, Y. (2005) Structure of the apoptotic protease-activating factor 1 bound to ADP. *Nature.* **434**: 926-933.

Riley, J.L., Westerheide, S.D., Price, J.A., Brown, J.A. and Boss, J.M. (1995) Activation of class II MHC genes requires both the X box region and the class II transactivator (CIITA). *Immunity.* **2**: 533-543.

Robbins, G.R., Truax, A.D., Davis, B.K., Zhang, L., Brickey, W.J. and Ting, J.P. (2012) Regulation of class I major histocompatibility complex (MHC) by nucleotide-binding domain, leucine-rich repeat-containing (NLR) proteins. *J Biol Chem.* **287**: 24294-24303.

Roberts, T.L., Idris, A., Dunn, J.A., Kelly, G.M., Burnton, C.M., Hodgson, S.*, et al* (2009) HIN-200 proteins regulate caspase activation in response to foreign cytoplasmic DNA. *Science.* **323**: 1057-1060.

Rosenstiel, P., Fantini, M., Brautigam, K., Kuhbacher, T., Waetzig, G.H., Seegert, D. and Schreiber, S. (2003) TNF-alpha and IFN-gamma regulate the expression of the NOD2 (CARD15) gene in human intestinal epithelial cells. *Gastroenterology.* **124**: 1001-1009.

Rothenfusser, S., Goutagny, N., DiPerna, G., Gong, M., Monks, B.G., Schoenemeyer, A.*, et al* (2005) The RNA helicase Lgp2 inhibits TLR-independent sensing of viral replication by retinoic acid-inducible gene-I. *J Immunol.* **175**: 5260-5268.

Sabbah, A., Chang, T.H., Harnack, R., Frohlich, V., Tominaga, K., Dube, P.H.*, et al* (2009) Activation of innate immune antiviral responses by Nod2. *Nat Immunol.* **10**: 1073-1080.

Saitoh, S., Akashi, S., Yamada, T., Tanimura, N., Matsumoto, F., Fukase, K.*, et al* (2004a) Ligand-dependent Toll-like receptor 4 (TLR4)-oligomerization is directly linked with TLR4-signaling. *J Endotoxin Res.* **10**: 257-260.

Saitoh, S., Akashi, S., Yamada, T., Tanimura, N., Kobayashi, M., Konno, K.*, et al* (2004b) Lipid A antagonist, lipid IVa, is distinct from lipid A in interaction with Toll-like receptor 4 (TLR4)-MD-2 and ligand-induced TLR4 oligomerization. *Int Immunol.* **16**: 961-969.

Sancho, D. and Reis e Sousa, C. (2012) Signaling by myeloid C-type lectin receptors in immunity and homeostasis. *Annu Rev Immunol.* **30**: 491-529.

Sato, M., Suemori, H., Hata, N., Asagiri, M., Ogasawara, K., Nakao, K.*, et al* (2000) Distinct and essential roles of transcription factors IRF-3 and IRF-7 in response to viruses for IFN-alpha/beta gene induction. *Immunity.* **13**: 539-548.

Schattgen, S.A. and Fitzgerald, K.A. (2011) The PYHIN protein family as mediators of host defenses. *Immunol Rev.* **243**: 109-118.

Schmidt, A., Endres, S. and Rothenfusser, S. (2011) Pattern recognition of viral nucleic acids by RIG-I-like helicases. *J Mol Med (Berl).* **89**: 5-12.

Schnappauf, F., Hake, S.B., Camacho Carvajal, M.M., Bontron, S., Lisowska-Grospierre, B. and Steimle, V. (2003) N-terminal destruction signals lead to rapid degradation of the major histocompatibility complex class II transactivator CIITA. *Eur J Immunol.* **33**: 2337-2347.

Schneider, C.A., Rasband, W.S. and Eliceiri, K.W. (2012) NIH Image to ImageJ: 25 years of image analysis. *Nat Methods.* **9**: 671-675.

Scholl, T., Mahanta, S.K. and Strominger, J.L. (1997) Specific complex formation between the type II bare lymphocyte syndrome-associated transactivators CIITA and RFX5. *Proc Natl Acad Sci U S A.* **94**: 6330-6334.

Schubert, U., Anton, L.C., Gibbs, J., Norbury, C.C., Yewdell, J.W. and Bennink, J.R. (2000) Rapid degradation of a large fraction of newly synthesized proteins by proteasomes. *Nature.* **404**: 770-774.

Sehgal, P.B. and Gupta, S.L. (1980) Regulation of the stability of poly(I)xpoly(C)-induced human fibroblast interferon mRNA: selective inactivation of interferon mRNA and lack of involvement of 2',5'-oligo(A) synthetase activation during the shutoff of interferon production. *Proc Natl Acad Sci U S A.* **77**: 3489-3493.

Sehgal, P.B., Lyles, D.S. and Tamm, I. (1978) Superinduction of human fibroblast interferon production: further evidence for increased stability of interferon mRNA. *Virology.* **89**: 186-198.

Seth, R.B., Sun, L., Ea, C.K. and Chen, Z.J. (2005) Identification and characterization of MAVS, a mitochondrial antiviral signaling protein that activates NF-kappaB and IRF 3. *Cell.* **122**: 669-682.

Sharma, R.P., He, Q. and Johnson, V.J. (2003a) Deletion of IFN-gamma reduces fumonisin-induced hepatotoxicity in mice via alterations in inflammatory cytokines and apoptotic factors. *J Interferon Cytokine Res.* **23**: 13-23.

Sharma, S., tenOever, B.R., Grandvaux, N., Zhou, G.P., Lin, R. and Hiscott, J. (2003b) Triggering the interferon antiviral response through an IKK-related pathway. *Science.* **300**: 1148-1151.

Shimazu, R., Akashi, S., Ogata, H., Nagai, Y., Fukudome, K., Miyake, K. and Kimoto, M. (1999) MD-2, a molecule that confers lipopolysaccharide responsiveness on Toll-like receptor 4. *J Exp Med.* **189**: 1777-1782.

Sijts, E.J. and Kloetzel, P.M. (2011) The role of the proteasome in the generation of MHC class I ligands and immune responses. *Cell Mol Life Sci.* **68**: 1491-1502.

Smith, K.D., Andersen-Nissen, E., Hayashi, F., Strobe, K., Bergman, M.A., Barrett, S.L.*, et al* (2003) Toll-like receptor 5 recognizes a conserved site on flagellin required for protofilament formation and bacterial motility. *Nat Immunol.* **4**: 1247-1253.

Song, A., Nikolcheva, T. and Krensky, A.M. (2000) Transcriptional regulation of RANTES expression in T lymphocytes. *Immunol Rev.* **177**: 236-245.

Staehli, F., Ludigs, K., Heinz, L.X., Seguin-Estevez, Q., Ferrero, I., Braun, M.*, et al* (2012) NLRC5 deficiency selectively impairs MHC class I- dependent lymphocyte killing by cytotoxic T cells. *J Immunol.* **188**: 3820-3828.

Steimle, V. and Mach, B. (1995) Complementation cloning of mammalian transcriptional regulators: the example of MHC class II gene regulators. *Curr Opin Genet Dev.* **5**: 646-651.

Steimle, V., Otten, L.A., Zufferey, M. and Mach, B. (1993) Complementation cloning of an MHC class II transactivator mutated in hereditary MHC class II deficiency (or bare lymphocyte syndrome). *Cell.* **75**: 135-146.

Steimle, V., Siegrist, C.A., Mottet, A., Lisowska-Grospierre, B. and Mach, B. (1994) Regulation of MHC class II expression by interferon-gamma mediated by the transactivator gene CIITA. *Science.* **265**: 106-109.

Steimle, V., Durand, B., Barras, E., Zufferey, M., Hadam, M.R., Mach, B. and Reith, W. (1995) A novel DNA-binding regulatory factor is mutated in primary MHC class II deficiency (bare lymphocyte syndrome). *Genes Dev.* **9**: 1021-1032.

Takaoka, A., Wang, Z., Choi, M.K., Yanai, H., Negishi, H., Ban, T.*, et al* (2007) DAI (DLM-1/ZBP1) is a cytosolic DNA sensor and an activator of innate immune response. *Nature.* **448**: 501-505.

Takeda, K., Takeuchi, O. and Akira, S. (2002) Recognition of lipopeptides by Toll-like receptors. *J Endotoxin Res*. **8**: 459-463.

Tanabe, T., Chamaillard, M., Ogura, Y., Zhu, L., Qiu, S., Masumoto, J*., et al* (2004) Regulatory regions and critical residues of NOD2 involved in muramyl dipeptide recognition. *Embo J*. **23**: 1587-1597.

Tao, M., Scacheri, P.C., Marinis, J.M., Harhaj, E.W., Matesic, L.E. and Abbott, D.W. (2009) ITCH K63-Ubiquitinates the NOD2 Binding Protein, RIP2, to Influence Inflammatory Signaling Pathways. *Curr Biol*.

Tattoli, I., Carneiro, L.A., Jehanno, M., Magalhaes, J.G., Shu, Y., Philpott, D.J*., et al* (2008) NLRX1 is a mitochondrial NOD-like receptor that amplifies NF-kappaB and JNK pathways by inducing reactive oxygen species production. *EMBO Rep*. **9**: 293-300.

Ting, J.P. and Trowsdale, J. (2002) Genetic control of MHC class II expression. *Cell*. **109 Suppl**: S21-33.

Ting, J.P., Kastner, D.L. and Hoffman, H.M. (2006) CATERPILLERs, pyrin and hereditary immunological disorders. *Nat Rev Immunol*. **6**: 183-195.

Tong, Y., Cui, J., Li, Q., Zou, J., Wang, H.Y. and Wang, R.F. (2012) Enhanced TLR-induced NF-kappaB signaling and type I interferon responses in NLRC5 deficient mice. *Cell Res*. **22**: 822-835.

Unlu, S., Kumar, A., Waterman, W.R., Tsukada, J., Wang, K.Z., Galson, D.L. and Auron, P.E. (2007) Phosphorylation of IRF8 in a pre-associated complex with Spi-1/PU.1 and non-phosphorylated Stat1 is critical for LPS induction of the IL1B gene. *Mol Immunol*. **44**: 3364-3379.

Unterholzner, L., Keating, S.E., Baran, M., Horan, K.A., Jensen, S.B., Sharma, S*., et al* (2010) IFI16 is an innate immune sensor for intracellular DNA. *Nat Immunol*. **11**: 997-1004.

van den Elsen, P.J., Holling, T.M., Kuipers, H.F. and van der Stoep, N. (2004) Transcriptional regulation of antigen presentation. *Curr Opin Immunol*. **16**: 67-75.

van der Merwe, P.A. and Dushek, O. (2010) Mechanisms for T cell receptor triggering. *Nat Rev Immunol*. **11**: 47-55.

Venkataraman, T., Valdes, M., Elsby, R., Kakuta, S., Caceres, G., Saijo, S*., et al* (2007) Loss of DExD/H box RNA helicase LGP2 manifests disparate antiviral responses. *J Immunol*. **178**: 6444-6455.

Vijay-Kumar, M., Gentsch, J.R., Kaiser, W.J., Borregaard, N., Offermann, M.K., Neish, A.S. and Gewirtz, A.T. (2005) Protein kinase R mediates intestinal epithelial gene remodeling in response to double-stranded RNA and live rotavirus. *J Immunol*. **174**: 6322-6331.

Vyas, J.M., Van der Veen, A.G. and Ploegh, H.L. (2008) The known unknowns of antigen processing and presentation. *Nat Rev Immunol*. **8**: 607-618.

Wang, L., Manji, G.A., Grenier, J.M., Al-Garawi, A., Merriam, S., Lora, J.M*., et al* (2002) PYPAF7, a novel PYRIN-containing Apaf1-like protein that regulates activation of NF-kappa B and caspase-1-dependent cytokine processing. *J Biol Chem*. **277**: 29874-29880.

Wang, Y., Liu, L., Davies, D.R. and Segal, D.M. (2012) Dimerization of Toll-like receptor 3 (TLR3) is required for ligand binding. *J Biol Chem*. **285**: 36836-36841.

Wang, Z., Choi, M.K., Ban, T., Yanai, H., Negishi, H., Lu, Y*., et al* (2008) Regulation of innate immune responses by DAI (DLM-1/ZBP1) and other DNA-sensing molecules. *Proc Natl Acad Sci U S A*. **105**: 5477-5482.

Wilkins, C. and Gale, M., Jr. (2010) Recognition of viruses by cytoplasmic sensors. *Curr Opin Immunol.* **22**: 41-47.

Wright, K.L. and Ting, J.P. (2006) Epigenetic regulation of MHC-II and CIITA genes. *Trends Immunol.* **27**: 405-412.

Xia, X., Cui, J., Wang, H.Y., Zhu, L., Matsueda, S., Wang, Q.*, et al* (2011) NLRX1 negatively regulates TLR-induced NF-kappaB signaling by targeting TRAF6 and IKK. *Immunity.* **34**: 843-853.

Xu, L.G., Wang, Y.Y., Han, K.J., Li, L.Y., Zhai, Z. and Shu, H.B. (2005) VISA is an adapter protein required for virus-triggered IFN-beta signaling. *Mol Cell.* **19**: 727-740.

Xu, S., Liu, X., Bao, Y., Zhu, X., Han, C., Zhang, P.*, et al* (2012) Constitutive MHC class I molecules negatively regulate TLR-triggered inflammatory responses via the Fps-SHP-2 pathway. *Nat Immunol.* **13**: 551-559.

Yamaguchi, K., Shirakabe, K., Shibuya, H., Irie, K., Oishi, I., Ueno, N.*, et al* (1995) Identification of a member of the MAPKKK family as a potential mediator of TGF-beta signal transduction. *Science.* **270**: 2008-2011.

Yamamoto, M., Sato, S., Mori, K., Hoshino, K., Takeuchi, O., Takeda, K. and Akira, S. (2002) Cutting edge: a novel Toll/IL-1 receptor domain-containing adapter that preferentially activates the IFN-beta promoter in the Toll-like receptor signaling. *J Immunol.* **169**: 6668-6672.

Yamasaki, K., Muto, J., Taylor, K.R., Cogen, A.L., Audish, D., Bertin, J.*, et al* (2009) NLRP3/cryopyrin is necessary for interleukin-1beta (IL-1beta) release in response to hyaluronan, an endogenous trigger of inflammation in response to injury. *J Biol Chem.* **284**: 12762-12771.

Yao, Y., Wang, Y., Chen, F., Huang, Y., Zhu, S., Leng, Q.*, et al* (2012) NLRC5 regulates MHC class I antigen presentation in host defense against intracellular pathogens. *Cell Res.* **22**: 836-847.

Yoneyama, M. and Fujita, T. (2009) RNA recognition and signal transduction by RIG-I-like receptors. *Immunol Rev.* **227**: 54-65.

Yun, S., Gustafsson, K. and Fabre, J.W. (1997) Suppression of MHC class II expression by human class II trans-activator constructs lacking the N-terminal domain. *Int Immunol.* **9**: 1545-1553.

Zhang, S.Y., Jouanguy, E., Ugolini, S., Smahi, A., Elain, G., Romero, P.*, et al* (2007) TLR3 deficiency in patients with herpes simplex encephalitis. *Science.* **317**: 1522-1527.

Zhao, Y., Yang, J., Shi, J., Gong, Y.N., Lu, Q., Xu, H.*, et al* (2011) The NLRC4 inflammasome receptors for bacterial flagellin and type III secretion apparatus. *Nature.* **477**: 596-600.

Zhong, B., Yang, Y., Li, S., Wang, Y.Y., Li, Y., Diao, F.*, et al* (2008) The adaptor protein MITA links virus-sensing receptors to IRF3 transcription factor activation. *Immunity.* **29**: 538-550.

Zhou, H. and Glimcher, L.H. (1995) Human MHC class II gene transcription directed by the carboxyl terminus of CIITA, one of the defective genes in type II MHC combined immune deficiency. *Immunity.* **2**: 545-553.

Zhou, H., Su, H.S., Zhang, X., Douhan, J., 3rd and Glimcher, L.H. (1997) CIITA-dependent and -independent class II MHC expression revealed by a dominant negative mutant. *J Immunol.* **158**: 4741-4749.

Zhu, X.S., Linhoff, M.W., Li, G., Chin, K.C., Maity, S.N. and Ting, J.P. (2000) Transcriptional scaffold: CIITA interacts with NF-Y, RFX, and CREB to cause stereospecific regulation of the class II major histocompatibility complex promoter. *Mol Cell Biol.* **20**: 6051-6061.

Zigrino, P., Drescher, C. and Mauch, C. (2001) Collagen-induced proMMP-2 activation by MT1-MMP in human dermal fibroblasts and the possible role of alpha2beta1 integrins. *Eur J Cell Biol.* **80**: 68-77.

Zinzow-Kramer, W.M., Long, A.B., Youngblood, B.A., Rosenthal, K.M., Butler, R., Mohammed, A.U*., et al* (2012) CIITA promoter I CARD-deficient mice express functional MHC class II genes in myeloid and lymphoid compartments. *Genes Immun.* **13**: 299-310.

Zurek, B., Bielig, H. and Kufer, T.A. (2011) Cell-Based Reporter Assay to Analyze Activation of Nod1 and Nod2. *Methods Mol Biol.* **748**: 107-119.

Zurek, B., Proell, M., Wagner, R.N., Schwarzenbacher, R. and Kufer, T.A. (2012a) Mutational analysis of human NOD1 and NOD2 NACHT domains reveals different modes of activation. *Innate Immun.*

Zurek, B., Schoultz, I., Neerincx, A., Napolitano, L.M., Birkner, K., Bennek, E*., et al* (2012b) TRIM27 negatively regulates NOD2 by ubiquitination and proteasomal degradation. *PLoS One.* **7**: e41255.

7 Abstract

Nucleotide-binding domain, leucine-rich repeat (NLR)-containing proteins play important roles in the innate immune system as intracellular pattern recognition receptors. The most prominent members, NOD1, NOD2 and NLRP3 have been extensively shown to trigger NF-κB activation or IL-1β/IL-18 processing upon pathogen infection, respectively. Nonetheless, other functions beyond pathogen recognition have also been reported for some NLR proteins.

Here we report the first characterization of the human NLR protein NLRC5. NLRC5 lacks the typical N-terminal CARD or PYRIN domain of most NLR proteins, but harbours a death domain fold effector domain with yet unknown function. Interestingly, NACHT and LRR domain alignments reveal close homology to the MHC class II transcriptional activator (CIITA), which is responsible for the transcriptional induction of MHC class II molecules, and moderate homology to NOD1 and NOD2.

In the first part of this study, we addressed the expression and regulation of NLRC5 in different tissues and cell lines. We detected NLRC5 expression primarily in cells and tissues of the immune system, including CD4$^+$ and CD8$^+$ T cells and spleen, lymph node and bone marrow. Furthermore, we were able to induce a TLR3-dependent NLRC5 induction upon stimulation with the dsRNA-mimic poly(I:C) as well as an TLR3-independent NLRC5 induction using a Sendai Virus (SeV)-based infection model. In line with that, we revealed a role for NLRC5 in type I interferon (IFN) response against RNA viruses. Moreover, we adapted an infection model of primary human dermal fibroblasts (hFibr) with Sendai Virus (SeV), depicting a distinct role for NLRC5 in anti-viral immune processes.

In the second part, we investigated the role of NLRC5 in MHC class I promoter activation. Similar to MHC class II promoter activation by the non-DNA binding coactivator CIITA, we were able to obtain a clear role for NLRC5 in MHC class I expression and identified the domains, which are important for nuclear translocation and MHC class I promoter activation. We further analysed the involvement of a DNA-binding complex, the so-called enhanceosome, in NLRC5-dependent MHC class I expression, which is pivotal for CIITA-dependent MHC class II expression.

Finally, we generated NLRC5-CIITA-chimeric proteins to decipher the NLRC5-dependent MHC class I and CIITA-dependent class II activation in more detail. Domain swapping of the N-terminal effector domains revealed, that the NLRC5 N-terminal effector domain fused to the C-terminus of CIITA is sufficient to activate both MHC class I and MHC class II expression.

Taken together, in this study we identified a role for NLRC5 in anti-viral immune responses and further contributed to the understanding of NLRC5-mediated MHC class I expression.

8 Zusammenfassung

Mitglieder der intrazellulären NLR Proteinfamilie spielen als Mustererkennungs-Rezeptoren (PRRs) entscheidende Rollen im angeborenen Immunsystem. Zu den bekanntesten NLR Proteinen gehören NOD1, NOD2 und NLRP3, welche bereits ausgiebig im Hinblick auf ihre Fähigkeit NF-κB und IL-1β/IL-18 Signalwege auszulösen untersucht wurden. Neben diesen wurden ebenfalls rezeptorunabhängige Funktionen für einige NLR Proteine in der Literatur beschrieben.

Im Rahmen dieser Arbeit wurde eine erste Charakterisierung des menschlichen NLR Proteins NLRC5 durchgeführt. Zwar fehlt NLRC5 die typische N-terminale CARD- oder PYRIN-Domäne der meisten NLR Proteine, dennoch besitzt es eine todesdomänenartige (death domain fold) Struktur mit bislang ungeklärter Funktion. Interessanterweise zeigen die nukleotidbindende Domäne und die leuzinreiche Domäne eine starke Homologie zum MHC Klasse II Aktivator CIITA, welcher für die transkriptionelle Induktion von MHC Klasse II Molekülen verantwortlich ist, als auch eine mittelmäßige Homologie zu NOD1 und NOD2.

Im ersten Teil dieser Arbeit wurde die Expression und Regulation von NLRC5 in verschiedenen Geweben und Zelltypen untersucht. NLRC5 Expression war hauptsächlich in Zellen und Geweben des Immunsystems, wie zum Beispiel in CD4-positiven und CD8-positiven T-Zellen, sowie in Milz, Lymphknoten und Knochenmark, nachweisbar. Außerdem konnte die Expression von NLRC5 durch Stimulation des Toll-ähnlichen Rezeptors 3 (TLR3) mit dem doppelsträngigen RNA Analogon poly(I:C), sowie TLR3-unabhängig durch Sendaivirusinfektion induziert werden. Zusätzlich konnte eine Funktion von NLRC5 in RNA-virusabhängige Typ I Interferoninduktion aufgedeckt werden, welche zusätzlich in einem Sendaivirusinfektionsmodell von menschlichen primären Fibroblasten nachgewiesen werden konnte.

Im zweiten Teil der Arbeit wurde die Fähigkeit von NLRC5 den MHC Klasse I Promotor zu aktivieren untersucht. Vergleichbar mit der CIITA-induzierten MHC Klasse II Promoteraktivierung konnte eine klare Beteiligung von NLRC5 an der MHC Klasse I Expression nachgewiesen werden, sowie die Bedeutung des nukleären Transports herausgearbeitet werden. Außerdem wurde der Einfluss eines DNA-bindenden Multiproteinkomplexes namens Enhanceosome, welcher in der CIITA-abhängigen MHC Klasse II Expression unabdingbar ist, ebenfalls in der NLRC5-abhängigen MHC Klasse I Expression nachgewiesen.

Zum Schluss wurden NLRC5-CIITA-Chimären generiert, um die NLRC5-abhängige MHC Klasse I und die CIITA-abhängige MHC Klasse II Expression genauer zu untersuchen. Ein Domänenaustausch der N-terminalen Effektordomänen hat ergeben, dass die NLRC5 Effektordomäne zusammen mit der nukleotidbindenden Domäne und der leuzinreichen Domäne von CIITA ausreichend ist, um sowohl MHC Klasse I als auch MHC Klasse II Expression zu induzieren.

In dieser Arbeit konnte nicht nur eine Funktion von NLRC5 in der antiviralen Immun-abwehr identifiziert werden, sondern auch ein Beitrag zum Verständnis von NLRC5-abhängiger MHC Klasse I Expression geleistet werden.

Danksagung

Zuallererst möchte ich mich bei PD Dr. Thomas Kufer bedanken, der mir unter exzellenter Betreuung und Anleitung die Möglichkeit gegeben hat, in seiner Arbeitsgruppe meine Doktorarbeit anzufertigen. Darüber hinaus vielen Dank für die zahlreichen Anregungen und interessanten Diskussionen rund um das Thema Wissenschaft und Forschung, sowie die Möglichkeit, eigene Ideen in dieser Doktorarbeit umzusetzen und letztendlich für das Korrekturlesen dieser Arbeit.

Außerdem danke ich meinem Doktorvater Prof. Dr. Jonathan Howard für die Übernahme der Erstkorrektur und Begutachtung, sowie den zahlreichen hilfreichen Anmerkungen rund um das Thema dieser Arbeit.

Prof. Dr. Mats Paulsson danke ich für die Übernahme der Zweitkorrektur und Begutachtung dieser Arbeit sowie für Anmerkungen und Ratschlägen zu diesem Projekt.

Prof. Dr. Günther Schwarz danke ich für die Übernahme des Vorsitzes in meiner mündlichen Prüfung.

Bei Dr. Robert Schwarzenbacher möchte ich mich für die Unterstützung und gute Zusammenarbeit in der Anfangsphase dieses Projektes bedanken.

Außerdem bedanke ich mich bei Prof. Dr. Viktor Steimle für die hervorragende Zusammenarbeit und Expertise sowie Hilfe bei Fragen rund um CIITA.

Ferner gilt mein Dank der AG Kufer, bestehend aus Katja, Maureen, Anna D. und Christine, sowie den ehemaligen Kollegen, Harald und Birte. Vielen Dank für das angenehme Arbeitsklima und die Unterstützung und Hilfsbereitschaft bei zahlreichen Versuchen. Mein besonderer Dank gilt Maureen und Katja L. für die experimentelle Unterstützung, sowie Katja L. und Harald für das Korrekturlesen dieser Arbeit.

Nicht zuletzt möchte ich mich bei meinen Eltern Heinz und Liane Neerincx bedanken, die mir die Möglichkeit gegeben haben, mein Studium der Biologie durchzuführen.

Abschließend bedanke ich mich bei meiner Freundin Claudia Peters, sowie bei allen Freunden, die auch in stressigen Zeiten immer wieder eine willkommene Ablenkung anboten, sowie explizit bei Jan und Tina für das Korrekturlesen dieser Arbeit.

Erklärung

Ich versichere, dass ich die von mir vorgelegte Dissertation selbstständig angefertigt, die benutzten Quellen und Hilfsmittel vollständig angegeben und die Stellen der Arbeit – einschließlich Tabellen, Karten und Abbildungen –, die anderen Werken im Wortlaut oder dem Sinn nach entnommen sind, in jedem Einzelfall als Entlehnung kenntlich gemacht habe; dass diese Dissertation noch keiner anderen Fakultät oder Universität zur Prüfung vorgelegen hat; dass sie – abgesehen von unten angegebenen Teilpublikationen – noch nicht veröffentlicht worden ist sowie, dass ich eine solche Veröffentlichung vor Abschluss des Promotionsverfahrens nicht vornehmen werde.

Die Bestimmungen der Promotionsordnung sind mir bekannt. Die von mir vorgelegte Dissertation ist von Prof. Dr. Jonathan Howard und Prof. Dr. Mats Paulsson betreut worden.

Köln, im November 2012

_____

(Andreas Heinrich Neerincx)

Teilpublikationen

Neerincx, A., Rodriguez, G.M., Steimle, V. and Kufer, T.A. (2012) NLRC5 controls basal MHC class I gene expression in an MHC enhanceosome-dependent manner. *J Immunol*. **188**: 4940-4950.

Neerincx, A., Lautz, K., Menning, M., Kremmer, E., Zigrino, P., Hosel, M*., et al* (2010) A role for the human nucleotide-binding domain, leucine-rich repeat-containing family member NLRC5 in antiviral responses. *J Biol Chem*. **285**: 26223-26232.